How hearing loss across the lifespan affects the brain: Structural correlates of hearing loss assessed by coordinate mapping using quantitative metrics of gray and white matter trajectories - Systematic review, meta-analysis and meta-regression

Francis A. M. Manno DPhil, $PhD^{1,2\hat{}}$†, Raul Rodríguez-Cruces MD, PhD^{3}*, Rachit Kumar BS^{4}*, Yilai Shu MD, PhD^{5}, J. Tilak Ratnanather $DPhil^{6}$, Condon Lau PhD^{2}

1. School of Biomedical Engineering, Faculty of Engineering, University of Sydney, Sydney, New South Wales, Australia
2. Department of Physics, City University of Hong Kong, Kowloon, Hong Kong SAR, China
3. Montreal Neurological Institute, McGill University, Montreal, Canada
4. Wallace H. Coulter Department of Biomedical Engineering, Georgia Institute of Technology and Emory University, Atlanta, GA, USA
5. ENT Institute and Otorhinolaryngology Department of the Affiliated Eye and ENT Hospital, State Key Laboratory of Medical Neurobiology, Institutes of Biomedcial Sciences, Fudan University, Shanghai, China
6. Center for Imaging Science and Institute for Computational Medicine, Department of Biomedical Engineering, Johns Hopkins University, Baltimore, MD, USA

Data availability statement: The entire dataset, analyses and code used in this work can be downloaded by contacting the corresponding author and from the Open Science Framework: Manno, et al., 2018. "Profound Hearing Loss." OSF. https://osf.io/7y59j/.

Declaration of Interests: The authors declare no competing financial interests and no non-financial competing interests.

Author Contributions: Conceptualization, FAMM JTR, CL; Methodology, FAMM, RRC; Formal Analysis, FAMM, RRC, RK; Visualization FAMM, RRC, RK; Investigation, FAMM, JTR; Writing, Editing, Funding FAMM, RRC, RK, YS, JTR, CL.

†Corresponding Author:
Francis A.M. Manno
School of Biomedical Engineering
Faculty of Engineering, The University of Sydney
Sydney, New South Wales, Australia
Email: Francis.Manno@Sydney.edu.au

Keywords: sensorineural hearing loss, structural MRI, bilateral hearing loss, unilateral hearing loss, deaf

Contents

List of Tables

Methods

Literature research

- Literature Search Methodology (eFigure PRISMA)
    1. PubMed searches were performed to acquire the requisite background information for this review. The searches had the purpose of identifying all sources concerning structural MRI assessments of unilateral or bilateral hearing loss. All studies must have utilized MRI as a structural assessment for hearing loss.
    2. Search Terminology: *"Unilateral hearing loss OR single-sided deafness, "Bilateral hearing loss OR deafness", "AND MRI OR magnetic resonance imaging"*
- First Search Oct/Nov 2012
    1. A literature search in PubMed using MeSH and truncated (wildcard) terms was performed for studies pertaining to "unilateral hearing loss" or "bilateral hearing loss on Wed October 10, 2012 through Thurs November 1, 2012. The literature search returned precisely 3,057 results. All abstracts returned were read for descriptions of congenital unilateral/bilateral hearing loss using MRI. Approximately, 905 studies meet the following inclusion criteria. These studies were surveyed to ascertain whether they were relevant for inclusion based on the 'Review inclusion criteria.'
    2. The primary inclusion and exclusion criteria were predetermined by following recommendations on meta-analysis (Sutton, et al., 2000)
- Inclusion criteria
    1. Structural MRI study of bilateral or unilateral hearing loss
    2. Study had at least one cohort of participants whom had congenital unilateral/bilateral hearing loss
    3. The study, with a cohort of hearing impaired participants, had an adequate hearing control
    4. The normal hearing controls were sufficiently matched to the hearing impaired cohort (i.e age, gender, education, etc.)
    5. An experiment comparing the two cohorts was performed consisting of, but not limited to, MRI structural assessment
- Exclusion criteria
    1. All studies were first included in the review and then given an asterisk if deemed inappropriate for inclusion.
    2. Case studies (i.e., reports with only one patient)
    3. Manuscripts with insufficient power of replication (i.e., manuscript with 2 patients)
    4. Manuscripts with an inadequate or absent normal hearing control cohort (i.e., no control cohort was reported) – indicated in table.
    5. Normal hearing control cohort lacked matching demographic characteristics (i.e. the study had a group of hearing loss pediatric children and the normal hearing control group was adults)
    6. Manuscripts without an experiment comparing the hearing loss and normal cohort (i.e., bilateral hearing loss was not compared to hearing controls).
- Second Search June/July 2018
    1. Searches from first search and second search were combined along with personal correspondences of articles from JTR.
    2. Pubmed; (deafness OR "hearing loss" OR "bilateral hearing loss" OR "unilateral hearing loss" OR "conductive hearing loss" OR "sensorineural hearing Loss") AND ("magnetic resonance imaging" OR MRI OR DTI OR "diffusion tensor imaging") NOT (Review[Filter] OR Editorial[Filter] OR Comment[Filter])
    3. Returned 4,179 articles. Articles were checked again throughout June/July 2018. Final article list was checked through Scopus.
    4. All references we checked at date indicated in table.

5. Approximately 911 studies meet inclusion criteria
6. Approximately 178 studies were screened from both periods and invited
7. Approximately 118 were excluded based on exclusion criteria or not pertaining to inclusion criteria
8. A total of 51 studies were analyzed

- Controls
- Our requirements for duplicated studies were studies which used the identical participants but had different methodology, participants age was identical, or it was stated participants were used by authors in two studies
- Only included original statistics here from the studies. All derived effect sizes were from study information. Asymmetry statistics were created if a study included a left and a right side for an identical ROI. Statistics from our analysis could be derived from, example asymmetry as indicated above.
- Asymmetry if included was converted to: only for asymmetry (check asymmetry) (L - R) /[(L+R)/2], where positive result = LEFT, negative result = RIGHT
- If studies included acquired and congenital we only used congenital metrics.

Figure SI.1 Flow diagram

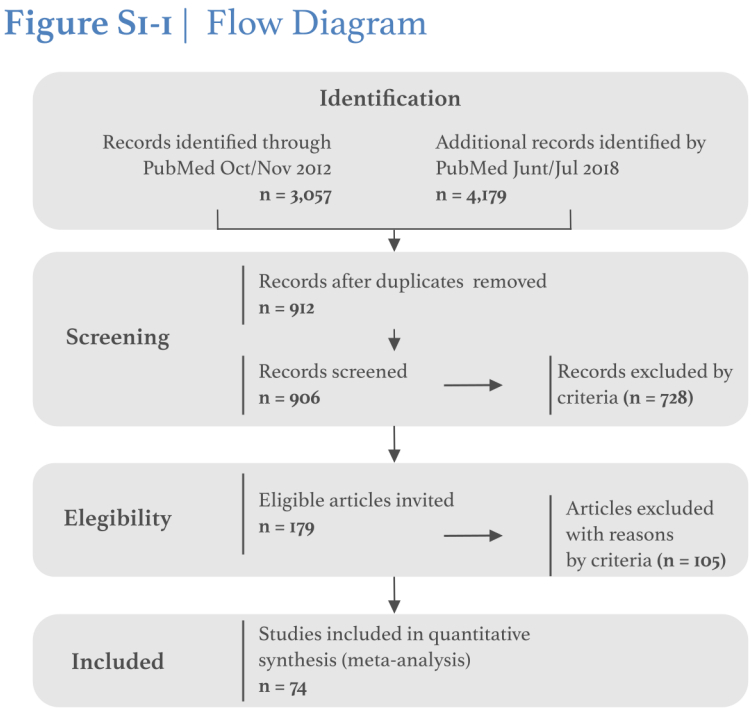

Figure 1: Flowchart of data-acquisition* All available bilateral/unilateral studies were analyzed.

Eligibility Criteria for the meta-regression

We included peer-review publications in English, involving patients with bilateral congenital and mixed hearing loss and controls with structural Magnetic Resonance Imaging. We included cross-sectional studies with control groups, that investigated the structural relation between MRI changes and the hearing loss. The most common MRI measures were **volume, FA, VBM and thickness.** Each measure was assignated

to a specific ROI and to a big brain area. (eg. HG and superior temporal lobe belong to **temporal lobe**). A total of 59 studies were included, 6 of them contained incomplete information. A total of 2778 patients and 4214 controls.
Notes for inclusion:

1. Xia et al. Chin J Rad, 2008 was excluded because it appears to be the same data as Xia et al. Chin J Med Img Tech, 2008.
2. Kim et al. Hear Res 2014 used two groups *prelingual deaf* and *post lingual deaf*, we used the average for the main table.
3. Xia et al. Chin J Med Img Tech, 2008 had 40 patients in total, in two groups 9-12 years and 19-22 years.
4. For some studies (eg. 2017, Ritgers et al. Front. Aging Neurosci) it was not possible to calculate the Hegdes'G variance and were not include in some specific meta-regressions.
5. Studies with *Mixed etiology* were excluded, due to a non representative low number (n=3).
6. Zheng et al. Sci Rep, 2017 this variables change; Con rangeLow Con rangeHigh. Why? I didn't find them on the orignal paper.

Tables of included studies

A total of **64** unique bilateral studies were included (19 acquires, 42 congenital and 3 mixed etiologies).

Table 1: Total unique studies 64

	Hearing Loss	Healthy
Total number of patients	7445	2924
Number mean	116.3	51.3
Number sd	479.3	204.3
Age mean	34.92	30.61
Age SD	23.08	19.45
%Female mean	50.41	54.97
%Female sd	12.2	12.64

Table 2: Acquired studies 19

	Hearing Loss	Healthy
Total number of patients	6469	1899
Number mean	340.5	146.1
Number sd	853.3	426.1
Age mean	65.31	56.44
Age SD	8.254	11.97
%Female mean	47.51	53.65
%Female sd	14.86	11.86

Table 3: Congenital studies 42

	Hearing Loss	Healthy
Total number of patients	927	976
Number mean	22.07	23.8
Number sd	17.06	14.63
Age mean	21.55	21.97
Age SD	12.21	12.68
%Female mean	51.16	55.23
%Female sd	10.95	13.2

Table 4: Mixed studies 3

	Hearing Loss	Healthy
Total number of patients	49	49
Number mean	16.33	16.33
Number sd	0.5774	0.5774
Age mean	25.26	25.13
Age SD	18.53	17.97
%Female mean	56.86	56.86
%Female sd	11.89	11.89

Table 5: Studies without Hedges'G (n=7). These studies do not have control population (NA)

Source	Etiology	Number.Control
2011, Peelle et al. J Neurosci	acquired	NA
2012, Chang et al., Clin Exp Otorhinolaryngo	congenital	NA
2012, Eckert et al. J Assoc Res Otolaryngol	acquired	NA
2013, Eckert et al. J Assoc Res Otolaryngol	acquired	NA
2017, Qian et al. Neuroimage Clin	acquired	NA
2017, Ritgers et al. Front. Aging Neurosci	acquired	NA
2018, Ritgers et al. Neurobiol Aging	acquired	NA

Table 6: Studies with Hedges'G (n=57, mixed etiology=3)

Source	Etiology	all.techniques	all.measures
2010, Liu et al. Chin J Med Img Tech	congenital	CT	FA
2012, Li et al. Brain Res	congenital	CT	Thickness
2015, Li et al. Restor Neurol Neurosci	mixed	CT	volume
2016, Shiell et al. Neural Plasticity	congenital	CT	Thickness
2016, Smittenaar et al. Open Neuroimag J	congenital	CT	CT
2018, Ren et al. Front Neurosci	acquired	CT, VBM	Thickness, volume
2004, Chang et al. Neuroreport	congenital	DTI	asymmetry, FA
2009, Wang et al. Chin J Med Img Tech	congenital	DTI	FA
2012, Li et al. Hum Brain Mapp	congenital	DTI	AD, FA, RD
2013, Miao et al. Am J Neuroradiol	congenital	DTI	FA, RD
2014, Lyness et al. Neuroimage	congenital	DTI	FA, MD, RD
2015, Huang et al. PLoS One	congenital	DTI	FA, MD
2016, Chinnadurai et al. Magn Reson Imaging	congenital	DTI	AD, Axial Kurtosis, FA, Mean Kurtosis, Radial Kurtosis, RD
2016, Ma et al. AJNR Am J Neuroradiol	acquired	DTI	AD, FA, MD, RD
2017, Karns et al. Hear Res	congenital	DTI	AD, FA, RD, volume
2017, Kim et al. Neuroreport	congenital	DTI	FA
2017, Shiell & Zatorre. Hear Res	congenital	DTI	AD, MD, RD, volume
2017, Zheng et al. Sci Rep	congenital	DTI	FA, Mean Kurtosis
2018, Benetti et al. Neuroimage	congenital	DTI	AD, FA, RD
2018, Park et al. Biomed Res Int	congenital	DTI	FA
2018, Zou et al. Otol Neurotol	congenital	DTI	AK, FA, MK, RK
2009, Kim et al. Neuroreport	congenital	DTI, VBM	FA, volume
2010, Husain et al. Brain Res	acquired	DTI, VBM	FA, volume
2014, Hribar et al. Hear Res	congenital	DTI, VBM	AD, FA, Thickness
2014, Profant et al. Neuroscience	acquired	DTI, VBM	AD, CT, FA, MD, RD, Surface, volume
2019, Luan et al. Front Neurosci	acquired	DTI, VBM	FA, MD, volume
2000, Bavelier et al. J Neurosci	congenital	VBM	volume
2003, Emmorey et al. PNAS	congenital	VBM	asymmetry, GM+WM, ratio GM/WM, volume
2003, Penhune et al. Neuroimage	congenital	VBM	asymmetry, ratio GM/WM, volume
2006, Kara et al. J Neuroradiol	congenital	VBM	length, Thickness, volume
2007, Meyer et al. Restor Neurol Neurosci	congenital	VBM	volume
2007, Shibata DK. Am J Neuroradiol	congenital	VBM	volume

Source	Etiology	all.techniques	all.measures
2008, Allen et al. J Neurosci	congenital	VBM	asymmetry, ratio GM/WM, Vol proportion, volume
2008, Xia et al. Chin J Med Img Tech	congenital	VBM	volume
2010, Leporé et al. Hum Brain Mapp	congenital	VBM	VBM
2010, Li, et al. J Clin Rad	congenital	VBM	volume
2011, Smith et al. Cereb Cortex	congenital	VBM	asymmetry, ratio GM/WM, volume
2013, Allen et al. Front Neuroanat	congenital	VBM	asymmetry, volume
2013, Boyen et al. Hear Res	acquired	VBM	volume
2013, Li et al. Restor Neurol Neurosci	mixed	VBM	Thickness
2013, Pénicaud et al. Neuroimage	congenital	VBM	volume
2014, Kim et al. Hear Res	congenital	VBM	volume
2014, Lin et al. Neuroimage	acquired	VBM	volume
2014, Olulade et al. J Neurosci	congenital	VBM	volume
2015, Tae Investig Magn Reson Imaging	congenital	VBM	VBM
2016, Amaral et al. Eur J Neurosci	congenital	VBM	asymmetry, Thickness
2016, Shi et al. Neuroreport	congenital	VBM	volume
2016, Wu et al. Brain Res	congenital	VBM	ADC, FA
2018, Alfandari et al. Trends Hear	mixed	VBM	volume
2018, Chen et al. Behav Neurosci	acquired	VBM	volume
2018, Feng et al. PNAS	congenital	VBM	VBM
2018, Kumar U, Mishra M. Brain Res	congenital	VBM	Thickness, VBM
2018, Pereira-Jorge et al. Neural Plast	acquired	VBM	volume
2018, Uchida et al. Front Aging Neurosci	acquired	VBM	volume
2019, Belkhiria et al. Front. Aging Neurosci	acquired	VBM	CT, volume
2019, Ponticorvo et al. Hum Brain Mapp	acquired	VBM	volume
2019, Xu et al. J Magn Reson Imaging	acquired	VBM	volume

Effect size calculation

Effect size direction was directly include in the Cohen's D value by mutipliying by -1 if the effect was decrease and by 1 if it was none of increased. The value of $Cohen'sD$ r_{Y1}, was calculated using the means and standard deviations of two groups (M_1=treatment and M_2=control):

$$Cohen's\ D = \frac{M_1 - M_2}{S_{pooled}}$$

where

$$S_{pooled} = \sqrt{\frac{(n_1 - 1) \times s_1^2 + (n_2 - 1) \times s_2^2}{n_1 + n_2 - 2}}$$

and the effect-size correlation is:

$$r_{Y1} = \frac{d}{\sqrt{d^2 + 4}}$$

We calculate the value of Cohen's d and the effect size correlation, r_{Y1}, using the t test value for a between subjects $t - test$ and the degrees of freedom, the following formula was used:

$$Cohen's\ D = \frac{2t}{\sqrt{df}}\ and\ r_{Y1} = \sqrt{\frac{t^2}{t^2 + df}}$$

Effects were summarized across studies using the generic inverse-variance weighting method with DerSimonian and Laird random effects. Studies were weighted by $1/SE$š (where SE is the standard error). For the effect size we used Hedges'G, wich takes into account the sample size.

$$Hedges'G = \frac{X_1 - X_2}{\sqrt{\frac{(n_1-1)s_1^2+(n_2-1)s_2^2}{n_1+n_2-2}}}$$

Finally, the variance was estimated using the cohen's D and sample size of each study. Our estimated variance was used for all meta-regressions, therefore we could have and additional bias in-between studies variance and heterogeneity calculations. We should have calculated the effect size from the mean and standard deviation from each study. Variance was estimated using the following formula:

$$Variance = \frac{n1 + n2}{n1 \times n2} + \frac{Hedges'G^2}{2 \times (n1 + n2 - 2)}$$

Estimatimation of heterogeneity per model

We estimated heterogeneity in results using the τ statistic, which represents the standard deviation in the meta-regression models, we used the heterogeneity test $x2$ and $I2$.
We performed a multi-level meta-analytic model, over our multiple effect size estimates nested withing variables: Etiology, side and Big brain area. We expected that the underlying true effects are more similar for the same level of the grouping variables than thrue effects arising from different levels.
We can account for the correlation in the true effects by adding a random effect to the model at the level corresponding to the grouping variable.
The dataset contains the result from 54 studies, each comparing different measurements between patients and controls. The diference of between groups was quantified in terms of Hedges'G and Cohen's D.

References (64 bilateral studies)

[1] "Emmorey K, Allen JS, Bruss J, Schenker N, Damasio H., A morphometric analysis of auditory brain regions in congenitally deaf adults., Proc Natl Acad Sci U S A. 2003 Aug 19;100(17):10049-54. , https://doi.org/10.1073/pnas.1730169100, emmorey@salk.edu"
[2] "Allen JS, Emmorey K, Bruss J, Damasio H., Morphology of the insula in relation to hearing status and sign language experience., J Neurosci. 2008 Nov 12;28(46):11900-5., https://doi.org/10.1523/JNEUROSCI.3141-08.2008, kemmorey@mail.sdsu.edu"
[3] "Allen JS, Emmorey K, Bruss J, Damasio H., Neuroanatomical differences in visual, motor, and language cortices between congenitally deaf signers, hearing signers, and hearing non-signers., Front Neuroanat. 2013 Aug 2;7:26., https://doi.org/10.3389/fnana.2013.00026, Hanna Damasio: hdamasio@college.usc.edu; Karen Emmorey: kemmorey@mail.sdsu.edu"
[4] "Shibata DK., Differences in brain structure in deaf persons on MR imaging studied with voxel-based morphometry., AJNR Am J Neuroradiol. 2007 Feb;28(2):243-9. , http://www.ajnr.org/content/28/2/243, shibatad@u.washington.edu"
[5] "Li J, Li W, Xian J, Li Y, Liu Z, Liu S, Wang X, Wang Z, He H., Cortical thickness analysis and optimized voxel-based morphometry in children and adolescents with prelingually profound sensorineural hearing loss., Brain Res. 2012 Jan 9;1430:35-42., https://doi.org/10.1016/j.brainres.2011.09.057, cjr.wzhch@vip.163.com (Z. Wang); huiguang.he@ia.ac.cn (H. He)"
[6] "Miao W, Li J, Tang M, Xian J, Li W, Liu Z, Liu S, Sabel BA, Wang Z, He H., Altered white matter integrity in adolescents with prelingual deafness: A high-resolution tract-based spatial statistics imaging study., AJNR Am J Neuroradiol. 2013 Jun-Jul;34(6):1264-70., https://doi.org/10.3174/ajnr.a3370, huiguang.he@ia.ac.cn & cjr.xianjunfang@vip.163.com"
[7] "Liu Z.-H, Li M, Xian J.-F, He H.-G, Z.-C, Li Y, Li J.-H, Wang X.-C, Liu S., Investigation of the white matter with tract-based spatial statistics in congenitally deaf patients., Chinese Journal of Medical Imaging Technology. 2010: 26(7):1226-1229., www.cjmit.com/cjmit/ch/reader/view_abstract.aspx?flag=1&file_no=20100708&journal_id=cjmit, cjr.xianjunfang@vip.163.com; lzhtrhos@sina.com"
[8] "Li W, Li J, Wang Z, Li Y, Liu Z, Yan F, Xian J, He H., Grey matter connectivity within and between auditory, language and visual systems in prelingually deaf adolescents., Restor Neurol Neurosci. 2015;33(3):279-90., https://doi.org/10.3233/rnn-140437, huiguang.he@ia.ac.cn; cjr.xianjunfang@vip.163.com"
[9] "Wenjing Li, Yong Li, Junxi X, Zhaohui L, Xiaocui W, Sha L, Zhenchang W, Huiguang H., A voxel-based morphometric analysis of brain in congenitally deaf patients., J Clin Rad. 2010; 29(2):166-169., https://doi.org/10.13437/j.cnki.jcr.2010.02.031, wenjing.li@bjut.edu.cn"
[10] "Li W, Li J, Xian J, Lv B, Li M, Wang C, Li Y, Liu Z, Liu S, Wang Z, He H, Sabel BA., Alterations of grey matter asymmetries in adolescents with prelingual deafness: A combined VBM and cortical thickness analysis., Restor Neurol Neurosci. 2013;31(1):1-17., https://doi.org/10.3233/RNN-2012-120269, huiguang.he@ia.ac.cn; cjr.xianjunfang@vip.163.com"
[11] "Meyer M, Toepel U, Keller J, Nussbaumer D, Zysset S, Friederici AD., Neuroplasticity of sign language:

implications from structural and functional brain imaging., Restor Neurol Neurosci. 2007;25(3-4):335-51., https://content.iospress.com/articles/restorative-neurology-and-neuroscience/rnn253415, mmeyer@access.uzh.ch"
[12] "Park KH, Chung WH, Kwon H, Lee JM., Evaluation of cerebral white matter in prelingually deaf children using diffusion tensor imaging., Biomed Res Int. 2018 Feb 4;2018:6795397., https://doi.org/10.1155/2018/6795397, whchung@skku.edu"
[13] "Penhune VB, Cismaru R, Dorsaint-Pierre R, Petitto LA, Zatorre RJ., The morphometry of auditory cortex in the congenitally deaf measured using MRI., Neuroimage. 2003 Oct;20(2):1215-25., https://doi.org/10.1016/s1053-8119(03)00373-2, vpenhune@vax2.concordia.ca"
[14] "Smith KM, Mecoli MD, Altaye M, Komlos M, Maitra R, Eaton KP, Egelhoff JC, Holland SK., Morphometric differences in the Heschl's gyrus of hearing impaired and normal hearing infants., Cereb Cortex. 2011 May;21(5):991-8., https://doi.org/10.1093/cercor/bhq164, scott.holland@cchmc.org"
[15] "Chang Y, Lee SH, Lee YJ, Hwang MJ, Bae SJ, Kim MN, Lee J, Woo S, Lee H, Kang DS., Auditory neural pathway evaluation on sensorineural hearing loss using diffusion tensor imaging., Neuroreport. 2004 Aug 6;15(11):1699-703., https://doi.org/10.1097/01.wnr.0000134584.10207.1a, leeshu@knu.ac.kr"
[16] "Chang Y, Lee HR, Paik JS, Lee KY, Lee SH., Voxel-wise analysis of diffusion tensor imaging for clinical outcome of cochlear implantation: retrospective study., Clin Exp Otorhinolaryngol. 2012 Apr;5 Suppl 1:S37-42., https://doi.org/10.3342/ceo.2012.5.s1.s37, leeshu@knu.ac.kr"
[17] "Shiell MM, Zatorre RJ., White matter structure in the right planum temporale region correlates with visual motion detection thresholds in deaf people., Hear Res. 2017 Jan;343:64-71., https://doi.org/10.1016/j.heares.2016.06.011, martha.shiell@mail.mcgill.ca; Robert.Zatorre@mcgill.ca"
[18] "Shiell MM, Champoux F, Zatorre RJ., The right hemisphere planum temporale supports enhanced visual motion detection ability in deaf people the right hemisphere planum temporale supports enhanced visual motion detection ability in deaf people., Neural Plasticity 2016: 7217630., https://doi.org/10.1155/2016/7217630, francois.champoux@umontreal.ca; martha.shiell@mail.mcgill.ca; Robert.Zatorre@mcgill.ca"
[19] "Kim DJ, Park SY, Kim J, Lee DH, Park HJ., Alterations of white matter diffusion anisotropy in early deafness., Neuroreport. 2009 Jul 15;20(11):1032-6., https://doi.org/10.1097/wnr.0b013e32832e0cdd, parkhj@yuhs.ac; hjpark0@gmail.com"
[20] "Kim J, Choi JY, Eo J, Park HJ., Comparative evaluation of the white matter fiber integrity in patients with prelingual and postlingual deafness., Neuroreport. 2017 Nov 8;28(16):1103-1107, https://doi.org/10.1097/wnr.0000000000000894, parkhj@yuhs.ac; hjpark0@gmail.com"
[21] "Amaral L, Ganho-Ávila A, Osório A, Soares MJ, He D, Chen Q, Mahon BZ, Gonçalves OF, Sampaio A, Fang F, Bi Y, Almeida J., Hemispheric asymmetries in subcortical visual and auditory relay structures in congenital deafness., Eur J Neurosci. 2016 Sep;44(6):2334-9., https://doi.org/10.1111/ejn.13340, Jorge Almeida: jorgealmeida@fpce.uc.pt"
[22] "Lyness RC, Alvarez I, Sereno MI, MacSweeney M., Microstructural differences in the thalamus and thalamic radiations in the congenitally deaf., Neuroimage. 2014 Oct 15;100:347-57., https://doi.org/10.1016/j.neuroimage.2014.05.077, c.rebeccalyness@gmail.com"
[23] "Karns CM, Stevens C, Dow MW, Schorr EM, Neville HJ., Atypical white-matter microstructure in congenitally deaf adults: A region of interest and tractography study using diffusion-tensor imaging., Hear Res. 2017 Jan;343:72-82., https://doi.org/10.1016/j.heares.2016.07.008, ckarns@uoregon.edu"
[24] "Hribar M, Suput D, Carvalho AA, Battelino S, Vovk A., Structural alterations of brain grey and white matter in early deaf adults., Hear Res. 2014 Dec;318:1-10., https://doi.org/10.1016/j.heares.2014.09.008, andrej.vovk@mf.uni-lj.s"
[25] "Huang L, Zheng W, Wu C, Wei X, Wu X, Wang Y, Zheng H., Diffusion tensor imaging of the auditory neural pathway for clinical outcome of cochlear implantation in pediatric congenital sensorineural hearing loss patients., PLoS One. 2015 Oct 20;10(10):e0140643., https://doi.org/10.1371/journal.pone.0140643, hwenb@126.com"
[26] "Olulade OA, Koo DS, LaSasso CJ, Eden GF., Neuroanatomical profiles of deafness in the context of native language experience., J Neurosci. 2014 Apr 16;34(16):5613-20., https://doi.org/10.1523/jneurosci.3700-13.2014, edeng@georgetown.edu"
[27] "Wu C, Huang L, Tan H, Wang Y, Zheng H, Kong L, Zheng W., Diffusion tensor imaging and MR spectroscopy of microstructural alterations and metabolite concentration changes in the auditory neural pathway of pediatric congenital sensorineural hearing loss patients., Brain Res. 2016 May 15;1639:228-34., https://doi.org/10.1016/j.brainres.2014.12.025, hwenb@126.com"
[28] "Kim E, Kang H, Lee H, Lee HJ, Suh MW, Song JJ, Oh SH, Lee DS., Morphological brain network assessed using graph theory and network filtration in deaf adults., Hear Res. 2014 Sep;315:88-98., https://doi.org/10.1016/j.heares.2014.06.007, shaoh@snu.ac.kr; dsl@plaza.snu.ac.kr"
[29] "Pénicaud S, Klein D, Zatorre RJ, Chen JK, Witcher P, Hyde K, Mayberry RI., Structural brain changes linked to delayed first language acquisition in congenitally deaf individuals., Neuroimage. 2013 Feb 1;66:42-9., https://doi.org/10.1016/j.neuroimage.2012.09.076, sidonie.p@gmail.com (S. Pénicaud); denise.klein@mcgill.ca (D. Klein); robert.zatorre@mcgill.ca (R.J. Zatorre); jen-kai.chen@mcgill.ca (J.-K. Chen); krista.hyde@mail.mcgill.ca (K. Hyde); rmayberry@ucsd.edu (R.I. Mayberry)" [30] "Chinnadurai V, Sreedhar CM, Khushu S., Assessment of cochlear nerve deficiency and its effect on normal maturation of auditory tract by diffusion kurtosis imaging and diffusion tensor imaging: A correlational approach., Magn Reson Imaging. 2016 Nov;34(9):1305-1313., https://doi.org/10.1016/j.mri.2016.07.010, vijayakumar@inmas.drdo.in; vijayininmas@gmail.com"
[31] "Kara A, Hakan Ozturk A, Kurtoglu Z, Umit Talas D, Aktekin M, Saygili M, Kanik A., Morphometric comparison of the human corpus callosum in deaf and hearing subjects: An MRI study., J Neuroradiol. 2006 Jun;33(3):158-63., https://doi.org/10.1016/s0150-9861(06)77253-4, alevkara@mersin.edu.tr"
[32] "Xia S, Qi J, Li Q., High-resolution MR study of auditory cortex in prelingual sensorineural hearing loss., Chinese Journal of Medical Imaging Technology. 2008; 24(11):1705-1707., http://www.cjmit.com/cjmit/ch/reader/view_abstract.aspx?flag=1&file_no=20081111&journal_id=cjmit, xiashuang77@163.com; cjr.qiji@vip.163.com"
[33] "Benetti S, Novello L, Maffei C, Rabini G, Jovicich J, Collignon O., White matter connectivity between occipital and temporal regions involved in face and voice processing in hearing and early deaf individuals., Neuroimage. 2018 Oct 1;179:263-274., https://doi.org/10.1016/j.neuroimage.2018.06.044, stefania.benetti@unitn.it; olivier.collignon@uclouvain.be"

[34] “Wang S, Li Y.-H, Zhou Y, Yu C.-S, Xu C.-L, Qin W, Liu Y, Jiang T.-Z., Diffusion tensor imaging observation of brain white matter in congenitally deaf., Chinese Journal of Medical Imaging Technology. 2009: 25(4):585-587., http://www.cjmit.com/cjmit/ch/reader/view_abstract.aspx?flag=1&file_no=20090418&journal_id=cjmit, wang_sh2006@lzu.cn; jiangtz@nlpr.ia.ac.cn”
[35] “Tae, W.-S. 2015., Reduced gray matter volume of auditory cortical and subcortical areas in congenitally deaf adolescents: A voxel-based morphometric study., Investig Magn Reson Imaging 19, 1-9., https://doi.org/10.13104/imri.2015.19.1.1, wstae@kangwon.ac.kr”
[36] “Feng G, Ingvalson EM, Grieco-Calub TM, Roberts MY, Ryan ME, Birmingham P, Burrowes D, Young NM, Wong PCM., Neural preservation underlies speech improvement from auditory deprivation in young cochlear implant recipients., Proc Natl Acad Sci U S A. 2018 Jan 30;115(5):E1022-E1031., https://doi.org/10.1073/pnas.1717603115, p.wong@cuhk.edu.hk”
[37] “Kumar U, Mishra M., Pattern of neural divergence in adults with prelingual deafness: Based on structural brain analysis., Brain Res. 2018 Jul 23. pii: S0006-8993(18)30405-0., https://doi.org/10.1016/j.brainres.2018.07.021, uttam@cbmr.res.in”
[38] “Leporé N, Vachon P, Lepore F, Chou YY, Voss P, Brun CC, Lee AD, Toga AW, Thompson PM., 3D mapping of brain differences in native signing congenitally and prelingually deaf subjects., Hum Brain Mapp. 2010 Jul;31(7):970-8., https://doi.org/10.1002/hbm.20910, nlepore@loni.ucla.edu”
[39] “Li Y, Ding G, Booth JR, Huang R, Lv Y, Zang Y, He Y, Peng D., Sensitive period for white-matter connectivity of superior temporal cortex in deaf people., Hum Brain Mapp. 2012 Feb;33(2):349-59., https://doi.org/10.1002/hbm.21215, Dinggsh@bnu.edu.cn; pdl3507@bnu.edu.cn”
[40] “Zheng W, Wu C, Huang L, Wu R., Diffusion kurtosis imaging of microstructural alterations in the brains of paediatric patients with congenital sensorineural hearing loss., Sci Rep 2017 May 8. 7;1543., https://doi.org/10.1038/s41598-017-01263-9, rhwu@stu.edu.cn”
[41] “Alfandari D, Vriend C, Heslenfeld DJ, Versfeld NJ, Kramer SE, Zekveld AA., Brain volume differences associated with hearing impairment in adults., Trends Hear. 2018 Jan-Dec;22:1-8., https://doi.org/10.1177/2331216518763689 , aa.zekveld@vumc.nl”
[42] “Ponticorvo S, Manara R, Pfeuffer J, Cappiello A, Cuoco S, Pellecchia MT, Saponiero R, Troisi D, Cassandro C, John M, Scarpa A, Cassandro E, Di Salle F, Esposito F., Cortical pattern of reduced perfusion in hearing loss revealed by ASL-MRI., Hum Brain Mapp. 2019 Feb 4., https://doi.org/10.1002/hbm.24538, faesposito@unisa.it”
[43] “Shi B, Yang LZ, Liu Y, Zhao SL, Wang Y, Gu F, Yang Z, Zhou Y, Zhang P, Zhang X., Early-onset hearing loss reorganizes the visual and auditory network in children without cochlear implantation., Neuroreport. 2016 Feb 10;27(3):197-202., https://doi.org/10.1097/wnr.0000000000000524, felice828@126.com”
[44] “Pereira-Jorge MR, Andrade KC, Palhano-Fontes FX, Diniz PRB, Sturzbecher M, Santos AC, Araujo DB., Anatomical and functional MRI changes after one year of auditory rehabilitation with hearing aids., Neural Plast. 2018 Sep 10;2018:9303674., https://doi.org/10.1155/2018/9303674 , draulio@neuro.ufrn.br”
[45] “Peelle JE, Troiani V, Grossman M, Wingfield A., Hearing loss in older adults affects neural systems supporting speech comprehension., J Neurosci. 2011 Aug 31;31(35):12638-43. , https://doi.org/10.1523/jneurosci.2559-11.2011, peelle@gmail.com”
[46] “Ren F, Ma W, Li M, Sun H, Xin Q, Zong W, Chen W, Wang G, Gao F, Zhao B., Gray matter atrophy is associated with cognitive impairment in patients with presbycusis: A comprehensive morphometric study., Front Neurosci. 2018 Oct 23;12:744., https://doi.org/10.3389/fnins.2018.00744, Fei Gao: feigao6262@163.com; Bin Zhao: qpqpoo6262@163.com”
[47] “Eckert MA, Cute SL, Vaden KI Jr, Kuchinsky SE, Dubno JR., Auditory cortex signs of age-related hearing loss., J Assoc Res Otolaryngol. 2012 Oct;13(5):703-13., https://doi.org/10.1007/s10162-012-0332-5, eckert@musc.edu”
[48] “Boyen K, Langers DR, de Kleine E, van Dijk P., Gray matter in the brain: Differences associated with tinnitus and hearing loss., Hear Res. 2013 Jan;295:67-78., https://doi.org/10.1016/j.heares.2012.02.010, k.boyen@umcg.nl (K. Boyen), d.r.m.langers@umcg.nl, (D.R.M. Langers), e.de.kleine@umcg.nl (E. de Kleine), p.van.dijk@umcg.nl (P. van Dijk)”
[49] “Luan Y, Wang C, Jiao Y, Tang T, Zhang J, Teng GJ., Prefrontal-temporal pathway mediates the cross-modal and cognitive reorganization in sensorineural hearing loss with or without tinnitus: A multimodal MRI study., Front Neurosci. 2019 Mar 12;13:222., https://doi.org/10.3389/fnins.2019.00222, gjteng@vip.sina.com”
[50] “Belkhiria C, Vergara RC, Martín SS, Leiva A, Marcenaro B, Martínez M, Delgado C, Delano PH., Cingulate cortex atrophy is associated with hearing loss in presbycusis with cochlear amplifier dysfunction., Front. Aging Neurosci., 26 April 2019, https://doi.org/10.3389/fnagi.2019.00097, pdelano@med.uchile.cl; phdelano@gmail.com”
[51] “Uchida Y, Nishita Y, Kato T, Iwata K, Sugiura S, Suzuki H, Sone M, Tange C, Otsuka R, Ando F, Shimokata H, Nakamura A., Smaller hippocampal volume and degraded peripheral hearing among Japanese community dwellers., Front Aging Neurosci. 2018 Oct 16;10:319., https://doi.org/10.3389/fnagi.2018.00319, yasueu@aichi-med-u.ac.jp”
[52] “Chen YC, Chen H, Jiang L, Bo F, Xu JJ, Mao CN, Salvi R, Yin X, Lu G, Gu JP., Presbycusis disrupts spontaneous activity revealed by resting-state functional MRI., Front Behav Neurosci. 2018 Mar 13;12:44., https://doi.org/10.3389/fnbeh.2018.00044 , Guangming Lu; cjr.luguangming@vip.163.com; Jian-Ping Gu; cjr.gujianping@vip.163.com”
[53] “Rigters SC, Bos D, Metselaar M, Roshchupkin GV, Baatenburg de Jong RJ, Ikram MA, Vernooij MW, Goedegebure A., Hearing impairment is associated with smaller brain volume in aging., Front Aging Neurosci. 2017 Jan 20;9:2, https://doi.org/10.3389/fnagi.2017.00002 , s.rigters@erasmusmc.nl”
[54] “Zou Y, Yang Y, Fan W, Yu Q, Wang M, Han P, Ma H., Microstructural alterations in the brains of adults with prelingual sensorineural hearing loss: A diffusion kurtosis imaging study., Otol Neurotol. 2018 Dec;39(10):e936-e943., https://doi.org/10.1097/mao.0000000000002000, cjr.hanping@vip.163.com; 1363191284@qq.com”
[55] “Smittenaar CR, MacSweeney M, Sereno MI, Schwarzkopf DS., Does congenital deafness affect the structural and functional architecture of primary visual cortex?, Open Neuroimag J. 2016 Feb 29;10:1-19., https://doi.org/10.2174/1874440001610010001, c.rebeccalyness@gmail.com”
[56] “Bavelier D, Tomann A, Hutton C, Mitchell T, Corina D, Liu G, Neville H., Visual attention to the periphery is enhanced in congenitally deaf individuals., J Neurosci. 2000 Sep 1;20(17):RC93., https://doi.org/10.1523/JNEUROSCI.20-17-j0001.2000 , daphne@bcs.rochester.edu”
[57] “Husain FT, Medina RE, Davis CW, Szymko-Bennett Y, Simonyan K, Pajor NM, Horwitz B., Neuroanatomical

changes due to hearing loss and chronic tinnitus: a combined VBM and DTI study., Brain Res. 2011 Jan 19;1369:74-88., https://doi.org/10.1016/j.brainres.2010.10.095, husainf@illinois.edu"
[58] "Xu XM, Jiao Y, Tang TY, Zhang J, Lu CQ, Salvi R, Teng GJ., Sensorineural hearing loss and cognitive impairments: Contributions of thalamus using multiparametric MRI., J Magn Reson Imaging. 2019 Jan 29., https://doi.org/10.1002/jmri.26665, gjteng@seu.edu.cn"
[59] "Profant O, Škoch A, Balogová Z, Tintěra J, Hlinka J, Syka J., Diffusion tensor imaging and MR morphometry of the central auditory pathway and auditory cortex in aging. Diffusion tensor imaging and MR morphometry of the central auditory pathway and auditory cortex in aging., Neuroscience. 2014 Feb 28;260:87-97., https://doi.org/10.1016/j.neuroscience.2013.12.010, profant@biomed.cas.cz"
[60] "Lin FR, Ferrucci L, An Y, Goh JO, Doshi J, Metter EJ, Davatzikos C, Kraut MA, Resnick SM., Association of hearing impairment with brain volume changes in older adults., Neuroimage. 2014 Apr 15;90:84-92., https://doi.org/10.1016/j.neuroimage.2013.12.059, flin1@jhmi.edu"
[61] "Eckert MA, Kuchinsky SE, Vaden KI, Cute SL, Spampinato MV, Dubno JR., White matter hyperintensities predict low frequency hearing in older adults., J Assoc Res Otolaryngol. 2013 Jun;14(3):425-33., https://doi.org/10.1007/s10162-013-0381-4, eckert@musc.edu"
[62] "Rigters SC, Cremers LGM, Ikram MA, van der Schroeff MP, de Groot M, Roshchupkin GV, Niessen WJN, Baatenburg de Jong RJ, Goedegebure A, Vernooij MW., White-matter microstructure and hearing acuity in older adults: a population-based cross-sectional DTI study., Neurobiol Aging. 2018 Jan;61:124-131., https://doi.org/10.1016/j.neurobiolaging.2017.09.018, s.rigters@erasmusmc.nl"
[63] "Qian ZJ, Chang PD, Moonis G, Lalwani AK., A novel method of quantifying brain atrophy associated with age-related hearing loss., Neuroimage Clin. 2017 Jul 24;16:205-209., https://doi.org/10.1016/j.nicl.2017.07.021, anil.lalwani@columbia.edu"
[64] "Ma W, Li M, Gao F, Zhang X, Shi L, Yu L, Zhao B, Chen W, Wang G, Wang X., DTI analysis of presbycusis using voxel-based analysis., AJNR Am J Neuroradiol. 2016 Nov;37(11):2110-2114., https://doi.org/10.3174/ajnr.A4870, wgb7932596@hotmail.com"

Unilateral hearing loss (total n=8)

- VBM studies
    1. Fan et al. Otol Neurotol. 2015 Dec;36(10):1622-7. (Unilateral SNHL adult mixed cause) –VBM –SPM
    2. Yang et al. Hear Res. 2014 Oct;316:37-43. (Right unilateral SHNL adult) –SPM – VBM
    3. Wang et al. Sci Rep. 2016 May 13;6:25811.(Adult acquired unilateral) SPM -VBM
- DTI
    1. Wu et al. AJNR Am J Neuroradiol. 2009 Oct;30(9):1773-7. (Congenital Unilateral deaf children) - DTI-Studio
    2. Lin et al. J Magn Reson Imaging. 2008 Sep;28(3):598-603. (Bilateral and unilateral SNHL Adult) - DTI-Studio
    3. Rachakonda et al. Front Syst Neurosci. 2014 May 26;8:87. (Unilateral left and right, adolescent) – Not indicated
    4. Wu et al. Audiol Neurootol. 2009;14(4):248-53. (Unilateral mixed left/right SNHL mixed congenital/unknown adult)-DTI Studio
    5. Vos et al. Hear Res. 2015 May;323:1-8. (Unilateral mixed left and right SNHL adult) – DTI Tractography - ExploreDTI

Signed differential mapping (SDM) table

SDM: congenital

MNI.coordinate	SDM.Z	P	Voxels	Description	Direction
-8,52,-20	4.350	0.0000068	916	Left gyrus rectus, BA 11	positive
-16,-100,-6	3.835	0.0000628	950	Left calcarine fissure / surrounding cortex, BA 17	positive
-22,-38,60	3.621	0.0001470	755	(undefined), BA 3	positive
26,-76,38	3.187	0.0007187	508	Right superior occipital gyrus, BA 19	positive
30,-32,56	3.494	0.0002378	457	Right postcentral gyrus, BA 3	positive
-8,38,12	3.387	0.0003530	419	Left anterior cingulate / paracingulate gyri, BA 32	positive
-4,-28,32	2.901	0.0018615	399	Left median cingulate / paracingulate gyri, BA 23	positive
62,2,10	2.817	0.0024230	319	Right rolandic operculum, BA 6	positive
14,-44,-10	3.679	0.0001172	259	Right cerebellum, hemispheric lobule IV / V, BA 30	positive
-8,-52,-8	2.704	0.0034276	287	Left cerebellum, hemispheric lobule IV / V, BA 18	positive
-26,-92,20	3.424	0.0003090	240	Left middle occipital gyrus, BA 18	positive
8,-72,22	2.994	0.0013756	102	Corpus callosum	positive
-42,-36,22	2.463	0.0068921	70	Left superior temporal gyrus, BA 48	positive
-56,10,30	2.664	0.0038628	52	Left precentral gyrus, BA 44	positive
-18,40,30	2.625	0.0043344	36	Corpus callosum	positive
44,-4,-10	1.938	0.0263297	39	Right superior temporal gyrus	positive
-32,-16,-12	2.134	0.0164014	35	Corpus callosum	positive
62,-32,-6	2.029	0.0212226	33	Right middle temporal gyrus, BA 21	positive
36,-22,-14	2.677	0.0037128	24	Right hippocampus, BA 20	positive
6,-34,56	1.959	0.0250691	21	Right paracentral lobule	positive
-26,20,-16	2.194	0.0141032	19	Left frontal orbito-polar tract	positive
-22,40,36	1.988	0.0234269	8	Left superior frontal gyrus, dorsolateral, BA 9	positive
34,-68,-46	1.865	0.0311240	7	Right cerebellum, hemispheric lobule VIIB	positive
-36,-10,-42	1.762	0.0390477	2	Left inferior temporal gyrus, BA 20	positive
-18,42,40	1.660	0.0484373	2	Left superior frontal gyrus, dorsolateral, BA 9	positive
52,2,-4	1.673	0.0471951	1	Right superior temporal gyrus, BA 38	positive
-20,46,36	1.670	0.0475018	1	Left superior frontal gyrus, dorsolateral, BA 9	positive
52,-14,-10	1.655	0.0489883	1	Right superior temporal gyrus, BA 22	positive
8,-54,-38	-2.751	0.0029747	714	Right cerebellum, hemispheric lobule IX	negative
-50,-16,-14	-3.909	0.0000463	521	Left middle temporal gyrus, BA 20	negative
42,12,-34	-3.013	0.0012935	323	Right temporal pole, middle temporal gyrus, BA 20	negative
-6,26,44	-3.092	0.0009937	214	Left superior frontal gyrus, medial, BA 8	negative
-48,-52,40	-2.485	0.0064724	223	Left inferior parietal (excluding supramarginal and angular) gyri, BA 40	negative
-44,8,-30	-2.333	0.0098195	190	Left temporal pole, middle temporal gyrus, BA 20	negative
16,-12,-10	-2.861	0.0021141	164	Right cortico-spinal projections	negative
38,-22,36	-3.305	0.0004744	149	Right superior longitudinal fasciculus III	negative
46,-58,42	-3.349	0.0004056	141	Right angular gyrus, BA 39	negative
-20,-54,12	-3.587	0.0001674	109	Corpus callosum	negative
-36,32,18	-3.168	0.0007666	123	Left inferior frontal gyrus, triangular part, BA 48	negative
22,36,48	-4.063	0.0000243	103	Right superior frontal gyrus, dorsolateral, BA 9	negative
-46,-6,-26	-2.997	0.0013640	97	Left inferior network, inferior longitudinal fasciculus	negative
-4,-32,22	-2.655	0.0039663	100	Corpus callosum	negative
-14,-66,-32	-2.564	0.0051706	68	(undefined)	negative
-30,-58,-58	-2.242	0.0124691	60	Left cerebellum, hemispheric lobule VIII	negative
28,42,28	-2.263	0.0118076	52	Right middle frontal gyrus, BA 46	negative
-46,-70,-46	-2.622	0.0043685	37	Left cerebellum, crus II	negative
26,-12,-2	-2.269	0.0116403	42	Right cortico-spinal projections	negative
4,-54,18	-2.683	0.0036445	31	Right precuneus, BA 30	negative
-54,-26,26	-2.386	0.0085091	28	Left superior longitudinal fasciculus III	negative
44,12,54	-2.203	0.0137867	25	Right middle frontal gyrus, BA 9	negative
44,6,20	-2.171	0.0149726	24	Right superior longitudinal fasciculus III	negative
10,-70,40	-1.972	0.0242994	23	Right precuneus, BA 7	negative
-40,-48,58	-2.064	0.0195199	17	Left inferior parietal (excluding supramarginal and angular) gyri, BA 40	negative
-30,-66,-48	-1.896	0.0289586	18	Left cerebellum, hemispheric lobule VIII	negative
0,-66,-10	-1.927	0.0269926	11	Cerebellum, vermic lobule VI	negative
34,-10,50	-1.989	0.0233668	10	Right superior longitudinal fasciculus II	negative
-2,26,-10	-1.831	0.0335253	9	Left anterior cingulate / paracingulate gyri, BA 11	negative
12,-80,48	-1.879	0.0301139	7	Right precuneus, BA 7	negative
60,-44,32	-1.917	0.0275989	7	Right supramarginal gyrus, BA 40	negative

MNI.coordinate	SDM.Z	P	Voxels	Description	Direction
24,-26,4	-1.898	0.0288799	7	Corpus callosum	negative
18,32,28	-1.950	0.0255769	4	Corpus callosum	negative
-26,-4,-16	-1.954	0.0253757	4	Left amygdala, BA 34	negative
-44,6,28	-1.778	0.0377381	4	Left inferior frontal gyrus, opercular part, BA 44	negative
40,-18,24	-1.931	0.0267345	3	Right superior longitudinal fasciculus III	negative
4,-66,-16	-1.760	0.0392402	3	Cerebellum, vermic lobule VI	negative
56,-38,24	-1.697	0.0448450	3	Right supramarginal gyrus, BA 48	negative
-42,4,22	-1.716	0.0430821	3	Left superior longitudinal fasciculus III	negative
-10,32,-10	-1.785	0.0371427	2	Left anterior cingulate / paracingulate gyri, BA 11	negative
-56,-46,38	-1.738	0.0411224	2	Left inferior parietal (excluding supramarginal and angular) gyri, BA 40	negative
42,-16,-10	-1.696	0.0449376	2	Right inferior network, inferior longitudinal fasciculus	negative
10,-80,38	-1.674	0.0471122	2	Right cuneus cortex, BA 19	negative
-32,-8,-28	-1.870	0.0307359	1	Left inferior network, inferior longitudinal fasciculus	negative
-18,-42,8	-1.828	0.0338045	1	Corpus callosum	negative
-24,-2,-28	-1.803	0.0357051	1	Left amygdala, BA 28	negative
-30,-52,-8	-1.784	0.0372359	1	Left fusiform gyrus, BA 37	negative
-18,-36,-8	-1.782	0.0373835	1	Left median network, cingulum	negative
-30,-64,10	-1.738	0.0410686	1	Corpus callosum	negative
-24,-32,-14	-1.723	0.0424798	1	Left median network, cingulum	negative
10,-82,44	-1.679	0.0466105	1	Right cuneus cortex, BA 19	negative
20,-6,-20	-1.666	0.0478409	1	Right hippocampus, BA 28	negative
34,28,40	-1.654	0.0490536	1	Right middle frontal gyrus, BA 9	negative

SDM: acquired

MNI.coordinate	SDM.Z	P	Voxels	Description	Direction
60,-24,16	3.668	0.0001223	651	Right superior temporal gyrus, BA 42	positive
52,-60,4	2.650	0.0040274	109	Right middle temporal gyrus, BA 37	positive
-44,-10,6	-2.782	0.0027017	858	Left rolandic operculum, BA 48	negative
6,-34,34	-1.853	0.0319374	65	Right median cingulate / paracingulate gyri, BA 23	negative
-54,-30,16	-1.663	0.0481477	1	Left superior temporal gyrus, BA 42	negative

SDM: pediatric

MNI.coordinate	SDM.Z	P	Voxels	Description	Direction
-6,-32,32	3.238	0.0006011	586	Left median network, cingulum	positive
26,-78,36	3.087	0.0010125	471	Right superior occipital gyrus, BA 19	positive
-10,52,-2	2.958	0.0015498	144	Left superior frontal gyrus, medial orbital, BA 10	positive
-18,-98,-6	2.835	0.0022947	131	Left calcarine fissure / surrounding cortex, BA 18	positive
6,-36,56	2.455	0.0070484	138	Right paracentral lobule	positive
-2,42,8	2.298	0.0107808	90	Left anterior cingulate / paracingulate gyri, BA 32	positive
-2,42,-22	2.094	0.0181222	26	Left gyrus rectus, BA 11	positive
-2,46,-26	1.726	0.0421527	1	Left gyrus rectus, BA 11	positive
10,52,-16	1.645	0.0499467	1	Corpus callosum	positive
46,-54,42	-3.111	0.0009324	269	Right inferior parietal (excluding supramarginal and angular) gyri, BA 40	negative
-48,-22,0	-3.096	0.0009812	211	Corpus callosum	negative
52,-24,2	-1.825	0.0340229	9	Corpus callosum	negative
-44,-16,-16	-1.789	0.0368080	6	Left inferior network, inferior longitudinal fasciculus	negative

SDM: adult

MNI.coordinate	SDM.Z	P	Voxels	Description	Direction
58,-2,-10	2.524	0.0057985	301	Right superior temporal gyrus, BA 21	positive
-22,-36,60	2.796	0.0025855	288	Left postcentral gyrus, BA 3	positive
44,12,-34	-2.342	0.0095819	84	Right temporal pole, middle temporal gyrus, BA 20	negative
-38,34,18	-2.212	0.0134751	30	Left inferior frontal gyrus, triangular part, BA 45	negative
-44,6,-30	-1.906	0.0283524	23	Left middle temporal gyrus, BA 20	negative
-58,-20,-14	-1.773	0.0380803	6	Left middle temporal gyrus, BA 21	negative

SDM: AgedAdult

MNI.coordinate	SDM.Z	P	Voxels	Description	Direction
58,-16,6	3.210	0.0006627	1782	Right superior temporal gyrus, BA 48	positive
54,-60,4	3.121	0.0009015	461	Right middle temporal gyrus	positive
16,-74,40	2.492	0.0063471	198	Right precuneus, BA 19	positive
14,-8,-8	2.328	0.0099693	36	Right cortico-spinal projections	positive
-10,42,-20	2.097	0.0180048	29	Left gyrus rectus, BA 11	positive
36,-44,-14	1.823	0.0341623	7	Right inferior network, inferior longitudinal fasciculus	positive
42,16,30	1.828	0.0337837	6	Right inferior frontal gyrus, opercular part, BA 44	positive
-4,-60,38	1.683	0.0462278	2	Left precuneus	positive
48,-10,-12	1.677	0.0467685	1	Right superior temporal gyrus, BA 48	positive
38,14,28	1.659	0.0485649	1	Right inferior frontal gyrus, opercular part, BA 48	positive
50,-16,-10	1.646	0.0498625	1	Right middle temporal gyrus, BA 48	positive
-32,-6,12	-1.738	0.0411015	6	Left insula, BA 48	negative
-32,-10,6	-1.736	0.0412629	4	(undefined), BA 48	negative
-34,-10,16	-1.717	0.0430003	3	Left insula, BA 48	negative
-28,-14,10	-1.691	0.0454556	3	Left striatum	negative

SDM: GM

MNI.coordinate	SDM.Z	P	Voxels	Description	Direction
62,-12,8	3.709	0.0001041	1093	Right superior temporal gyrus, BA 22	positive
-4,-90,8	2.378	0.0087125	198	Left calcarine fissure / surrounding cortex, BA 18	positive
22,-74,40	2.735	0.0031158	127	Right superior occipital gyrus, BA 7	positive
-10,-32,36	2.402	0.0081576	123	Left median network, cingulum	positive
-6,42,-20	2.746	0.0030164	100	Corpus callosum	positive
54,-62,4	2.426	0.0076259	58	Right middle temporal gyrus, BA 37	positive
0,-36,54	1.807	0.0353866	5	Left paracentral lobule	positive
-8,-96,-2	1.655	0.0489485	1	Left calcarine fissure / surrounding cortex, BA 17	positive
-4,24,44	-2.476	0.0066513	41	Left superior frontal gyrus, medial, BA 8	negative

SDM: WM

MNI.coordinate	SDM.Z	P	Voxels	Description	Direction
62,-14,-18	2.769	0.0028142	586	Right middle temporal gyrus, BA 21	positive
-22,-36,60	2.695	0.0035164	258	Left postcentral gyrus, BA 3	positive
10,38,10	2.847	0.0022033	142	Right median network, cingulum	positive
-14,56,-2	2.255	0.0120670	19	Corpus callosum	positive
44,-4,-10	1.788	0.0369088	6	Right superior temporal gyrus	positive
-50,-16,-14	-2.681	0.0036704	456	Left middle temporal gyrus, BA 20	negative
6,-64,-42	-2.665	0.0038518	240	Cerebellum, vermic lobule VIII	negative
-14,-64,-30	-3.205	0.0006742	176	(undefined)	negative
44,12,-34	-2.435	0.0074469	78	Right temporal pole, middle temporal gyrus, BA 20	negative
-38,34,18	-2.416	0.0078490	40	Left inferior frontal gyrus, triangular part, BA 45	negative
-2,-30,22	-2.348	0.0094253	39	Corpus callosum	negative
-38,-16,18	-1.811	0.0350648	4	Left rolandic operculum, BA 48	negative

Studies characteristics

Relation between hearing loss (dB) and age (Figure 2.D)

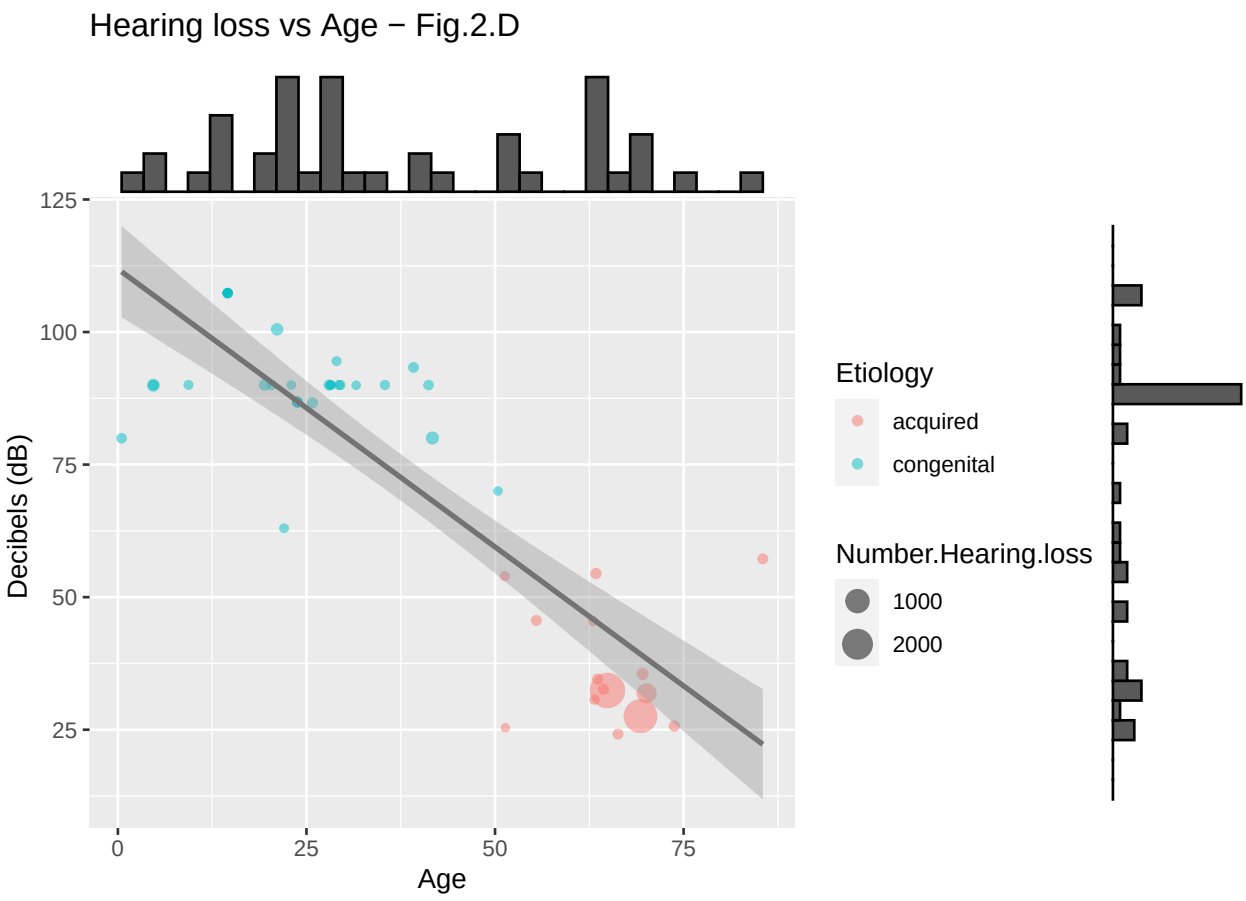

Studies characteristics (Figure 2.E, 2.F)

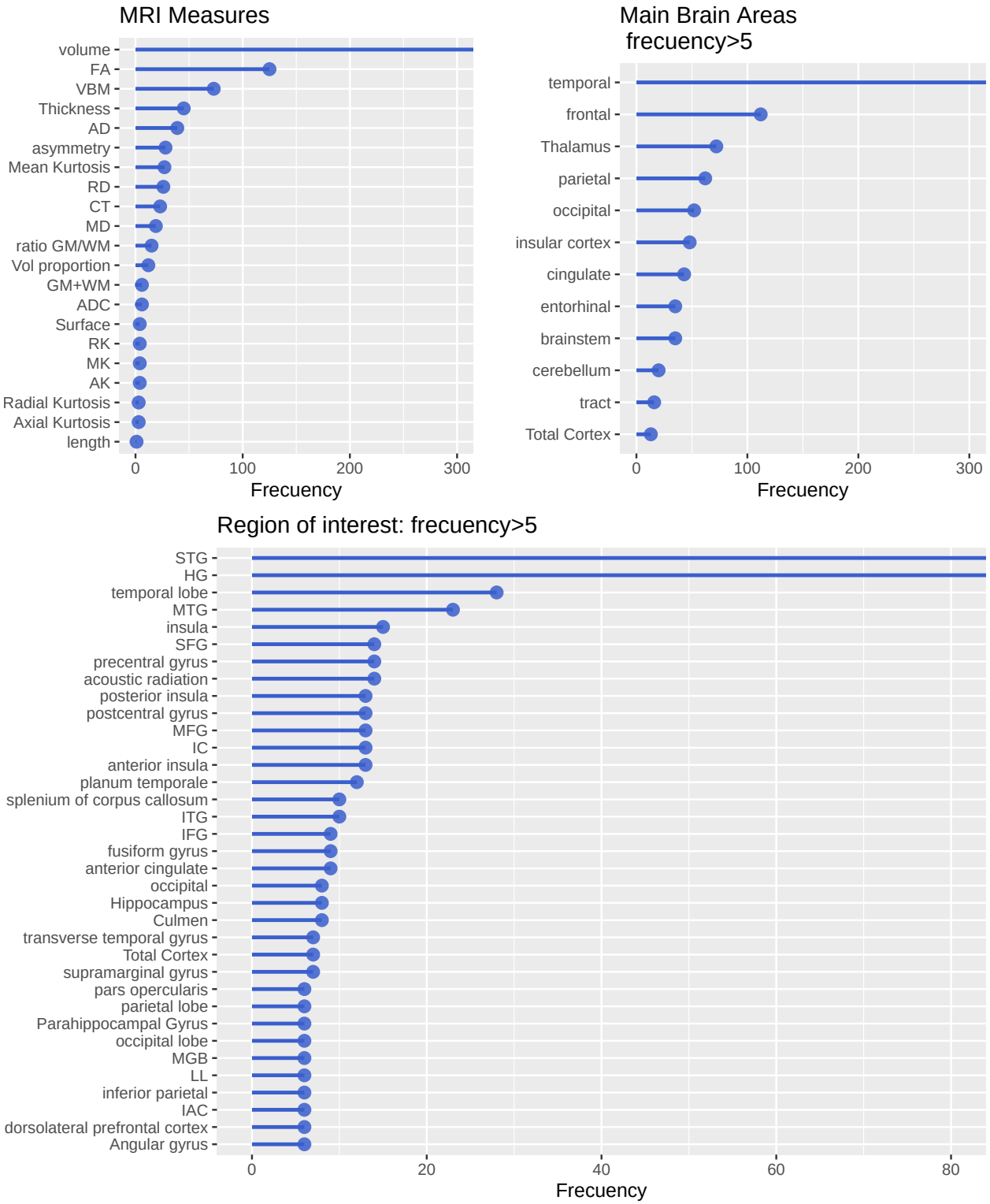

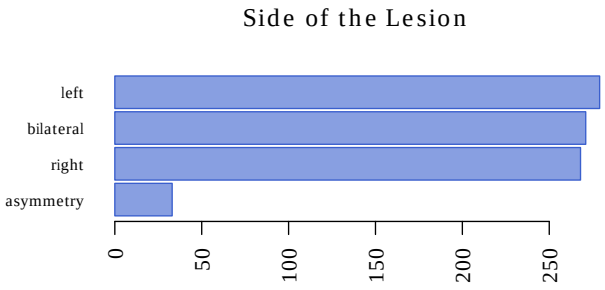

Fig.2.E − Severity

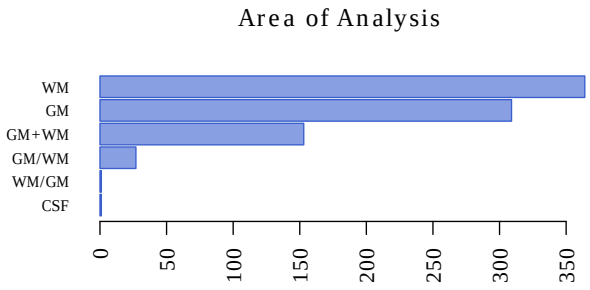

Fig.2.F − Effect direction

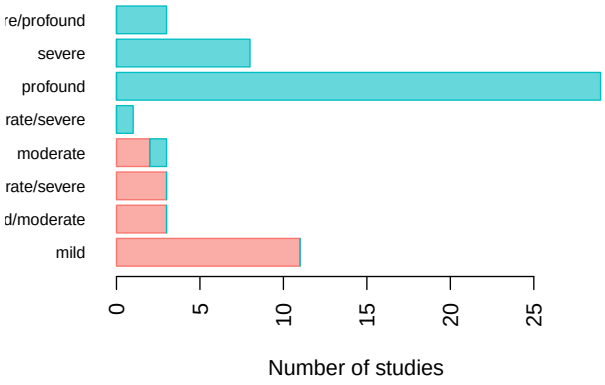

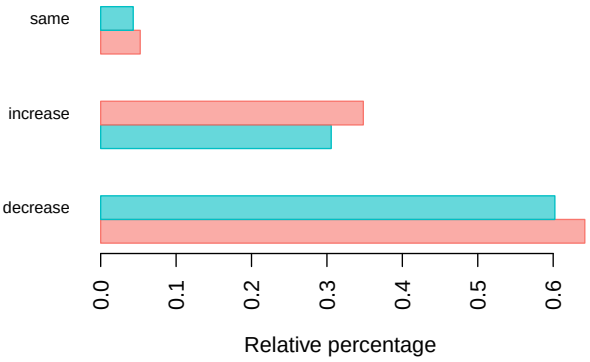

Brain structure (GM, WM) and MRI measures

Highlights
a. Most of the studies that measured Gray matter focus on cortical changes (volume, thicknes and VBM).
b. White matter studies are more heterogeneous in their measurements.
c. Diffusion tensor (DT) derived mesurements are the most frequent in white matter, followed by volume.
c.1 It is harder to interpret a meta-analysis of multiple white matter measurements because its effect varies widely in different directions. The measurements derived from DT have the most differences.

We conduct our meta-analysis using the **TWO** most frequent measurements for gray and white matter. We use *volume* for GM and *fractional anysotropy* for WM.

Further meta regressions can be found in the supplementary material.
Gray Matter
- thickness
- VBM

White Matter integrity
- mean diffusivity MD
- radial diffusivity RD
- axial diffusivity AD
- mean kurtosis

White Matter volume
- thickness (I am unsure how they did this)
- VBM
- volume

Biletareal - GM volume
- WM volume
- WM fractional anisotropy

Frequency table: Brain structure (GM, WM) and MRI measures

Table 7: Matter vs measure (continued below)

	AD	ADC	AK	asymmetry	Axial Kurtosis	CT	FA	GM+WM
GM	0	0	2	9	0	23	8	0
WM	39	6	2	8	3	0	117	0

Table 8: Table continues below

	length	MD	Mean Kurtosis	MK	Radial Kurtosis	ratio GM/WM	RD
GM	0	2	0	2	0	0	0
WM	1	17	27	2	3	0	26

	RK	Surface	Thickness	VBM	Vol proportion	volume
GM	2	4	14	43	6	194
WM	2	0	10	16	6	79

Table 10: Matter vs Side

	asymmetry	bilateral	left	right	total
GM	9	59	130	109	2
WM	13	164	91	95	1

Brain structure (GM, WM) and side

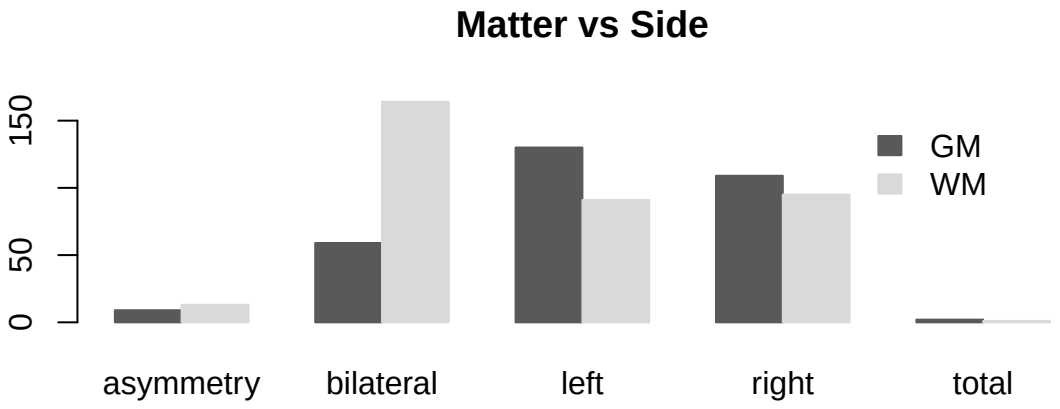

Studies characteristics (Figure 2.A, 2.B): Brain structure (GM, WM) by MRI measure (volume and FA)

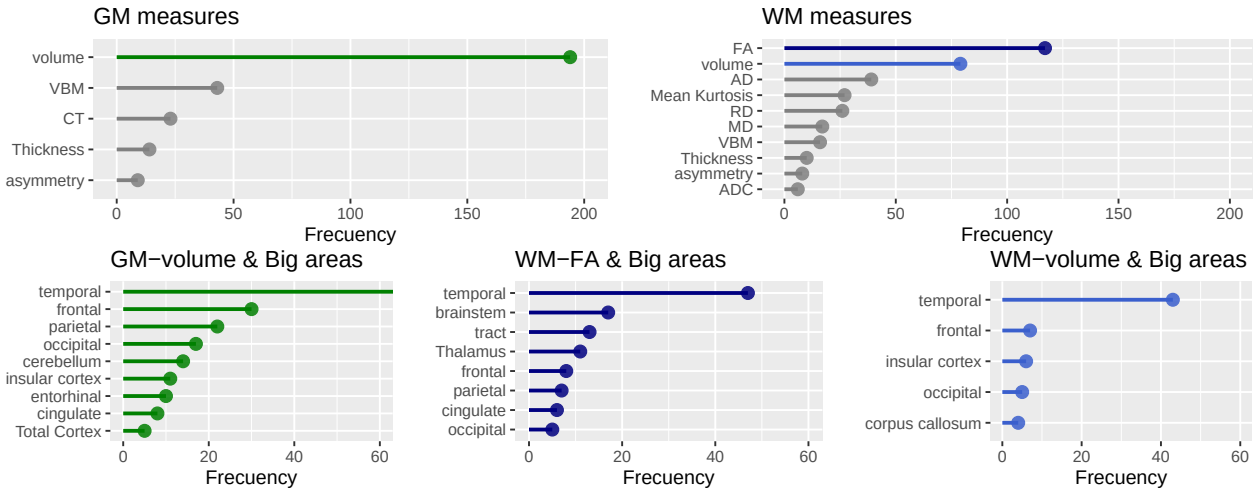

MRI measures by ROI (Figure 2.C)

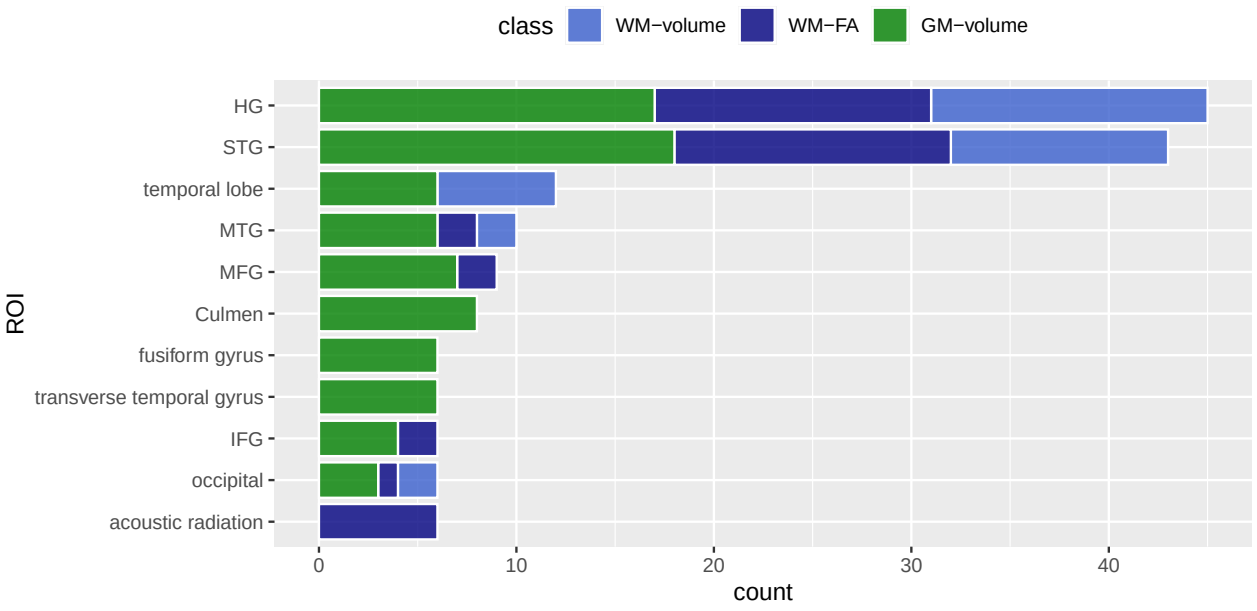

Relations of all MRI measurements of GM and WM with age

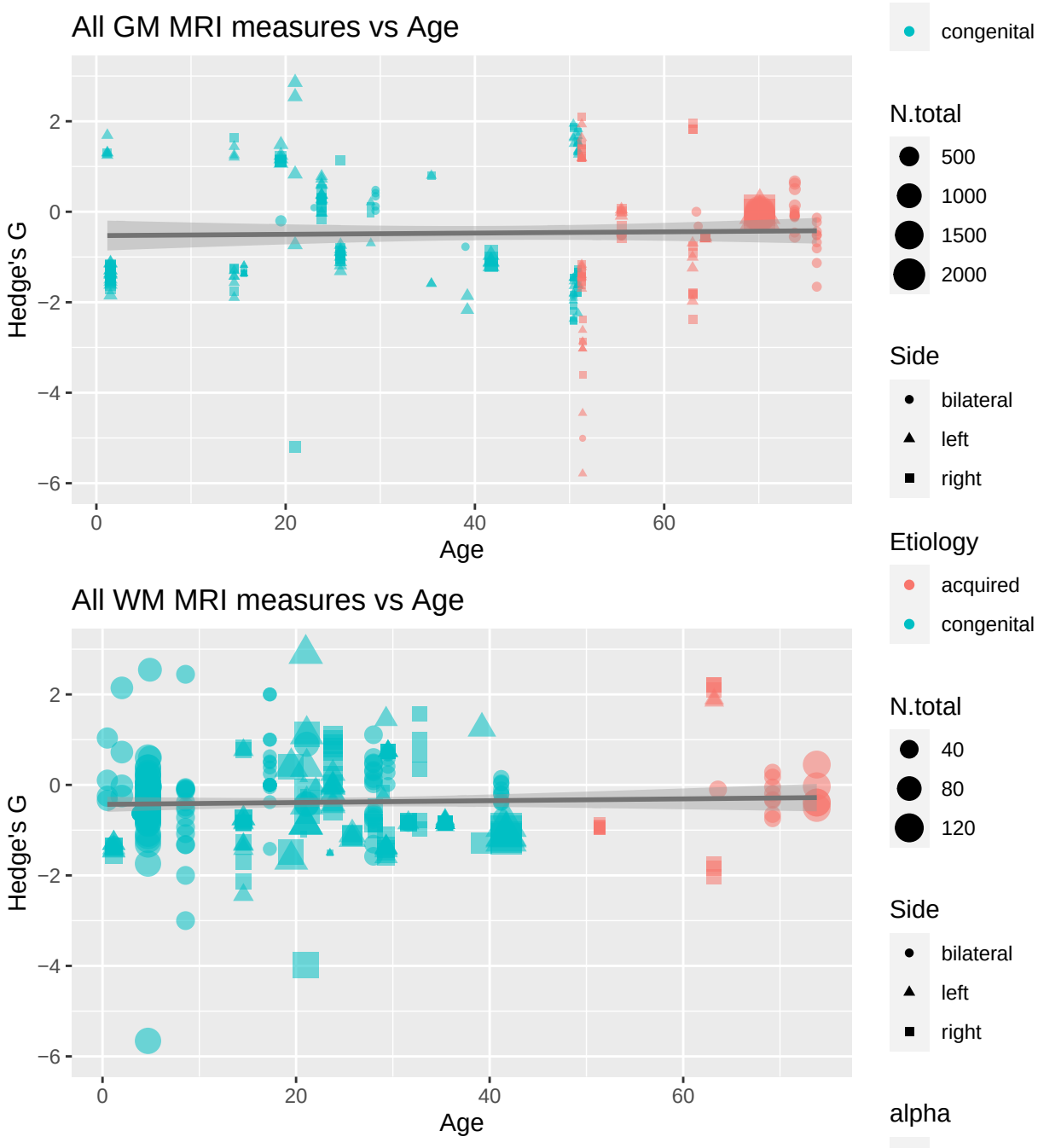

Gray matter relation with Age by volume (Figures 3.A and 3.B)

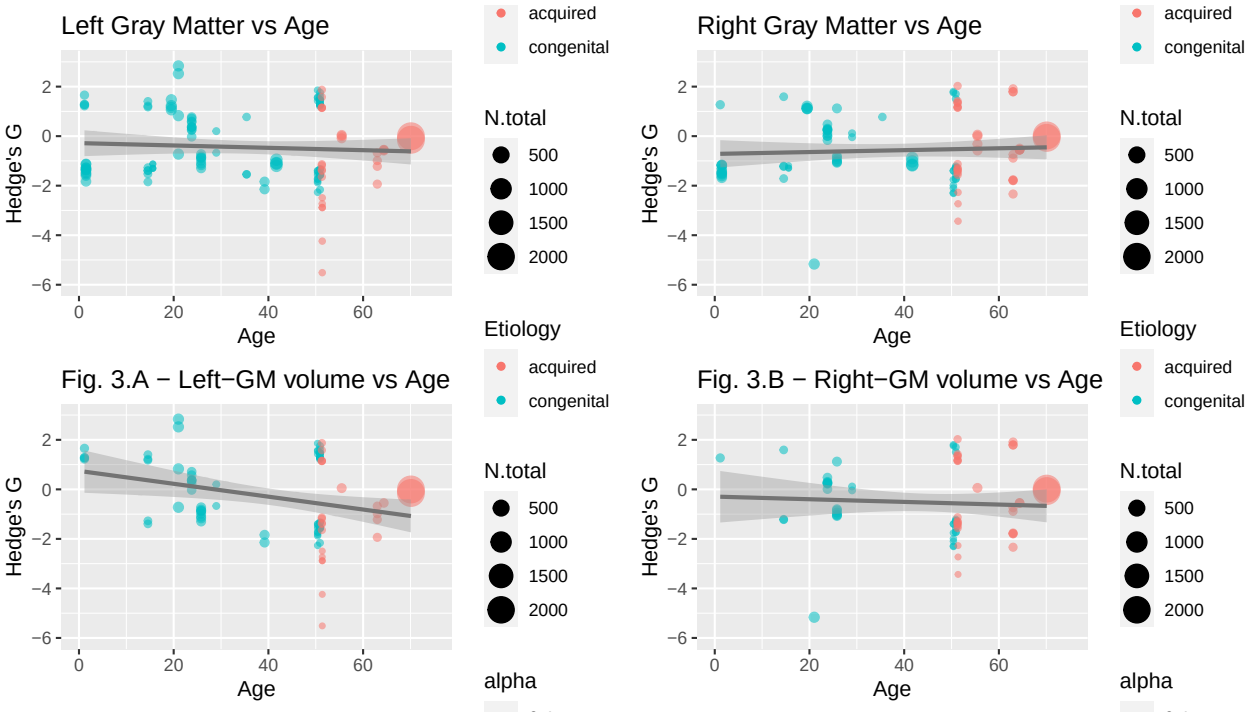

White matter relation with Age by volume and FA (Figures 3.C, 3.D and 3.F)

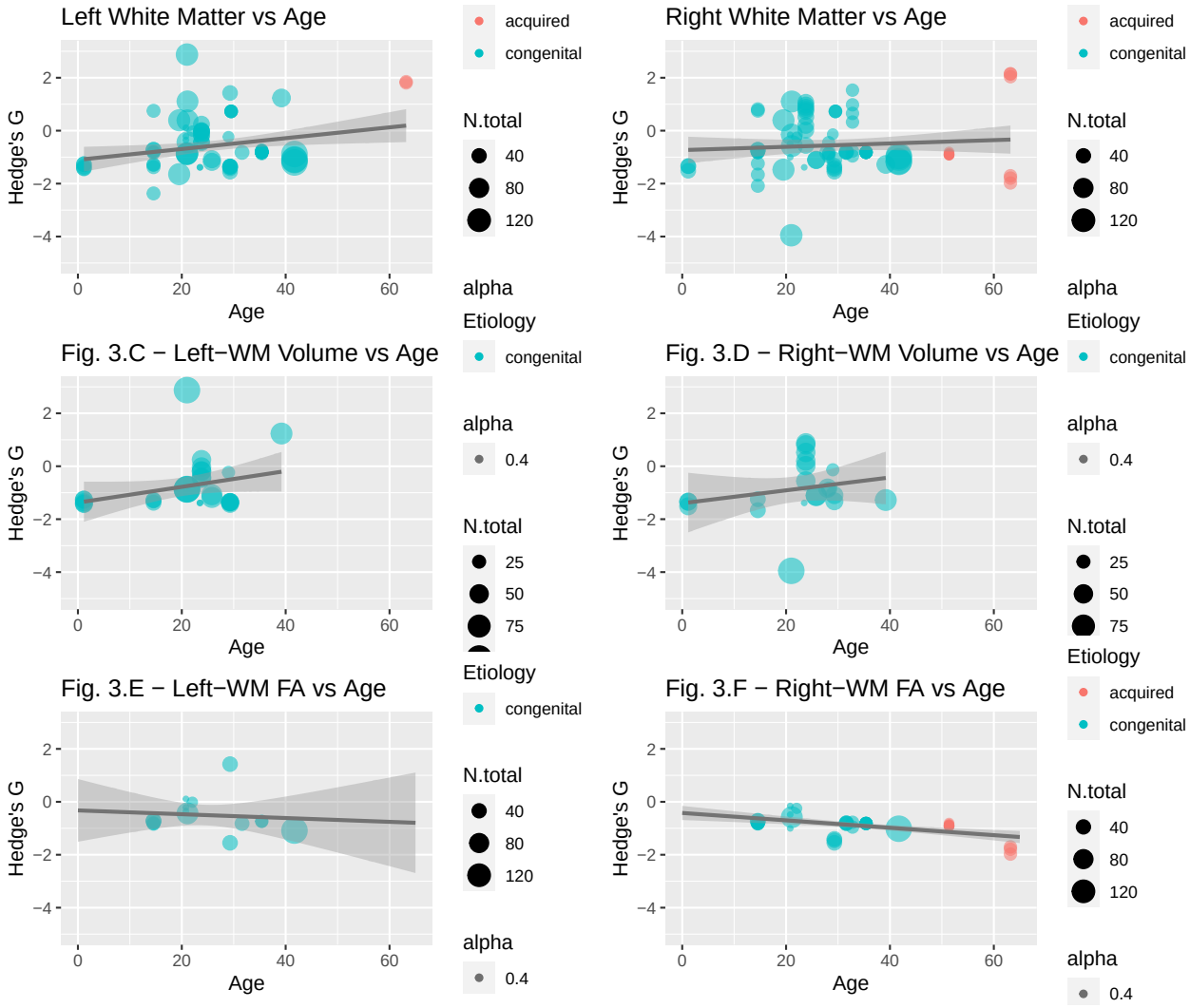

Gray and White matter relation with Age by asymmetry

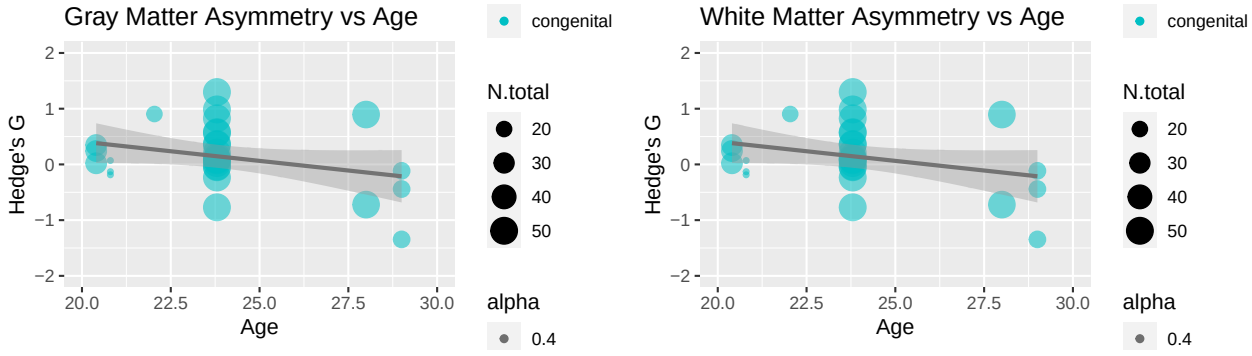

Table of estimates and meta-regression: WM and GM relation with age by MRI measures (volume and FA)

Model	r	p-value	t.stat	df
GM.vol.L	-0.27	0.0103	-2.62	85
WM.vol.L	0.26	0.1687	1.41	28
WM.fa.L	-0.09	0.7393	-0.34	13
GM.vol.R	-0.07	0.5343	-0.62	69
WM.vol.R	0.23	0.316	1.03	19
WM.fa.R	-0.55	2e-04	-4.04	38

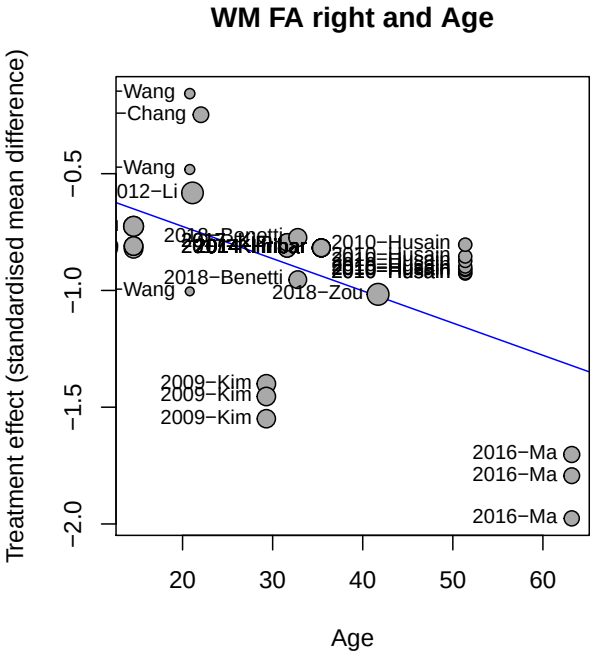

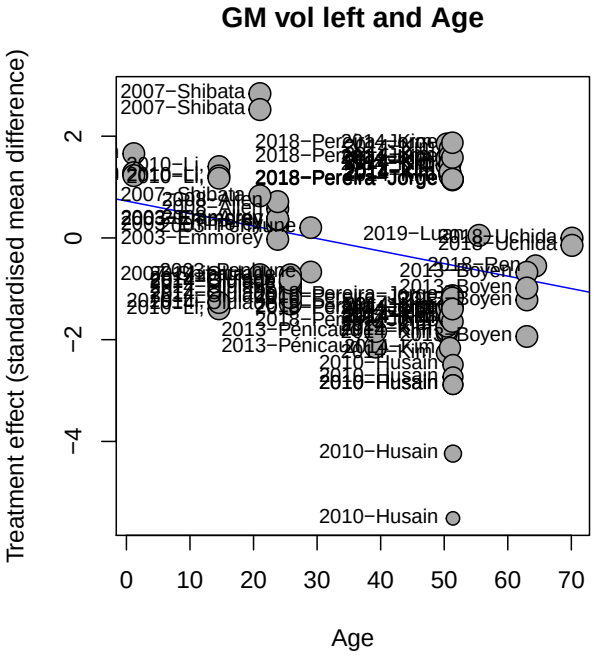

Meta-regression

Included variables by Etiology, Brain matter and MRI measure

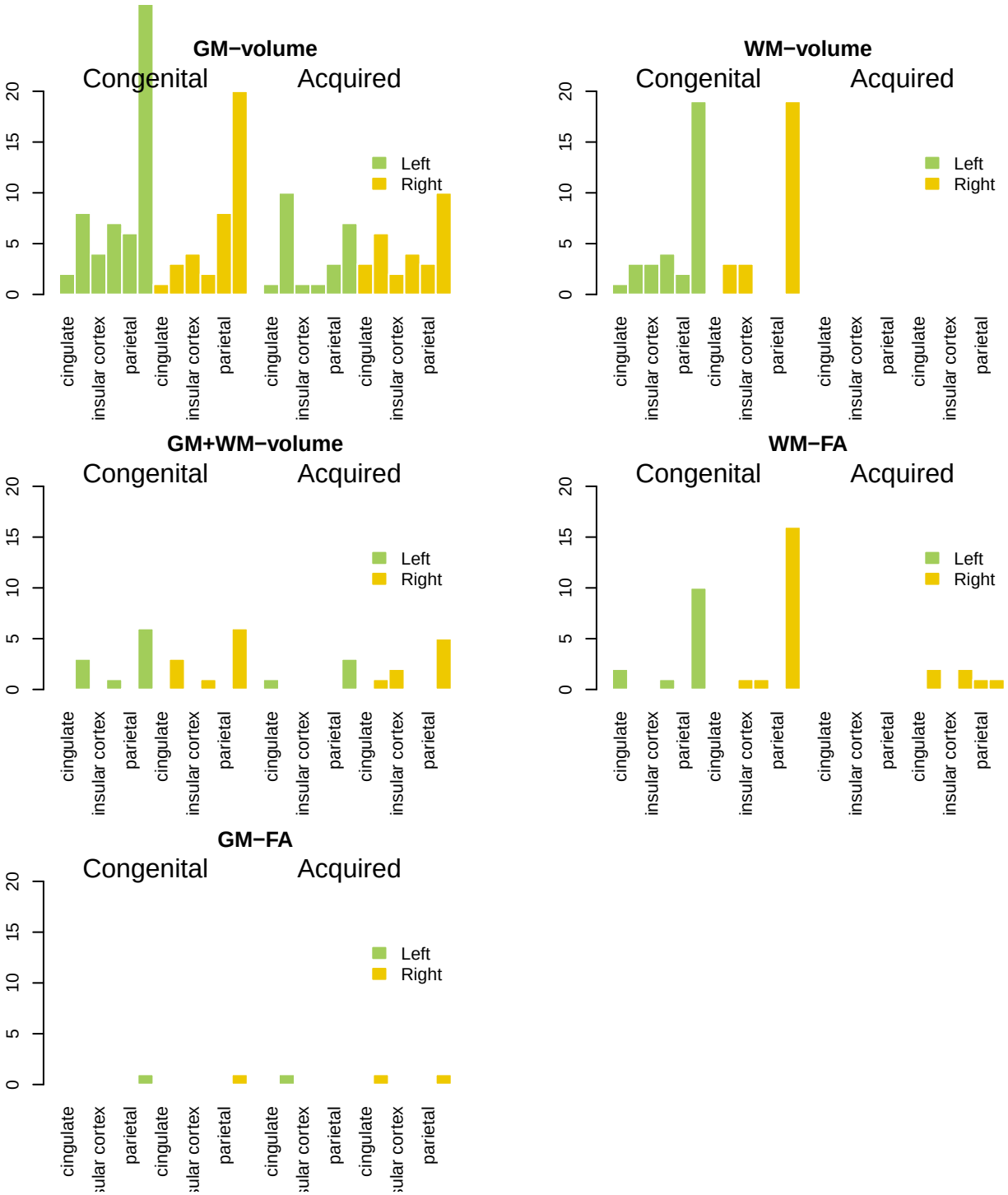

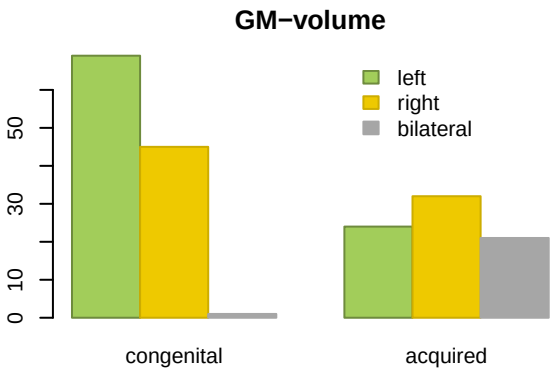
GM−volume
left
right
bilateral
0
10
30
50
congenital
acquired

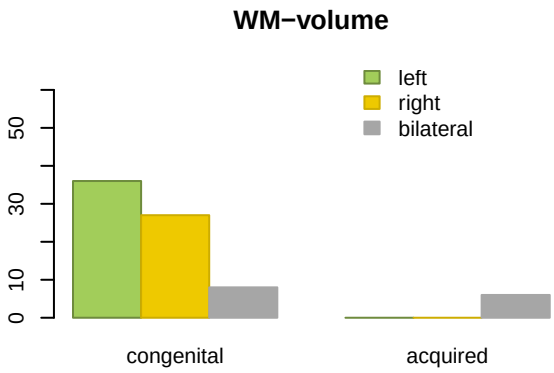
WM−volume
left
right
bilateral
0
10
30
50
congenital
acquired

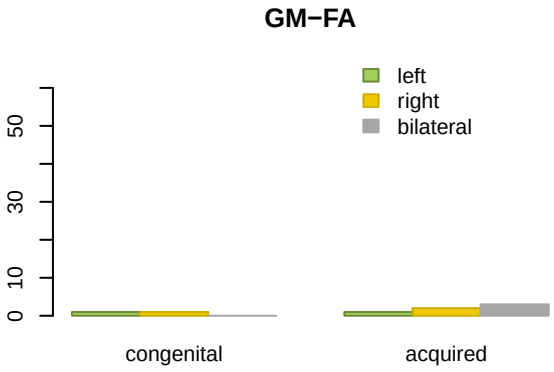
GM−FA
left
right
bilateral
0
10
30
50
congenital
acquired

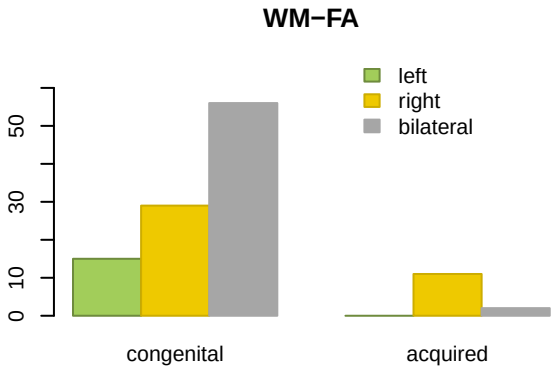
WM−FA
left
right
bilateral
0
10
30
50
congenital
acquired

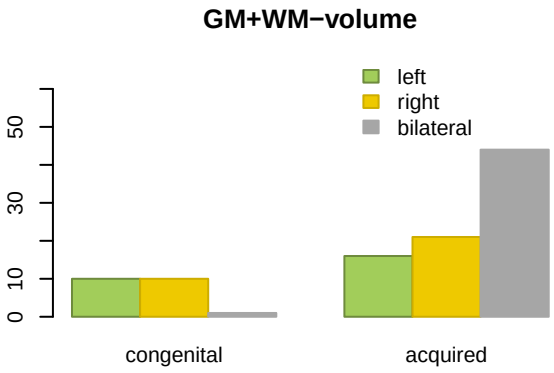
GM+WM−volume
left
right
bilateral
0
10
30
50
congenital
acquired

Acquired - Meta-regressions of Gray Matter Volume

Random effects model no intercept covariated by Big area

Table 12: REM by big area- Congenital - Gray Matter Volume

HedgeG	se	zval	ci.lo	ci.up	pval	N
0.9013104	0.3734628	2.4133872	0.1693367	1.6332841	0.0158050	11
1.4999543	0.9036636	1.6598593	-0.2711937	3.2711023	0.0969428	2
-0.5879845	0.4467854	-1.3160334	-1.4636677	0.2876988	0.1881628	8
0.0628005	0.6065046	0.1035449	-1.1259267	1.2515276	0.9175305	4
-0.5251523	0.4566856	-1.1499207	-1.4202396	0.3699351	0.2501765	7
-0.8874850	0.5149084	-1.7235784	-1.8966869	0.1217169	0.0847840	6
-0.1159681	0.2235026	-0.5188668	-0.5540252	0.3220890	0.6038537	30
1.2815547	1.2134567	1.0561191	-1.0967766	3.6598861	0.2909138	1
1.6815703	0.7283834	2.3086335	0.2539651	3.1091754	0.0209639	3
-0.8017506	1.1929769	-0.6720588	-3.1399424	1.5364411	0.5015462	1
0.0586466	0.6339350	0.0925119	-1.1838432	1.3011364	0.9262913	4
-2.5593121	0.7143293	-3.5828186	-3.9593717	-1.1592525	0.0003399	3
-0.1339176	0.5980210	-0.2239346	-1.3060172	1.0381821	0.8228082	4
-1.7301425	0.8957245	-1.9315566	-3.4857303	0.0254452	0.0534143	2
-1.1125014	0.4445211	-2.5026964	-1.9837468	-0.2412560	0.0123251	8
-0.5427415	0.2729266	-1.9885987	-1.0776678	-0.0078152	0.0467455	20

Table 13: Congenital - Gray Matter Volume

Test	Estimates
Mixed-effect model:	k= 114 : tau^2= 1.35 (SE= 0.22) I^2= 91.08 %, H^2= 11.21
Residual heterogeneity:	QE(df= 98)= 1048.28 , p.val= 7.08528565862191e-159
Test of moderators (big areas):	QM(df= 16)= 48.63 p.val= 3.78635028624703e-05

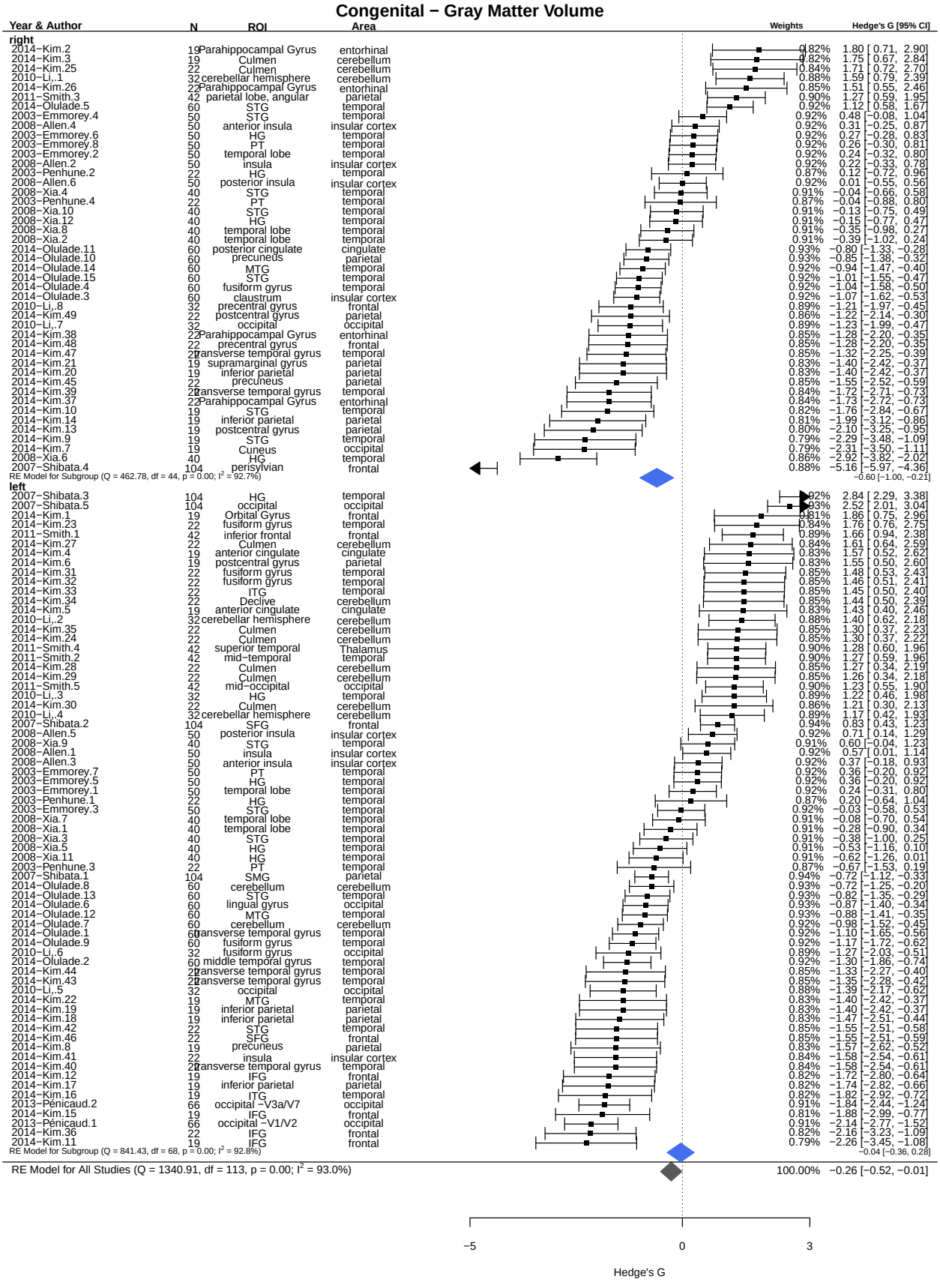
Congenital − Gray Matter Volume
Year & Author
N
ROI
Area
Weights
Hedge's G [95% CI]
right
2014−Kim.2 19 Parahippocampal Gyrus entorhinal 0.82% 1.80 [0.71, 2.90]
2014−Kim.3 19 Culmen cerebellum 0.82% 1.75 [0.67, 2.84]
2014−Kim.25 22 Culmen cerebellum 0.84% 1.71 [0.72, 2.70]
2010−Li,.1 32 cerebellar hemisphere cerebellum 0.88% 1.59 [0.79, 2.39]
2014−Kim.26 22 Parahippocampal Gyrus entorhinal 0.85% 1.51 [0.55, 2.46]
2011−Smith.3 42 parietal lobe, angular parietal 0.90% 1.27 [0.59, 1.95]
2014−Olulade.5 60 STG temporal 0.92% 1.12 [0.58, 1.67]
2003−Emmorey.4 50 STG temporal 0.92% 0.48 [−0.08, 1.04]
2008−Allen.4 50 anterior insula insular cortex 0.92% 0.31 [−0.25, 0.87]
2003−Emmorey.6 50 HG temporal 0.92% 0.27 [−0.28, 0.83]
2003−Emmorey.8 50 PT temporal 0.92% 0.26 [−0.30, 0.81]
2003−Emmorey.2 50 temporal lobe temporal 0.92% 0.24 [−0.32, 0.80]
2008−Allen.2 50 insula insular cortex 0.92% 0.22 [−0.33, 0.78]
2003−Penhune.2 22 HG temporal 0.87% 0.12 [−0.72, 0.96]
2008−Allen.6 50 posterior insula insular cortex 0.92% 0.01 [−0.55, 0.56]
2008−Xia.4 40 STG temporal 0.91% −0.04 [−0.66, 0.58]
2003−Penhune.4 22 PT temporal 0.87% −0.04 [−0.88, 0.80]
2008−Xia.10 40 STG temporal 0.91% −0.13 [−0.75, 0.49]
2008−Xia.12 40 HG temporal 0.91% −0.15 [−0.77, 0.47]
2008−Xia.8 40 temporal lobe temporal 0.91% −0.35 [−0.98, 0.27]
2008−Xia.2 40 temporal lobe temporal 0.91% −0.39 [−1.02, 0.24]
2014−Olulade.11 60 posterior cingulate cingulate 0.93% −0.80 [−1.33, −0.28]
2014−Olulade.10 60 precuneus parietal 0.93% −0.85 [−1.38, −0.32]
2014−Olulade.14 60 MTG temporal 0.92% −0.94 [−1.47, −0.40]
2014−Olulade.15 60 STG temporal 0.92% −1.01 [−1.55, −0.47]
2014−Olulade.4 60 fusiform gyrus temporal 0.92% −1.04 [−1.58, −0.50]
2014−Olulade.3 60 claustrum insular cortex 0.92% −1.07 [−1.62, −0.53]
2010−Li,.8 32 precentral gyrus frontal 0.89% −1.21 [−1.97, −0.45]
2014−Kim.49 22 postcentral gyrus parietal 0.86% −1.22 [−2.14, −0.30]
2010−Li,.7 32 occipital occipital 0.89% −1.23 [−1.99, −0.47]
2014−Kim.38 22 Parahippocampal Gyrus entorhinal 0.85% −1.28 [−2.20, −0.35]
2014−Kim.48 22 precentral gyrus frontal 0.85% −1.28 [−2.20, −0.35]
2014−Kim.47 22 transverse temporal gyrus temporal 0.85% −1.32 [−2.25, −0.39]
2014−Kim.21 19 supramarginal gyrus parietal 0.83% −1.40 [−2.42, −0.37]
2014−Kim.20 19 inferior parietal parietal 0.83% −1.40 [−2.42, −0.37]
2014−Kim.45 22 precuneus parietal 0.85% −1.55 [−2.52, −0.59]
2014−Kim.39 22 transverse temporal gyrus temporal 0.84% −1.72 [−2.71, −0.73]
2014−Kim.37 22 Parahippocampal Gyrus entorhinal 0.84% −1.73 [−2.72, −0.73]
2014−Kim.10 19 STG temporal 0.82% −1.76 [−2.84, −0.67]
2014−Kim.14 19 inferior parietal parietal 0.81% −1.99 [−3.12, −0.86]
2014−Kim.13 19 postcentral gyrus parietal 0.80% −2.10 [−3.25, −0.95]
2014−Kim.9 19 STG temporal 0.79% −2.29 [−3.48, −1.09]
2014−Kim.7 19 Cuneus occipital 0.79% −2.31 [−3.50, −1.11]
2008−Xia.6 40 HG temporal 0.86% −2.92 [−3.82, −2.02]
2007−Shibata.4 104 perisylvian frontal 0.88% −5.16 [−5.97, −4.36]
RE Model for Subgroup (Q = 462.78, df = 44, p = 0.00; I² = 92.7%) −0.60 [−1.00, −0.21]
left
2007−Shibata.3 104 HG temporal 2.84 [2.29, 3.38]
2007−Shibata.5 104 occipital occipital 2.52 [2.01, 3.04]
2014−Kim.1 19 Orbital Gyrus frontal 1.86 [0.75, 2.96]
2014−Kim.23 22 fusiform gyrus temporal 1.76 [0.76, 2.75]
2011−Smith.1 42 inferior frontal frontal 1.66 [0.94, 2.38]
2014−Kim.27 22 Culmen cerebellum 1.61 [0.64, 2.59]
2014−Kim.4 19 anterior cingulate cingulate 1.57 [0.52, 2.62]
2014−Kim.6 19 postcentral gyrus parietal 1.55 [0.50, 2.60]
2014−Kim.31 22 fusiform gyrus temporal 1.48 [0.53, 2.43]
2014−Kim.32 22 fusiform gyrus temporal 1.46 [0.51, 2.41]
2014−Kim.33 22 ITG temporal 1.45 [0.50, 2.40]
2014−Kim.34 22 Declive cerebellum 1.44 [0.50, 2.39]
2014−Kim.5 19 anterior cingulate cingulate 1.43 [0.40, 2.46]
2010−Li,.2 32 cerebellar hemisphere cerebellum 1.40 [0.62, 2.18]
2014−Kim.35 22 Culmen cerebellum 1.30 [0.37, 2.23]
2014−Kim.24 22 Culmen cerebellum 1.30 [0.37, 2.22]
2011−Smith.4 42 superior temporal Thalamus 1.28 [0.60, 1.96]
2011−Smith.2 42 mid−temporal temporal 1.27 [0.59, 1.96]
2014−Kim.28 22 Culmen cerebellum 1.27 [0.34, 2.19]
2014−Kim.29 22 Culmen cerebellum 1.26 [0.34, 2.18]
2011−Smith.5 42 mid−occipital occipital 1.23 [0.55, 1.90]
2010−Li,.3 32 HG temporal 1.22 [0.46, 1.98]
2014−Kim.30 22 Culmen cerebellum 1.21 [0.30, 2.13]
2010−Li,.4 32 cerebellar hemisphere cerebellum 1.17 [0.42, 1.93]
2007−Shibata.2 104 SFG frontal 0.83 [0.43, 1.23]
2008−Allen.5 50 posterior insula insular cortex 0.71 [0.14, 1.29]
2008−Xia.9 40 STG temporal 0.60 [−0.04, 1.23]
2008−Allen.1 50 insula insular cortex 0.57 [0.01, 1.14]
2008−Allen.3 50 anterior insula insular cortex 0.37 [−0.18, 0.93]
2003−Emmorey.7 50 PT temporal 0.36 [−0.20, 0.92]
2003−Emmorey.5 50 HG temporal 0.36 [−0.20, 0.92]
2003−Emmorey.1 50 temporal lobe temporal 0.24 [−0.31, 0.80]
2003−Penhune.1 22 HG temporal 0.20 [−0.64, 1.04]
2003−Emmorey.3 50 STG temporal −0.03 [−0.58, 0.53]
2008−Xia.7 40 temporal lobe temporal −0.08 [−0.70, 0.54]
2008−Xia.1 40 temporal lobe temporal −0.28 [−0.90, 0.34]
2008−Xia.3 40 STG temporal −0.38 [−1.00, 0.25]
2008−Xia.5 40 HG temporal −0.53 [−1.16, 0.10]
2008−Xia.11 40 HG temporal −0.62 [−1.26, 0.01]
2003−Penhune.3 22 PT temporal −0.67 [−1.53, 0.19]
2007−Shibata.1 104 SMG parietal −0.72 [−1.12, −0.33]
2014−Olulade.8 60 cerebellum cerebellum −0.72 [−1.25, −0.20]
2014−Olulade.13 60 STG temporal −0.82 [−1.35, −0.29]
2014−Olulade.6 60 lingual gyrus occipital −0.87 [−1.40, −0.34]
2014−Olulade.12 60 MTG temporal −0.88 [−1.41, −0.35]
2014−Olulade.7 60 cerebellum cerebellum −0.98 [−1.52, −0.45]
2014−Olulade.1 60 transverse temporal gyrus temporal −1.10 [−1.65, −0.56]
2014−Olulade.9 60 fusiform gyrus temporal −1.17 [−1.72, −0.62]
2010−Li,.6 32 fusiform gyrus occipital −1.27 [−2.03, −0.51]
2014−Olulade.2 60 middle temporal gyrus temporal −1.30 [−1.86, −0.74]
2014−Kim.44 22 transverse temporal gyrus temporal −1.33 [−2.27, −0.40]
2014−Kim.43 22 transverse temporal gyrus temporal −1.35 [−2.28, −0.42]
2010−Li,.5 32 occipital occipital −1.39 [−2.17, −0.62]
2014−Kim.22 19 MTG temporal −1.40 [−2.42, −0.37]
2014−Kim.19 19 inferior parietal parietal −1.40 [−2.42, −0.37]
2014−Kim.18 19 inferior parietal parietal −1.47 [−2.51, −0.44]
2014−Kim.42 22 STG temporal −1.55 [−2.51, −0.58]
2014−Kim.46 22 SFG frontal −1.55 [−2.51, −0.59]
2014−Kim.8 19 precuneus parietal −1.57 [−2.62, −0.52]
2014−Kim.41 22 insula insular cortex −1.58 [−2.54, −0.61]
2014−Kim.40 22 transverse temporal gyrus temporal −1.59 [−2.54, −0.61]
2014−Kim.12 19 IFG frontal −1.72 [−2.80, −0.64]
2014−Kim.17 19 inferior parietal parietal −1.74 [−2.82, −0.66]
2014−Kim.16 19 ITG temporal −1.82 [−2.92, −0.72]
2013−Pénicaud.2 66 occipital −V3a/V7 occipital −1.84 [−2.44, −1.24]
2014−Kim.15 19 IFG frontal −1.88 [−2.99, −0.77]
2013−Pénicaud.1 66 occipital −V1/V2 occipital −2.14 [−2.77, −1.52]
2014−Kim.36 22 IFG frontal −2.16 [−3.23, −1.09]
2014−Kim.11 19 IFG frontal −2.26 [−3.45, −1.08]
RE Model for Subgroup (Q = 841.43, df = 68, p = 0.00; I² = 92.8%) −0.04 [−0.36, 0.28]
RE Model for All Studies (Q = 1340.91, df = 113, p = 0.00; I² = 93.0%) 100.00% −0.26 [−0.52, −0.01]
−5
0
3
Hedge's G

Table 14: Acquired - Gray Matter Volume

Test	Estimates
Mixed-effect model:	k= 56 : tau^2= 2.49 (SE= 0.6) I^2= 98.57 %, H^2= 70.1
Residual heterogeneity:	QE(df= 41)= 412.31 , p.val= 8.01499990705428e-63
Test of moderators (big areas):	QM(df= 15)= 29.35 p.val= 0.014479351188099

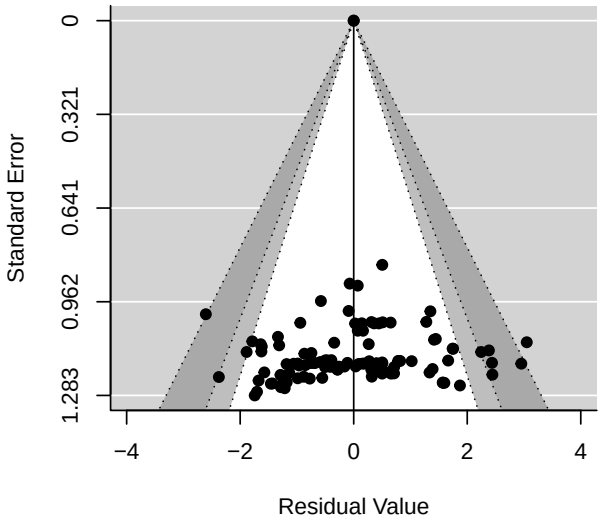

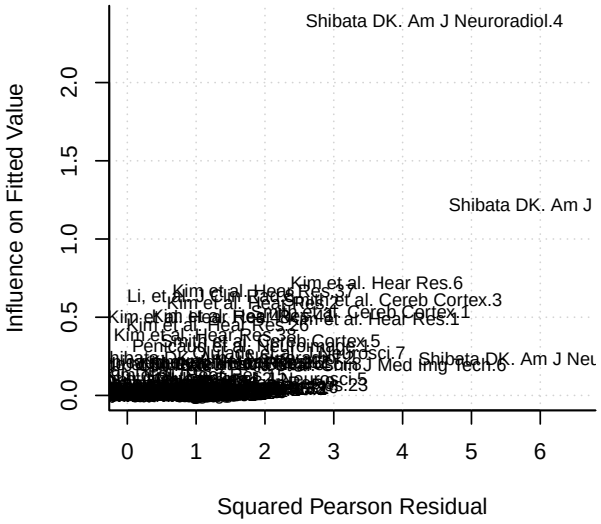

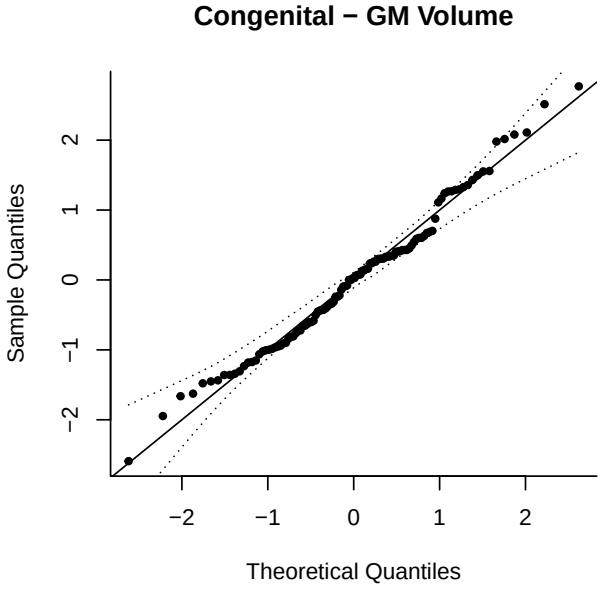

Acquired - Meta-regressions of Gray Matter by Volume

Random effects model no intercept covariated by Big area

Table 15: REM by big area- Congenital - Gray Matter Volume

HedgeG	se	zval	ci.lo	ci.up	pval	N
-2.8834593	1.7275069	-1.6691449	-6.269311	0.5023920	0.0950887	1
-1.1400688	0.5267737	-2.1642479	-2.172526	-0.1076114	0.0304453	10
-1.9371568	1.6261099	-1.1912828	-5.124274	1.2499600	0.2335426	1
-1.3534702	1.6409912	-0.8247883	-4.569754	1.8628133	0.4094918	1
-1.3978319	1.6417994	-0.8514023	-4.615700	1.8200359	0.3945459	1
0.3896201	0.9454302	0.4121088	-1.463389	2.2426292	0.6802597	3
-0.8301541	0.6236257	-1.3311735	-2.052438	0.3921299	0.1831319	7
-1.4826100	0.9540207	-1.5540648	-3.352456	0.3872362	0.1201690	3
0.0070725	1.1610972	0.0060912	-2.268636	2.2827812	0.9951399	2
-1.4376558	0.7012092	-2.0502524	-2.812001	-0.0633111	0.0403398	6
-2.0470474	1.1513226	-1.7779963	-4.303598	0.2095035	0.0754045	2
-1.5245544	1.1626676	-1.3112555	-3.803341	0.7542323	0.1897714	2
-1.5236790	0.8157812	-1.8677544	-3.122581	0.0752228	0.0617963	4
0.3405078	0.9458955	0.3599846	-1.513413	2.1944289	0.7188586	3
0.7270216	0.5141240	1.4140977	-0.280643	1.7346863	0.1573332	10

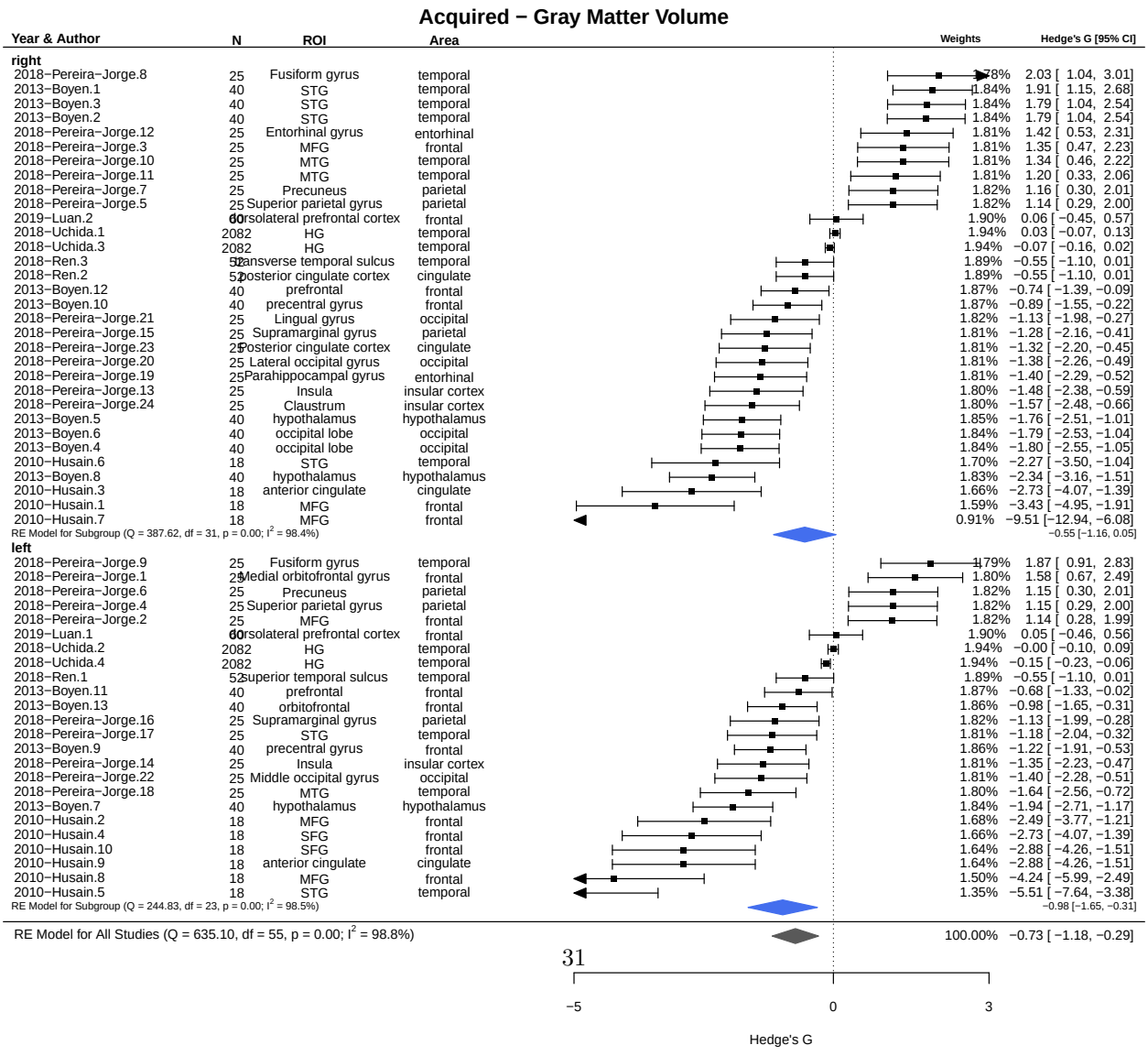

Table 16: Congenital White Matter Volume

Test	Estimates
Mixed-effect model:	k= 63 : tau^2= 0.83 (SE= 0.19) I^2= 89.36 %, H^2= 9.4
Residual heterogeneity:	QE(df= 50)= 462.69 , p.val= 3.35220276992225e-68
Test of moderators (big areas):	QM(df= 13)= 50.92 p.val= 2.07007590853841e-06

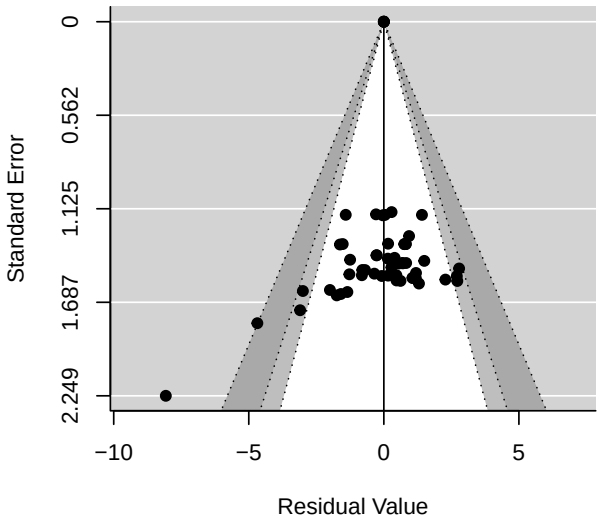

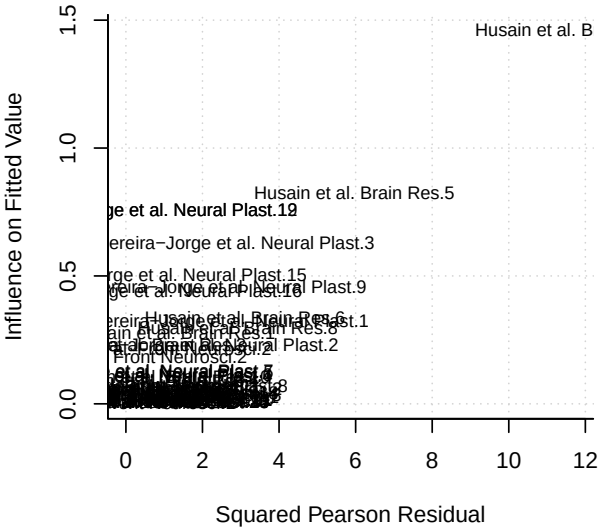

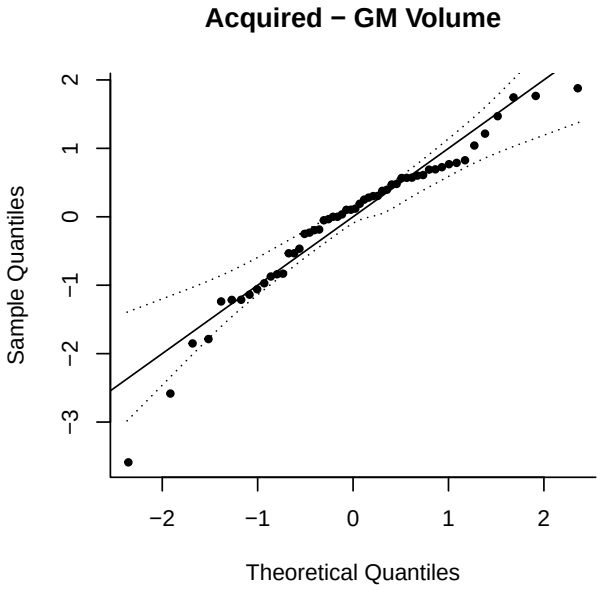

Congenital - White Matter by VOLUME

Random effects model no intercept covariated by Big area

Table 17: REM by big area- Congenital - Gray Matter Volume

HedgeG	se	zval	ci.lo	ci.up	pval	N
-1.1070810	0.6745058	-1.6413217	-2.4290881	0.2149260	0.1007306	2
-1.3786454	0.9926110	-1.3889080	-3.3241272	0.5668365	0.1648607	1
-1.3402379	0.5684006	-2.3579110	-2.4542825	-0.2261933	0.0183781	3
0.0079129	0.5504384	0.0143756	-1.0709265	1.0867523	0.9885303	3
0.5024402	0.4846477	1.0367123	-0.4474518	1.4523323	0.2998699	4
-1.3081390	0.6914333	-1.8919238	-2.6633233	0.0470452	0.0585011	2
-0.4780484	0.2210575	-2.1625524	-0.9113131	-0.0447837	0.0305756	19
-1.3856308	0.7930734	-1.7471658	-2.9400261	0.1687645	0.0806086	2
-1.5134943	0.9788737	-1.5461589	-3.4320516	0.4050629	0.1220662	1
-1.3856308	1.1215752	-1.2354328	-3.5838777	0.8126162	0.2166695	1
-2.3098509	0.5696811	-4.0546382	-3.4264054	-1.1932964	0.0000502	3
0.7369857	0.5521197	1.3348296	-0.3451490	1.8191204	0.1819321	3
-0.5528945	0.2217554	-2.4932631	-0.9875270	-0.1182620	0.0126575	19

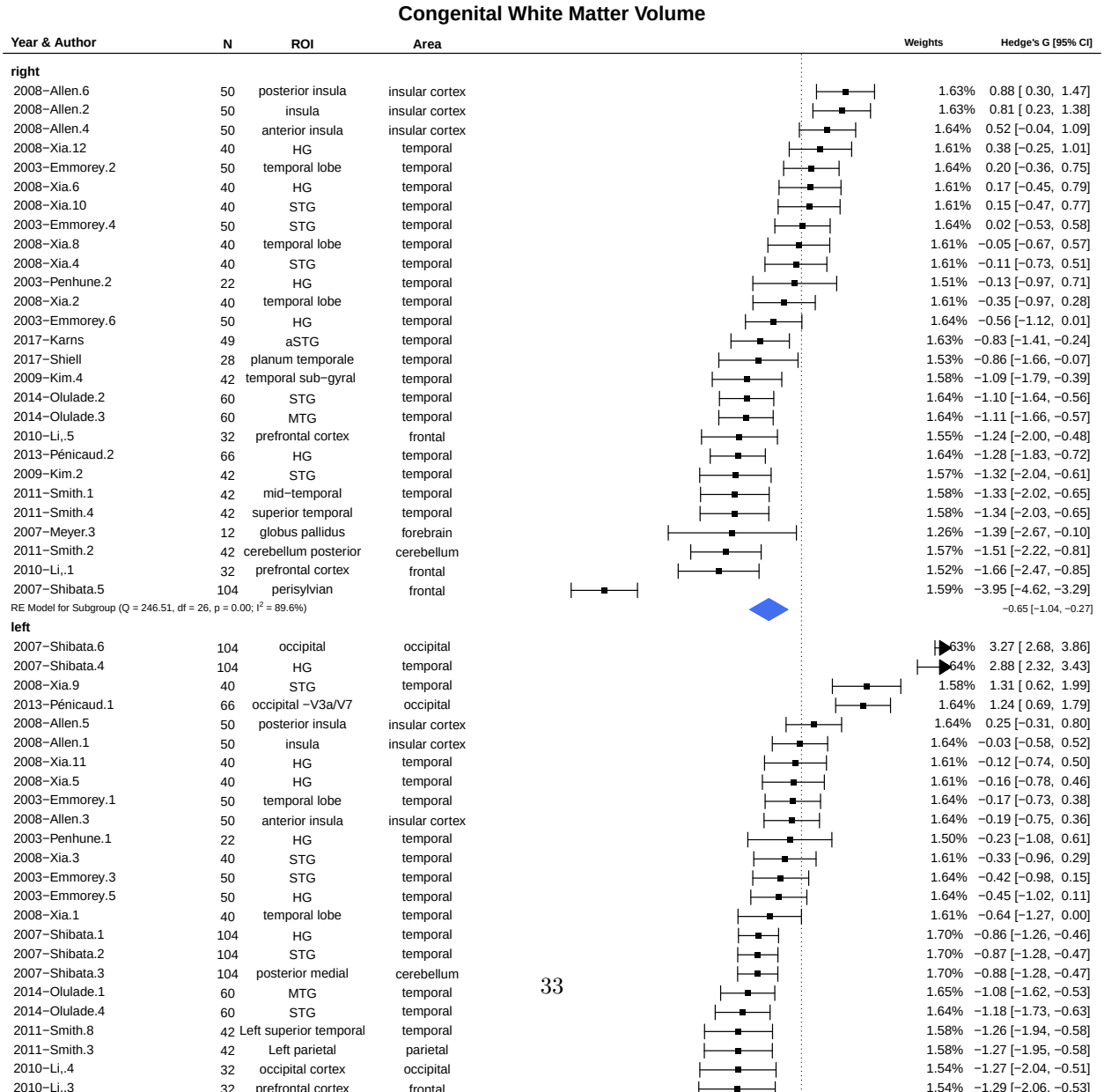

Table 18: acquired White Matter Volume

Test	Estimates
Mixed-effect model:	k= 6 : tau^2= 0.09 (SE= 0.21) I^2= 59.05 %, H^2= 2.44
Residual heterogeneity:	QE(df= 1)= 2.44 , p.val= 0.118106312179678
Test of moderators (big areas):	QM(df= 5)= 5.26 p.val= 0.385192885534552

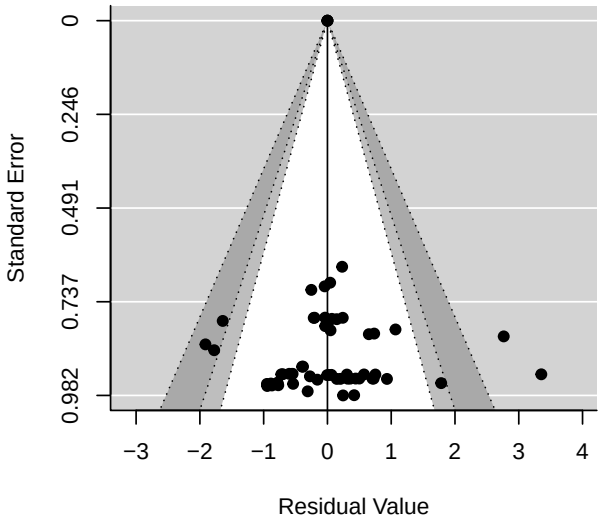

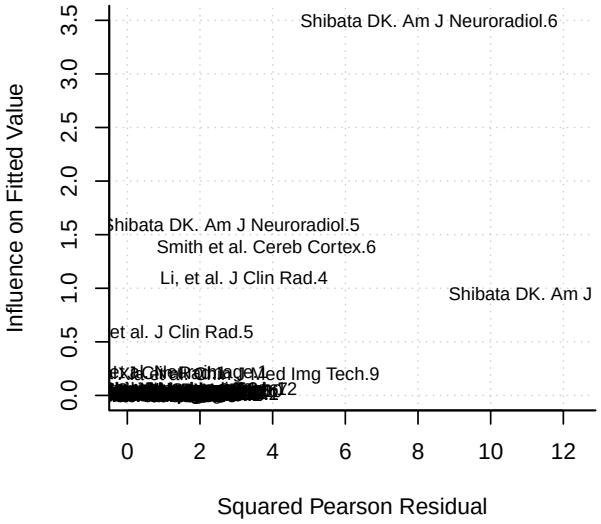

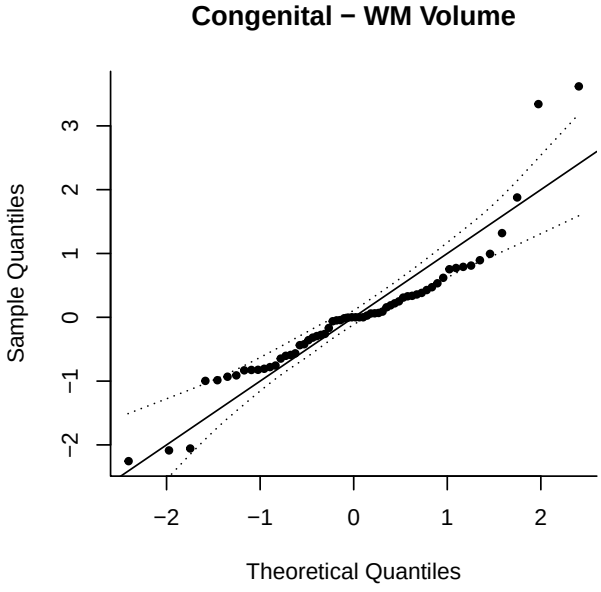

Acquired - White Matter by VOLUME (ONLY BILATERAL)

Not enough values for the Random effects model no intercept covariated by Big area and Side (left or right)

Table 19: REM by big area- Congenital - Gray Matter Volume

HedgeG	se	zval	ci.lo	ci.up	pval	N
-0.5069091	0.3500431	-1.4481334	-1.1929809	0.1791627	0.1475797	1
-0.3876364	0.3494280	-1.1093454	-1.0725027	0.2972300	0.2672812	1
-0.3876364	0.3494280	-1.1093454	-1.0725027	0.2972300	0.2672812	1
-0.0298182	0.3485651	-0.0855455	-0.7129932	0.6533569	0.9318277	1
0.2239473	0.2691216	0.8321415	-0.3035214	0.7514160	0.4053291	2

Table 20: Congenital White Matter FA

Test	Estimates
Mixed-effect model:	k= 44 : tau^2= 0.04 (SE= 0.04) I^2= 24.12 %, H^2= 1.32
Residual heterogeneity:	QE(df= 33)= 40.58 , p.val= 0.17085782139714
Test of moderators (big areas):	QM(df= 11)= 168.31 p.val= 2.63258401967927e-30

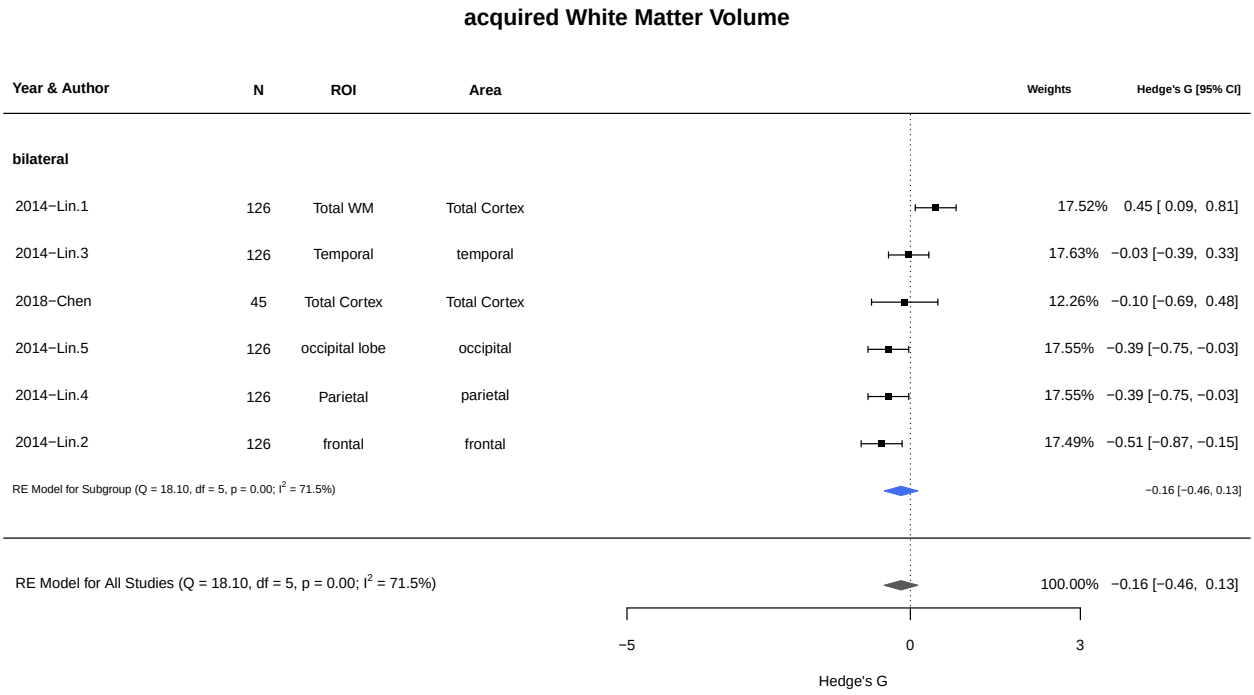

Nothing is significant

Congenital - White Matter by FA fractional anisotropy

Random effects model no intercept covariated by Big area

Table 21: REM by big area- Congenital - Gray Matter Volume

HedgeG	se	zval	ci.lo	ci.up	pval	N
-0.0155675	0.4891077	-0.0318283	-0.9742009	0.9430660	0.9746090	1
0.2970009	0.2964912	1.0017190	-0.2841112	0.8781129	0.3164793	2
-0.7254299	0.3790761	-1.9136787	-1.4684055	0.0175457	0.0556612	1
-0.6980338	0.1264916	-5.5184183	-0.9459528	-0.4501147	0.0000000	10
-1.5493057	0.4250056	-3.6453770	-2.3823013	-0.7163100	0.0002670	1
-0.2475694	0.4908382	-0.5043809	-1.2095945	0.7144557	0.6139937	1
-0.8177670	0.4415169	-1.8521760	-1.6831242	0.0475902	0.0640005	1
-0.7254299	0.3790761	-1.9136787	-1.4684055	0.0175457	0.0556612	1
-0.8298372	0.1035639	-8.0128036	-1.0328187	-0.6268557	0.0000000	16
-0.9238373	0.1788955	-5.1641181	-1.2744659	-0.5732086	0.0000002	6
-1.0039894	0.2156391	-4.6558783	-1.4266343	-0.5813446	0.0000032	4

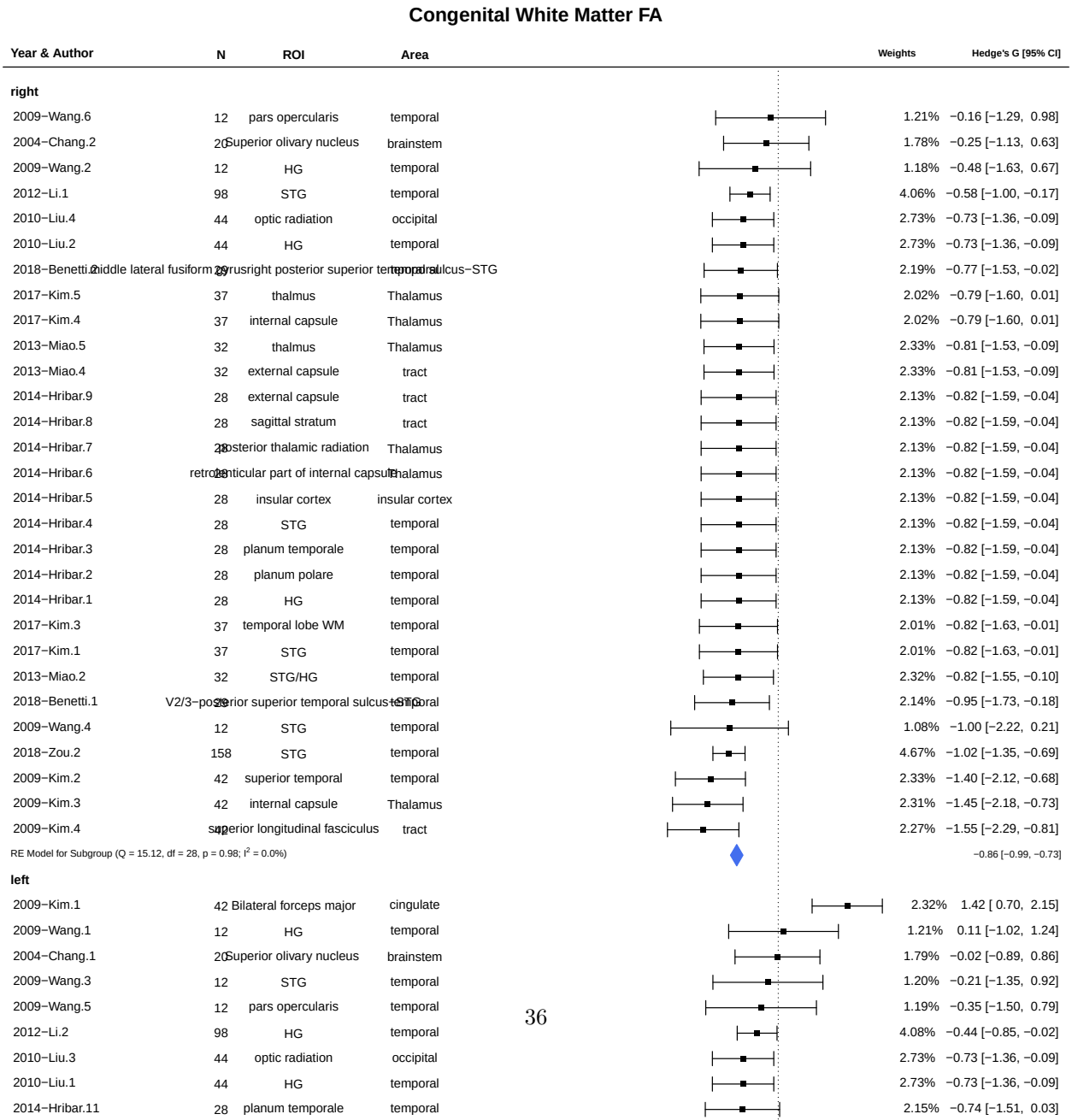

Table 22: acquired White Matter FA

Test	Estimates
Mixed-effect model:	k= 11 : tau^2= 0 (SE= 0.15) I^2= 0 %, H^2= 1
Residual heterogeneity:	QE(df= 6)= 2.64 , p.val= 0.852507484101014
Test of moderators (big areas):	QM(df= 5)= 71.74 p.val= 4.45450158997401e-14

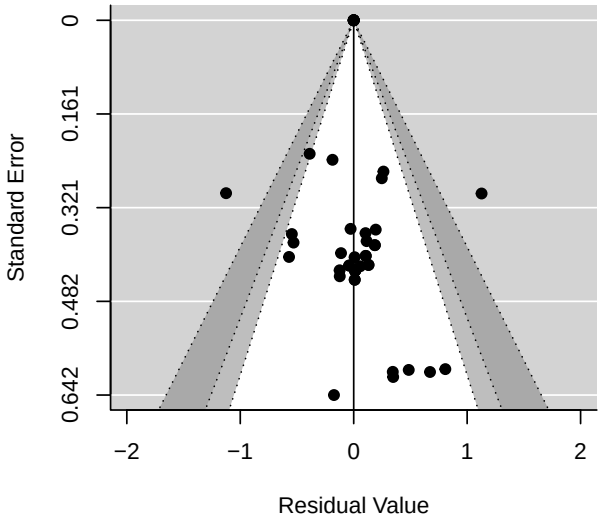

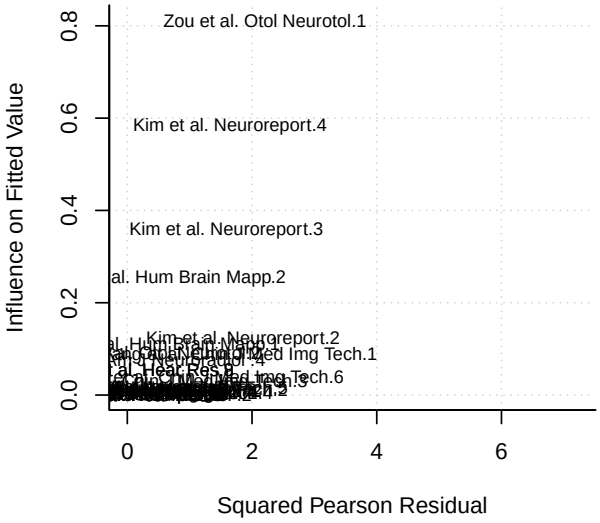

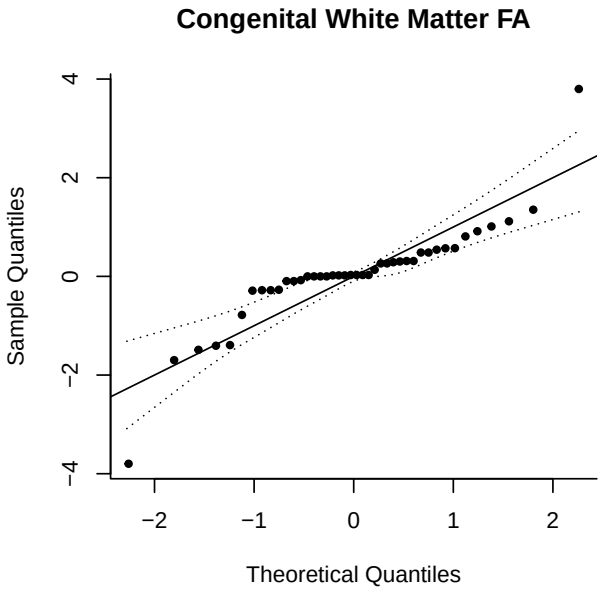

Acquired - White Matter by FA fractional anisotropy (ONLY RIGHT)

Random effects model no intercept covariated by Big area

Table 23: REM by big area- Congenital - Gray Matter Volume

HedgeG	se	zval	ci.lo	ci.up	p.val	N
-1.4804586	0.3403176	-4.350226	-2.147469	-0.8134483	0.0000136	2
-0.9104754	0.3603273	-2.526801	-1.616704	-0.2042469	0.0115107	2
-1.7025869	0.4379232	-3.887866	-2.560901	-0.8442731	0.0001011	1
-1.7933682	0.4445829	-4.033822	-2.664735	-0.9220018	0.0000549	1
-0.8811554	0.2271998	-3.878328	-1.326459	-0.4358519	0.0001052	5

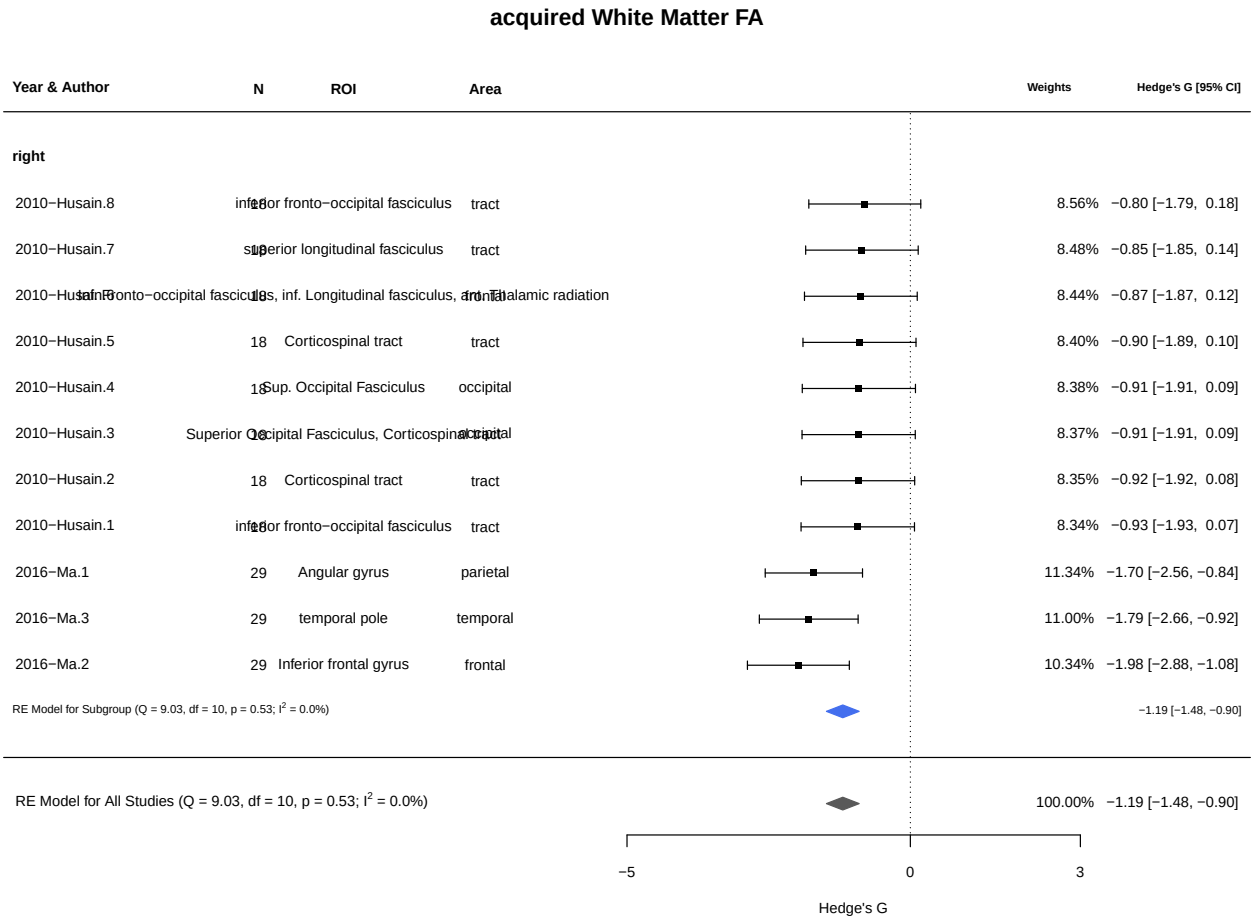

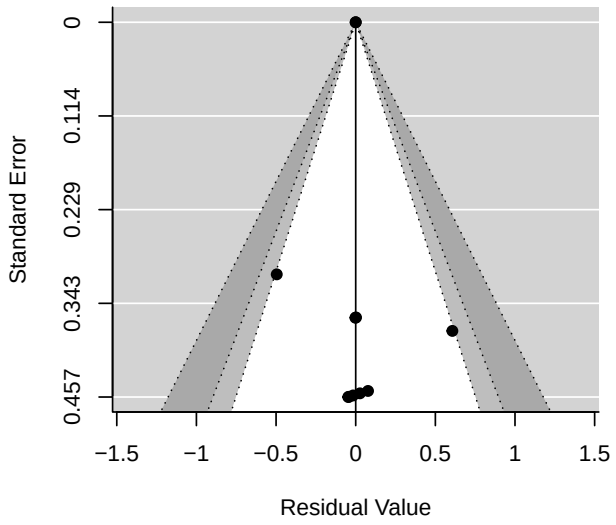
Standard Error
0
0.114
0.229
0.343
0.457
−1.5
−1
−0.5
0
0.5
1
1.5
Residual Value

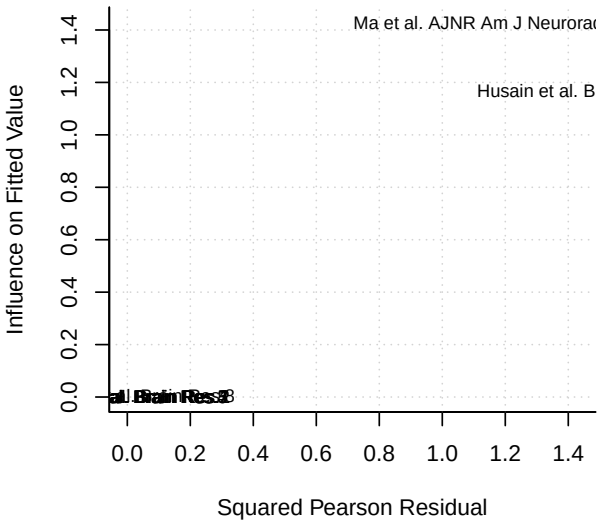
Ma et al. AJNR Am J Neurorad
Husain et al. B
Influence on Fitted Value
0.0
0.2
0.4
0.6
0.8
1.0
1.2
1.4
Squared Pearson Residual

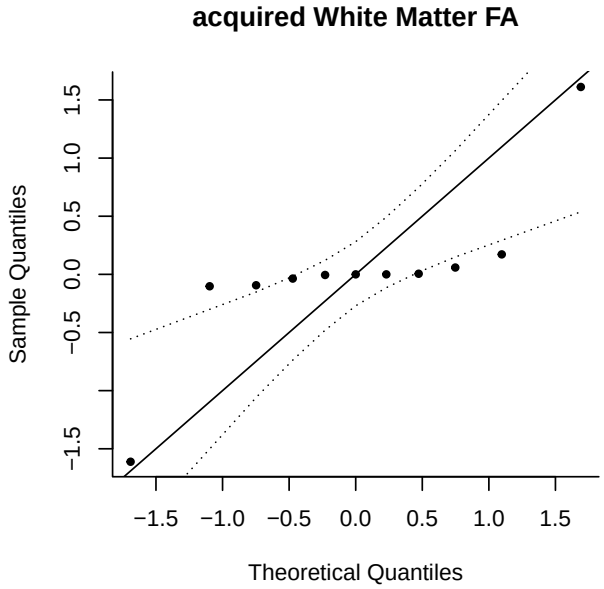
acquired White Matter FA
Sample Quantiles
−1.5
−0.5
0.0
0.5
1.0
1.5
−1.5
−1.0
−0.5
0.0
0.5
1.0
1.5
Theoretical Quantiles

Supplementary material: heterogeneity per model

Heterogeney: GM volume Right

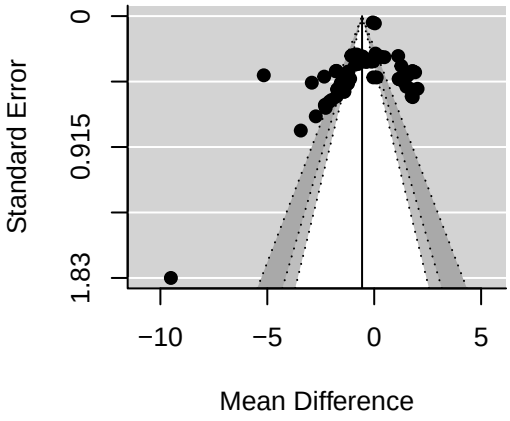

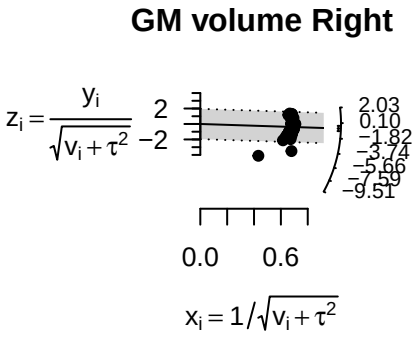

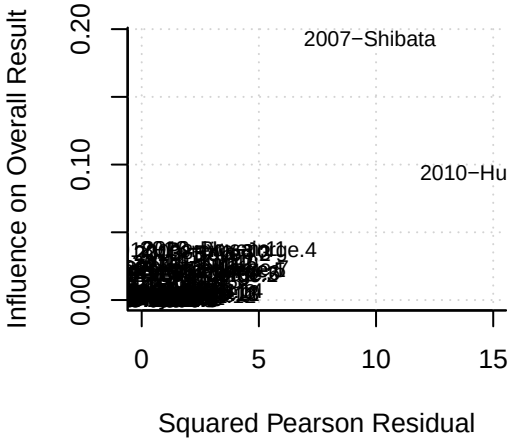

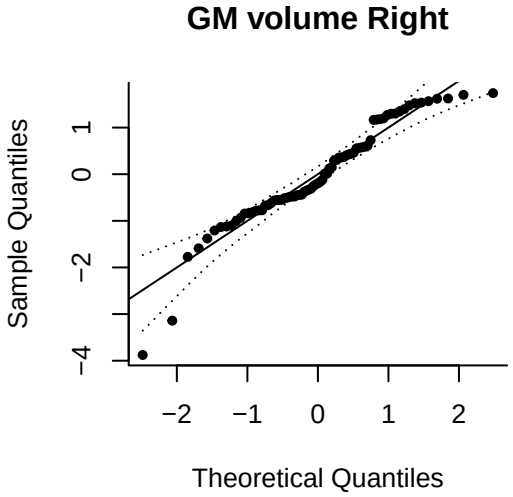

Heterogeneny: GM volume Left

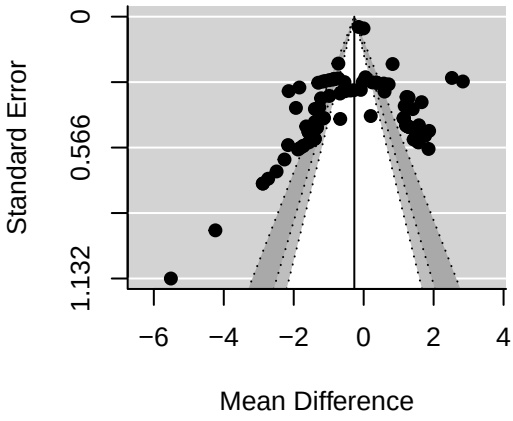

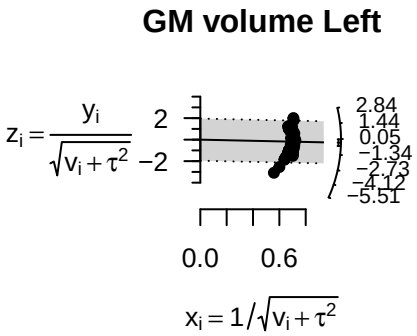

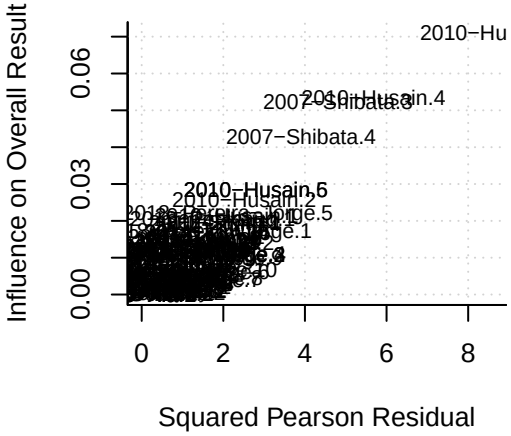

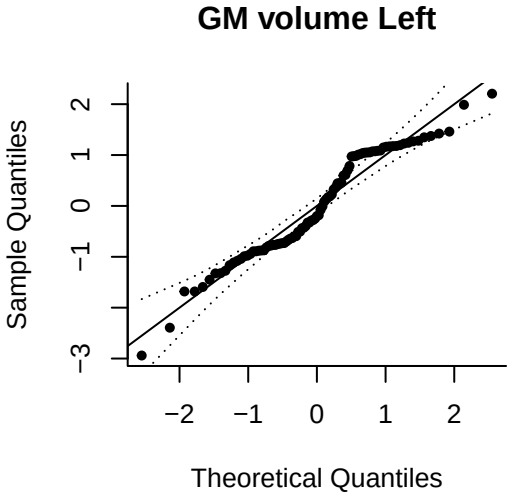

Heterogeney: WM FA Right

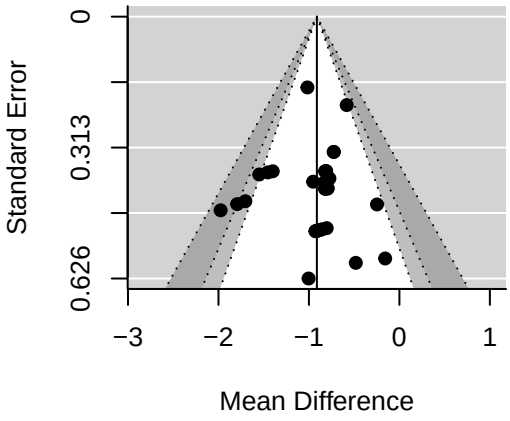

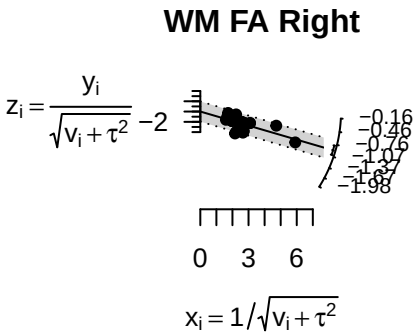

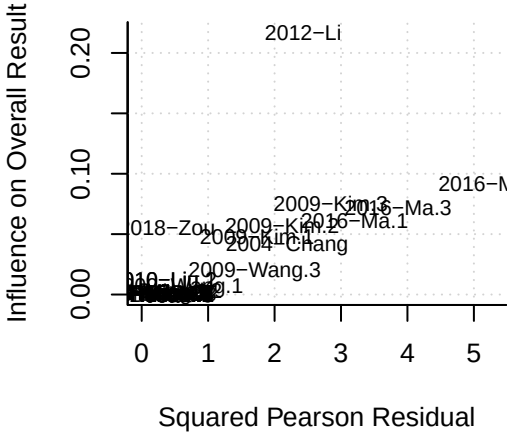

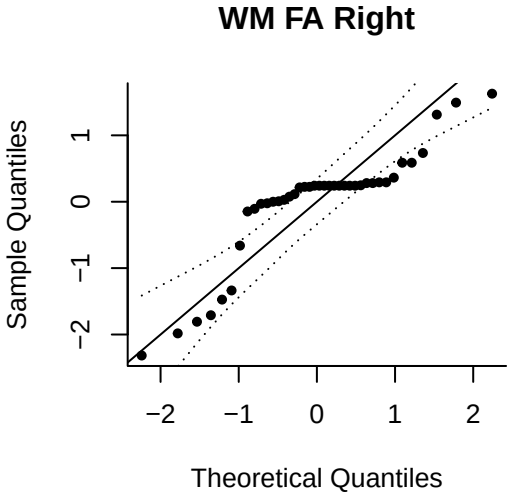

Heterogeney: WM FA Left

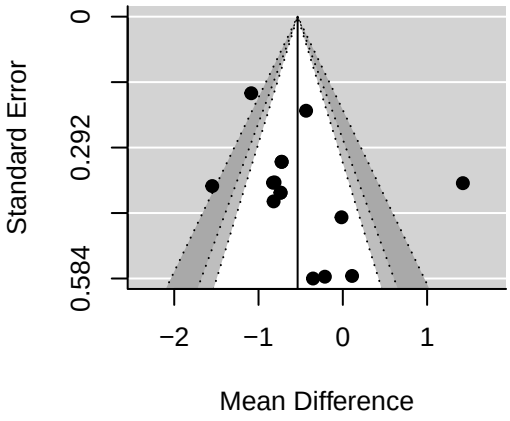

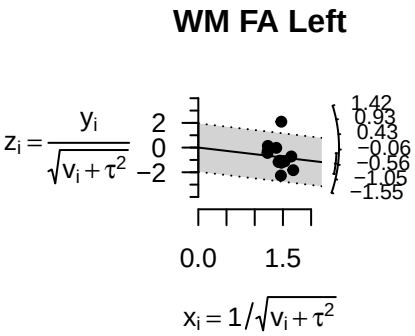

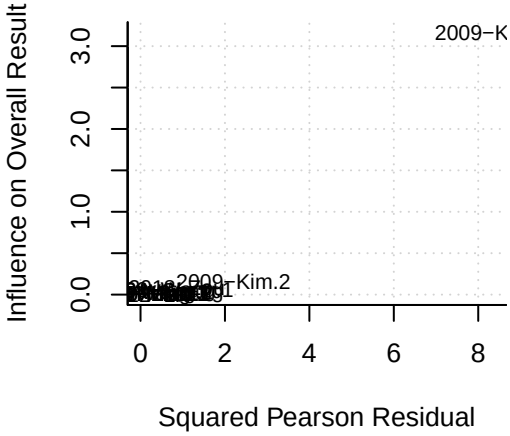

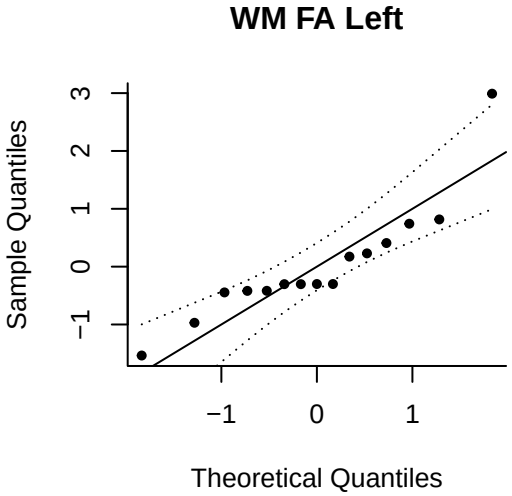

Heterogeney: WM volume Right

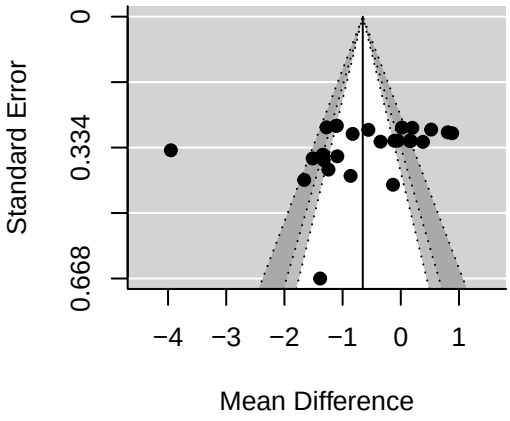

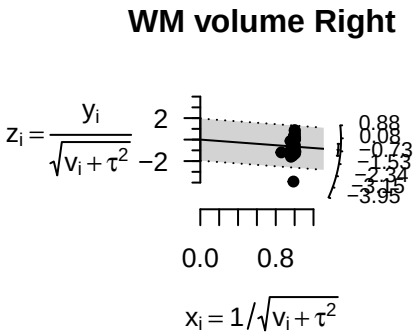

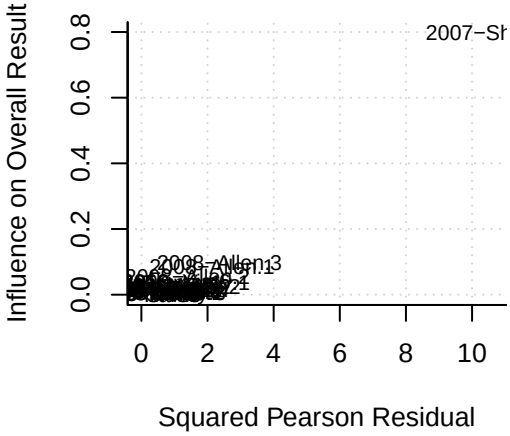

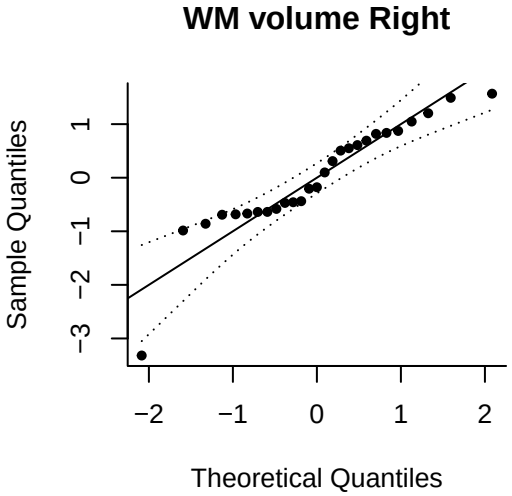

Heterogeneny: WM volume Left

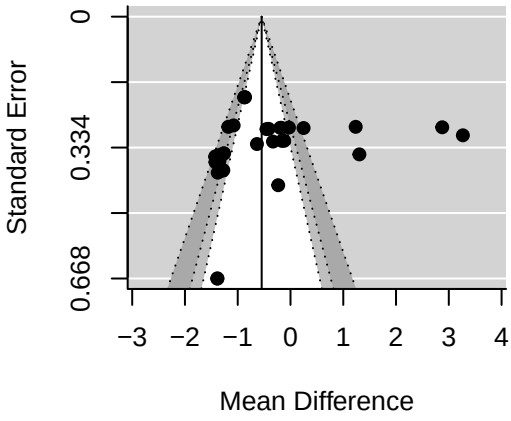

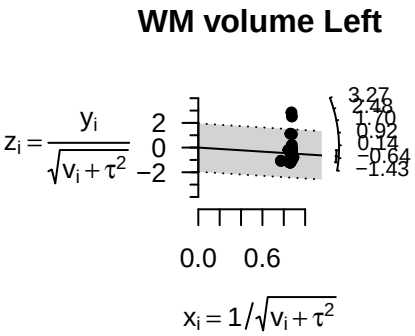

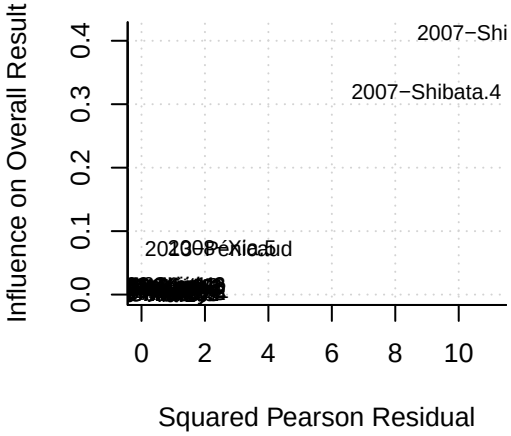

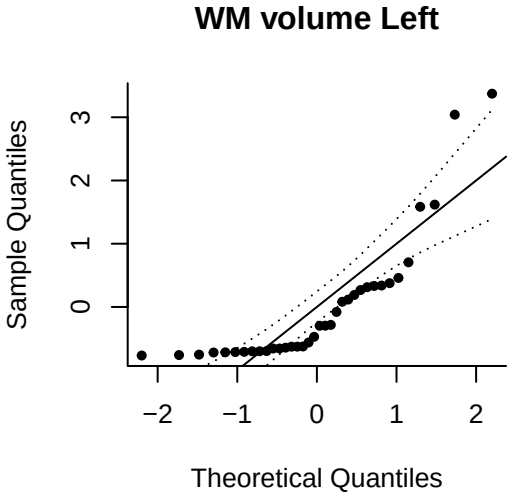

Meta-regressions of Gray Matter Volume & Brain Areas: Random effects model no intercept covariated by Side

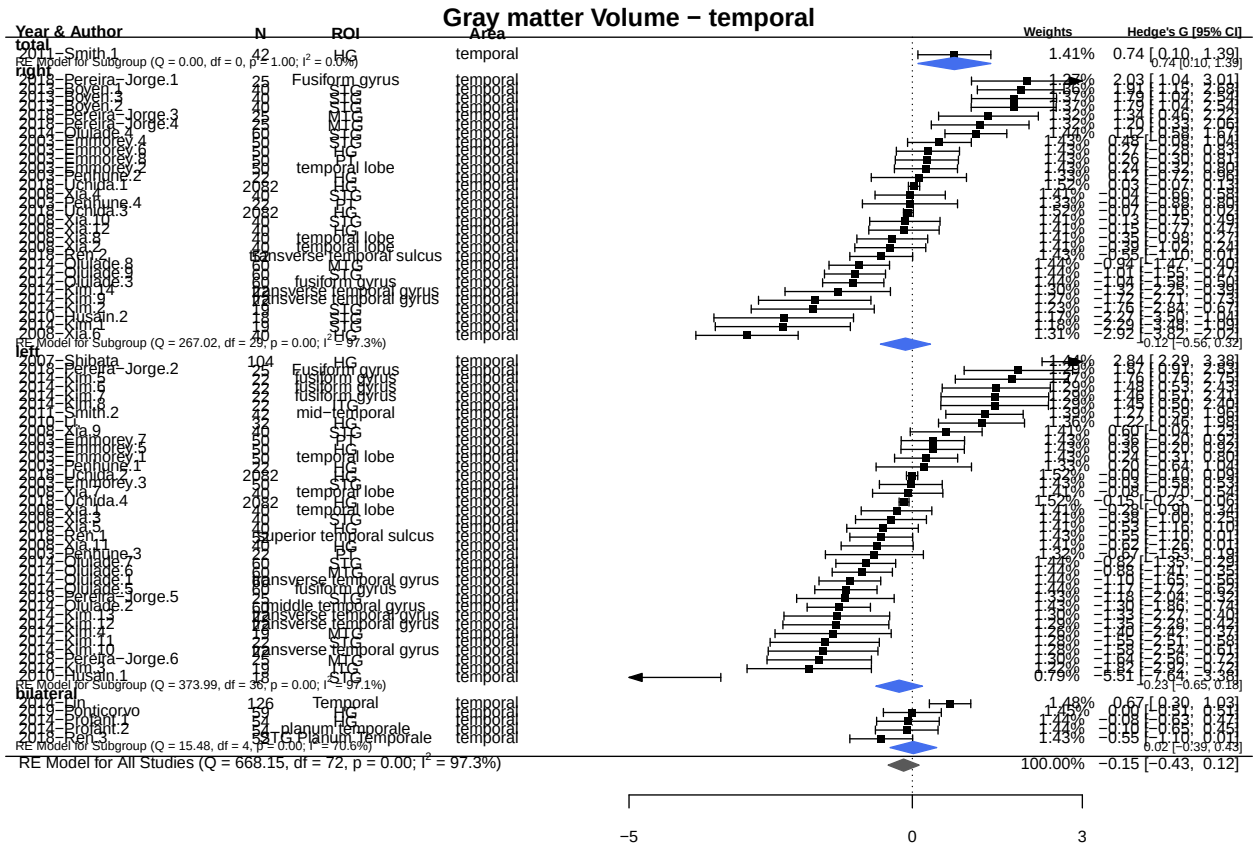

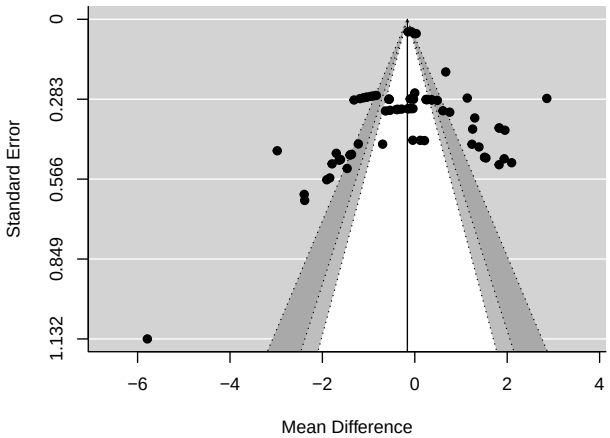

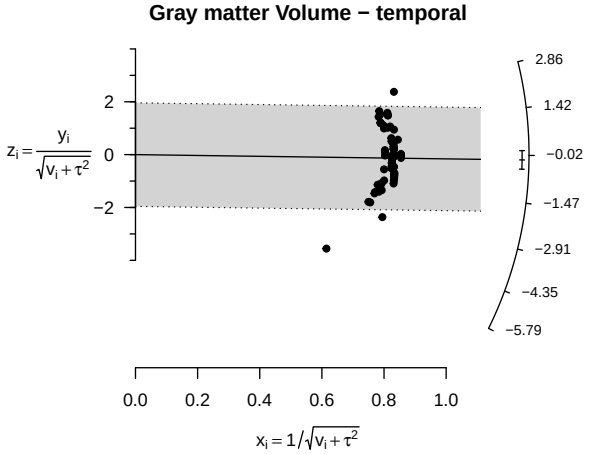

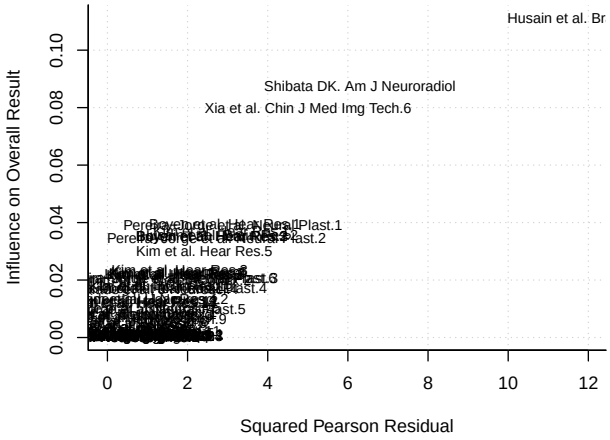

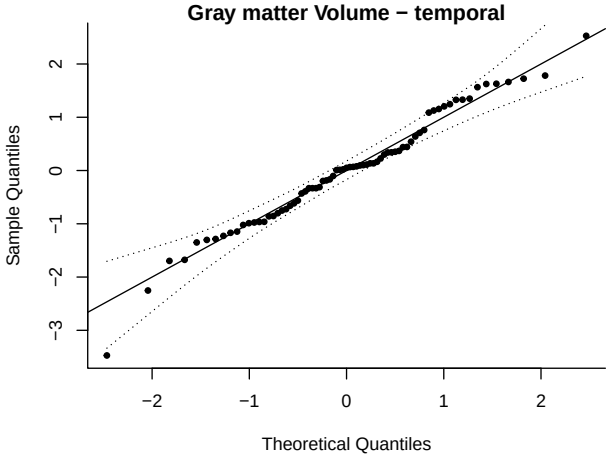

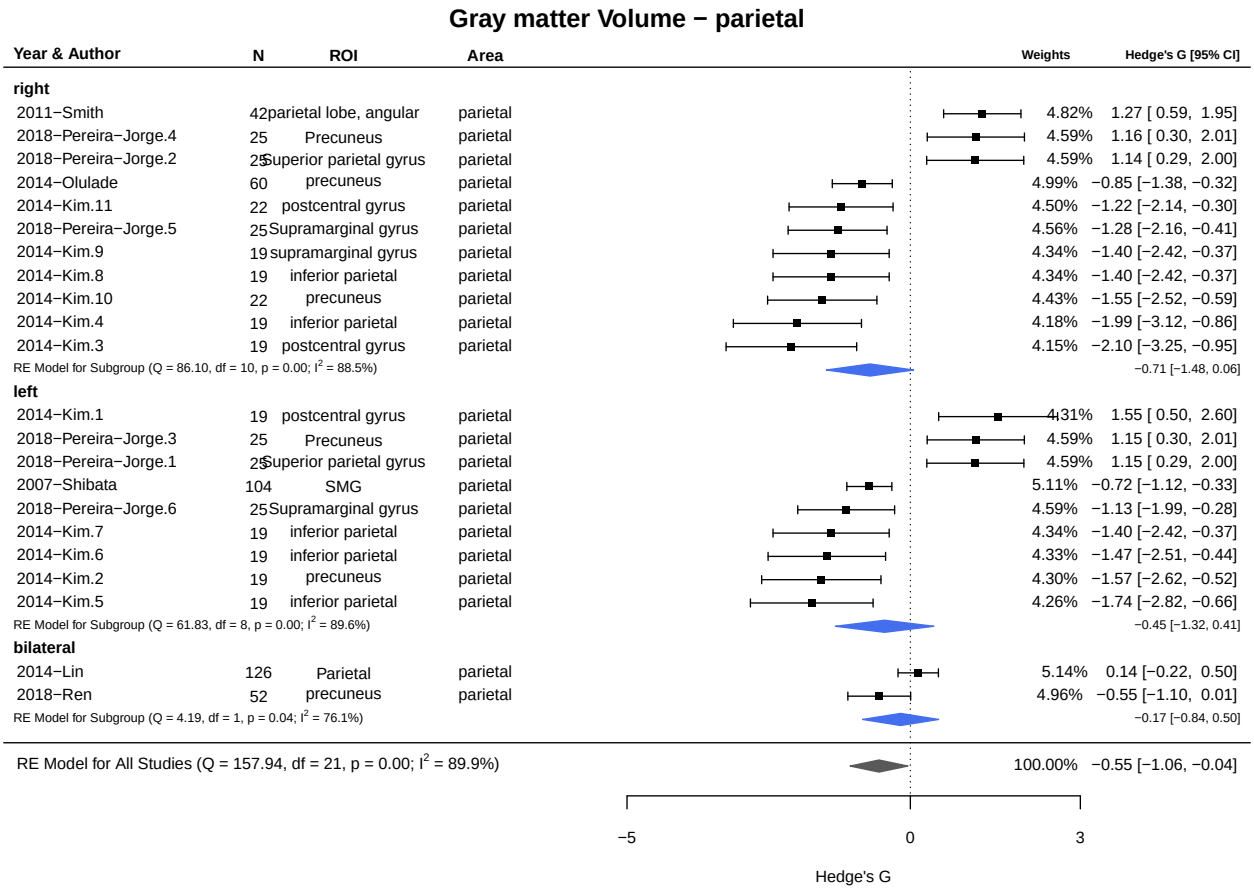
Gray matter Volume − parietal
Year & Author
N
ROI
Area
Weights
Hedge's G [95% CI]
right
2011−Smith 42 parietal lobe, angular parietal 4.82% 1.27 [0.59, 1.95]
2018−Pereira−Jorge.4 25 Precuneus parietal 4.59% 1.16 [0.30, 2.01]
2018−Pereira−Jorge.2 25 Superior parietal gyrus parietal 4.59% 1.14 [0.29, 2.00]
2014−Olulade 60 precuneus parietal 4.99% −0.85 [−1.38, −0.32]
2014−Kim.11 22 postcentral gyrus parietal 4.50% −1.22 [−2.14, −0.30]
2018−Pereira−Jorge.5 25 Supramarginal gyrus parietal 4.56% −1.28 [−2.16, −0.41]
2014−Kim.9 19 supramarginal gyrus parietal 4.34% −1.40 [−2.42, −0.37]
2014−Kim.8 19 inferior parietal parietal 4.34% −1.40 [−2.42, −0.37]
2014−Kim.10 22 precuneus parietal 4.43% −1.55 [−2.52, −0.59]
2014−Kim.4 19 inferior parietal parietal 4.18% −1.99 [−3.12, −0.86]
2014−Kim.3 19 postcentral gyrus parietal 4.15% −2.10 [−3.25, −0.95]
RE Model for Subgroup (Q = 86.10, df = 10, p = 0.00; I² = 88.5%) −0.71 [−1.48, 0.06]
left
2014−Kim.1 19 postcentral gyrus parietal 4.31% 1.55 [0.50, 2.60]
2018−Pereira−Jorge.3 25 Precuneus parietal 4.59% 1.15 [0.30, 2.01]
2018−Pereira−Jorge.1 25 Superior parietal gyrus parietal 4.59% 1.15 [0.29, 2.00]
2007−Shibata 104 SMG parietal 5.11% −0.72 [−1.12, −0.33]
2018−Pereira−Jorge.6 25 Supramarginal gyrus parietal 4.59% −1.13 [−1.99, −0.28]
2014−Kim.7 19 inferior parietal parietal 4.34% −1.40 [−2.42, −0.37]
2014−Kim.6 19 inferior parietal parietal 4.33% −1.47 [−2.51, −0.44]
2014−Kim.2 19 precuneus parietal 4.30% −1.57 [−2.62, −0.52]
2014−Kim.5 19 inferior parietal parietal 4.26% −1.74 [−2.82, −0.66]
RE Model for Subgroup (Q = 61.83, df = 8, p = 0.00; I² = 89.6%) −0.45 [−1.32, 0.41]
bilateral
2014−Lin 126 Parietal parietal 5.14% 0.14 [−0.22, 0.50]
2018−Ren 52 precuneus parietal 4.96% −0.55 [−1.10, 0.01]
RE Model for Subgroup (Q = 4.19, df = 1, p = 0.04; I² = 76.1%) −0.17 [−0.84, 0.50]
RE Model for All Studies (Q = 157.94, df = 21, p = 0.00; I² = 89.9%) 100.00% −0.55 [−1.06, −0.04]
−5
0
3
Hedge's G

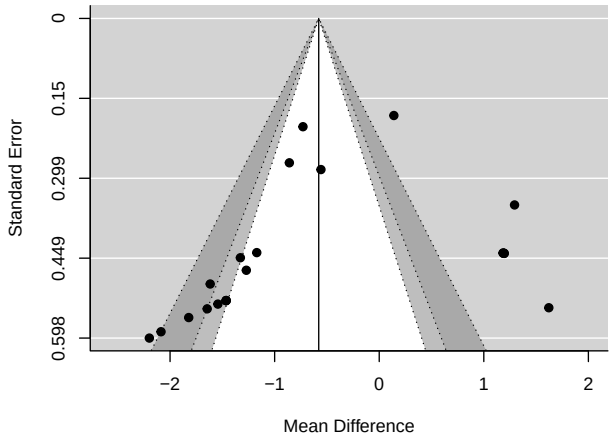
Standard Error
0
0.15
0.299
0.449
0.598
−2
−1
0
1
2
Mean Difference

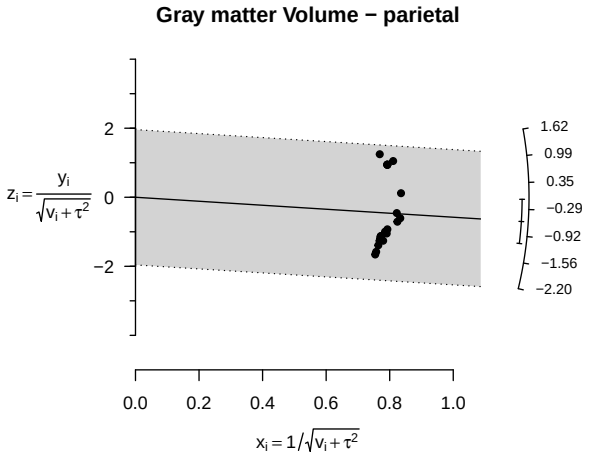
Gray matter Volume − parietal
$z_i = \frac{y_i}{\sqrt{v_i + \tau^2}}$
2
0
−2
1.62
0.99
0.35
−0.29
−0.92
−1.56
−2.20
0.0
0.2
0.4
0.6
0.8
1.0
$x_i = 1/\sqrt{v_i + \tau^2}$

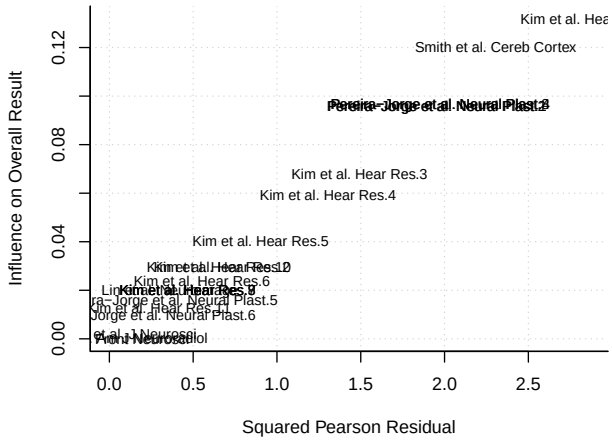
Influence on Overall Result
0.00
0.04
0.08
0.12
Kim et al. Hea
Smith et al. Cereb Cortex
Kim et al. Hear Res.3
Kim et al. Hear Res.4
Kim et al. Hear Res.5
0.0
0.5
1.0
1.5
2.0
2.5
Squared Pearson Residual

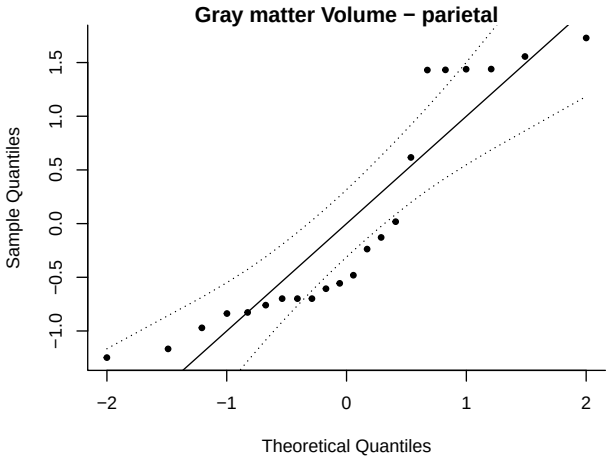
Gray matter Volume − parietal
Sample Quantiles
−1.0
−0.5
0.0
0.5
1.0
1.5
−2
−1
0
1
2
Theoretical Quantiles

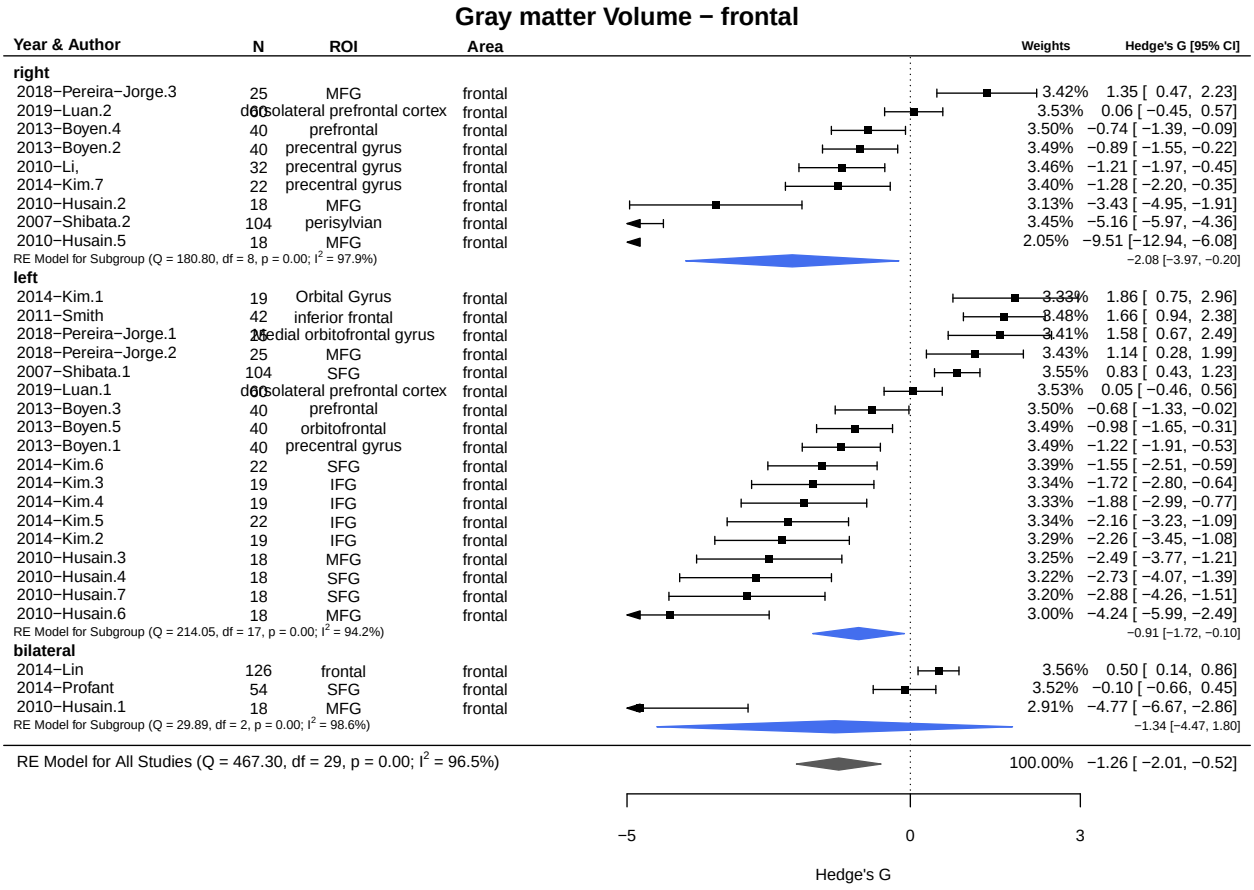
Gray matter Volume − frontal
Year & Author
N
ROI
Area
Weights
Hedge's G [95% CI]
right
2018−Pereira−Jorge.3 25 MFG frontal 3.42% 1.35 [0.47, 2.23]
2019−Luan.2 60 dorsolateral prefrontal cortex frontal 3.53% 0.06 [−0.45, 0.57]
2013−Boyen.4 40 prefrontal frontal 3.50% −0.74 [−1.39, −0.09]
2013−Boyen.2 40 precentral gyrus frontal 3.49% −0.89 [−1.55, −0.22]
2010−Li, 32 precentral gyrus frontal 3.46% −1.21 [−1.97, −0.45]
2014−Kim.7 22 precentral gyrus frontal 3.40% −1.28 [−2.20, −0.35]
2010−Husain.2 18 MFG frontal 3.13% −3.43 [−4.95, −1.91]
2007−Shibata.2 104 perisylvian frontal 3.45% −5.16 [−5.97, −4.36]
2010−Husain.5 18 MFG frontal 2.05% −9.51 [−12.94, −6.08]
RE Model for Subgroup (Q = 180.80, df = 8, p = 0.00; I² = 97.9%) −2.08 [−3.97, −0.20]
left
2014−Kim.1 19 Orbital Gyrus frontal 3.33% 1.86 [0.75, 2.96]
2011−Smith 42 inferior frontal frontal 3.48% 1.66 [0.94, 2.38]
2018−Pereira−Jorge.1 25 medial orbitofrontal gyrus frontal 3.41% 1.58 [0.67, 2.49]
2018−Pereira−Jorge.2 25 MFG frontal 3.43% 1.14 [0.28, 1.99]
2007−Shibata.1 104 SFG frontal 3.55% 0.83 [0.43, 1.23]
2019−Luan.1 60 dorsolateral prefrontal cortex frontal 3.53% 0.05 [−0.46, 0.56]
2013−Boyen.3 40 prefrontal frontal 3.50% −0.68 [−1.33, −0.02]
2013−Boyen.5 40 orbitofrontal frontal 3.49% −0.98 [−1.65, −0.31]
2013−Boyen.1 40 precentral gyrus frontal 3.49% −1.22 [−1.91, −0.53]
2014−Kim.6 22 SFG frontal 3.39% −1.55 [−2.51, −0.59]
2014−Kim.3 19 IFG frontal 3.34% −1.72 [−2.80, −0.64]
2014−Kim.4 19 IFG frontal 3.33% −1.88 [−2.99, −0.77]
2014−Kim.5 22 IFG frontal 3.34% −2.16 [−3.23, −1.09]
2014−Kim.2 19 IFG frontal 3.29% −2.26 [−3.45, −1.08]
2010−Husain.3 18 MFG frontal 3.25% −2.49 [−3.77, −1.21]
2010−Husain.4 18 SFG frontal 3.22% −2.73 [−4.07, −1.39]
2010−Husain.7 18 SFG frontal 3.20% −2.88 [−4.26, −1.51]
2010−Husain.6 18 MFG frontal 3.00% −4.24 [−5.99, −2.49]
RE Model for Subgroup (Q = 214.05, df = 17, p = 0.00; I² = 94.2%) −0.91 [−1.72, −0.10]
bilateral
2014−Lin 126 frontal frontal 3.56% 0.50 [0.14, 0.86]
2014−Profant 54 SFG frontal 3.52% −0.10 [−0.66, 0.45]
2010−Husain.1 18 MFG frontal 2.91% −4.77 [−6.67, −2.86]
RE Model for Subgroup (Q = 29.89, df = 2, p = 0.00; I² = 98.6%) −1.34 [−4.47, 1.80]
RE Model for All Studies (Q = 467.30, df = 29, p = 0.00; I² = 96.5%) 100.00% −1.26 [−2.01, −0.52]
−5
0
3
Hedge's G

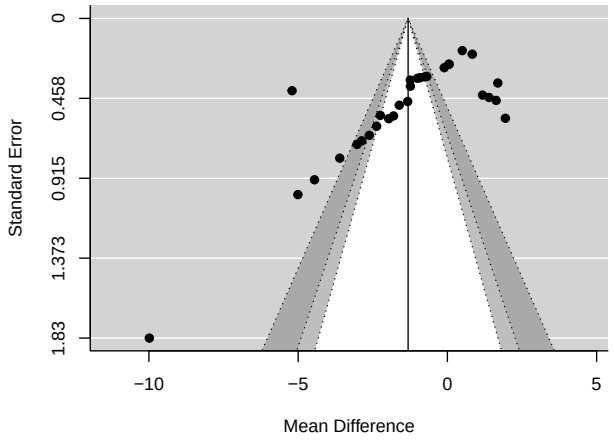
Standard Error
0
0.458
0.915
1.373
1.83
−10
−5
0
5
Mean Difference

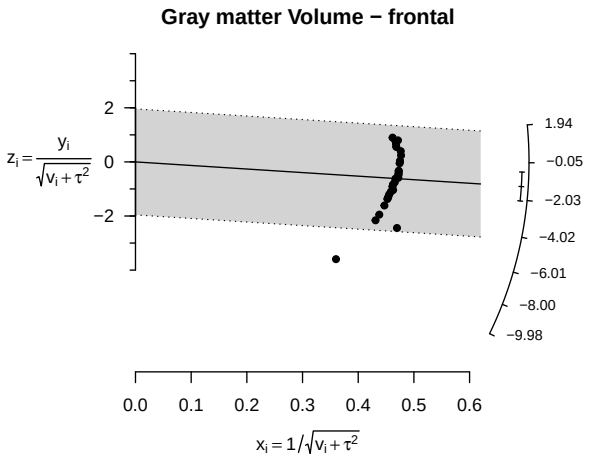
Gray matter Volume − frontal
$z_i = \frac{y_i}{\sqrt{v_i + \tau^2}}$
2
0
−2
1.94
−0.05
−2.03
−4.02
−6.01
−8.00
−9.98
0.0
0.1
0.2
0.3
0.4
0.5
0.6
$x_i = 1/\sqrt{v_i + \tau^2}$

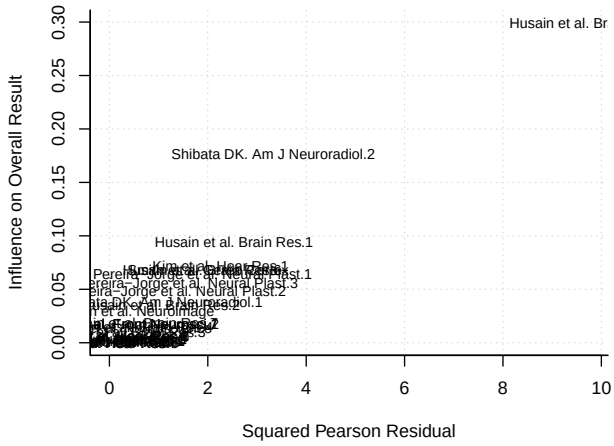
Influence on Overall Result
0.00
0.05
0.10
0.15
0.20
0.25
0.30
Husain et al. Br
Shibata DK. Am J Neuroradiol.2
Husain et al. Brain Res.1
0
2
4
6
8
10
Squared Pearson Residual

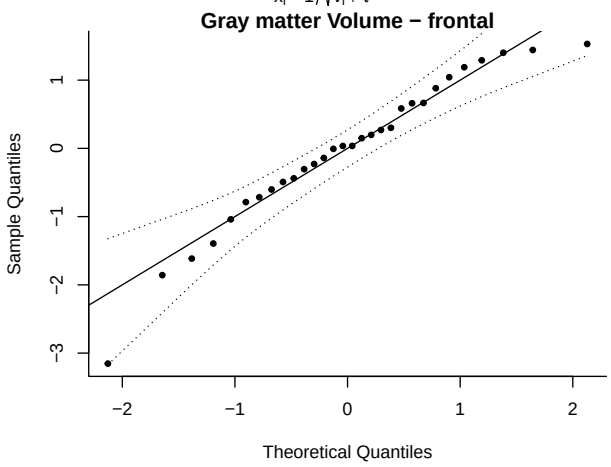
Gray matter Volume − frontal
Sample Quantiles
1
0
−1
−2
−3
−2
−1
0
1
2
Theoretical Quantiles

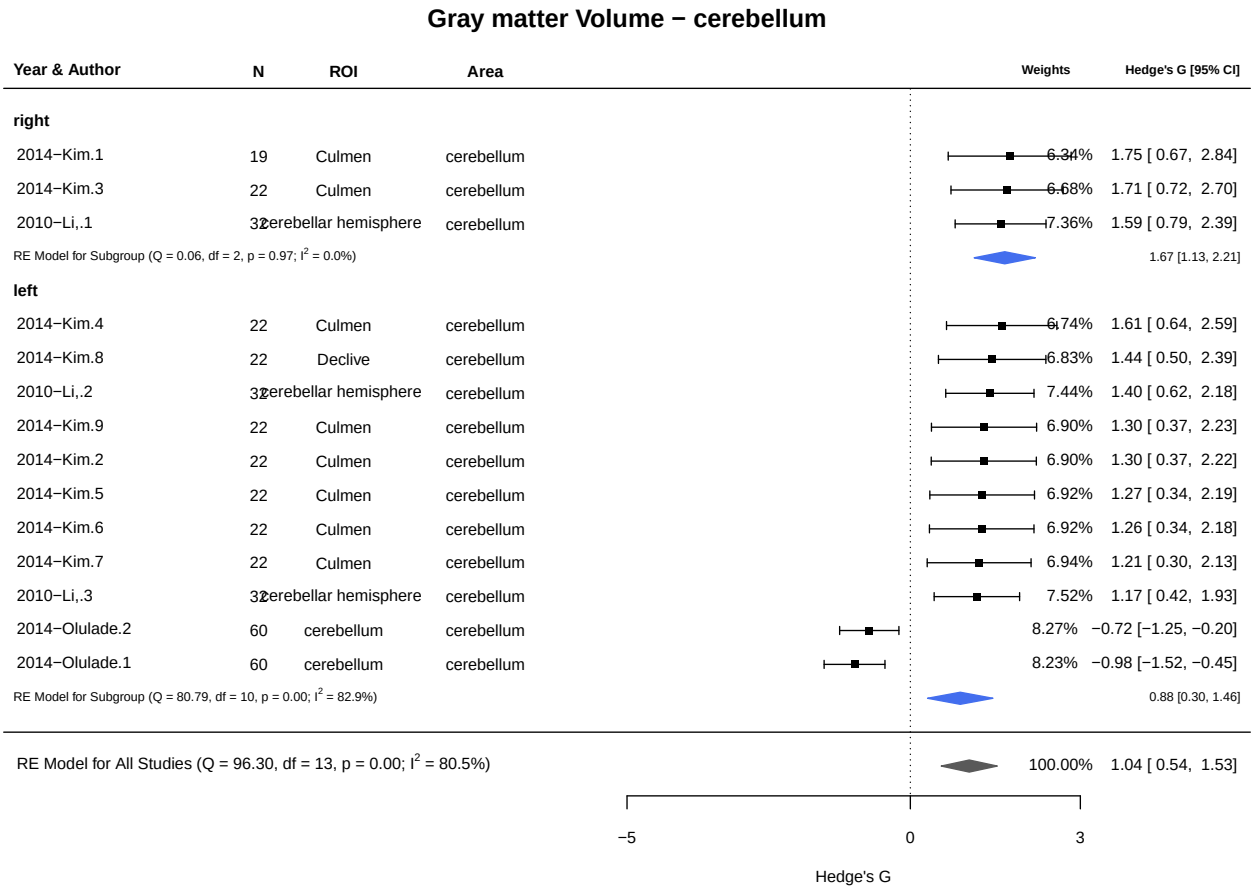
Gray matter Volume − cerebellum
Year & Author
N
ROI
Area
Weights
Hedge's G [95% CI]
right
2014−Kim.1 19 Culmen cerebellum 6.34% 1.75 [0.67, 2.84]
2014−Kim.3 22 Culmen cerebellum 6.68% 1.71 [0.72, 2.70]
2010−Li,.1 32 cerebellar hemisphere cerebellum 7.36% 1.59 [0.79, 2.39]
RE Model for Subgroup (Q = 0.06, df = 2, p = 0.97; I² = 0.0%) 1.67 [1.13, 2.21]
left
2014−Kim.4 22 Culmen cerebellum 6.74% 1.61 [0.64, 2.59]
2014−Kim.8 22 Declive cerebellum 6.83% 1.44 [0.50, 2.39]
2010−Li,.2 32 cerebellar hemisphere cerebellum 7.44% 1.40 [0.62, 2.18]
2014−Kim.9 22 Culmen cerebellum 6.90% 1.30 [0.37, 2.23]
2014−Kim.2 22 Culmen cerebellum 6.90% 1.30 [0.37, 2.22]
2014−Kim.5 22 Culmen cerebellum 6.92% 1.27 [0.34, 2.19]
2014−Kim.6 22 Culmen cerebellum 6.92% 1.26 [0.34, 2.18]
2014−Kim.7 22 Culmen cerebellum 6.94% 1.21 [0.30, 2.13]
2010−Li,.3 32 cerebellar hemisphere cerebellum 7.52% 1.17 [0.42, 1.93]
2014−Olulade.2 60 cerebellum cerebellum 8.27% −0.72 [−1.25, −0.20]
2014−Olulade.1 60 cerebellum cerebellum 8.23% −0.98 [−1.52, −0.45]
RE Model for Subgroup (Q = 80.79, df = 10, p = 0.00; I² = 82.9%) 0.88 [0.30, 1.46]
RE Model for All Studies (Q = 96.30, df = 13, p = 0.00; I² = 80.5%) 100.00% 1.04 [0.54, 1.53]
−5
0
3
Hedge's G

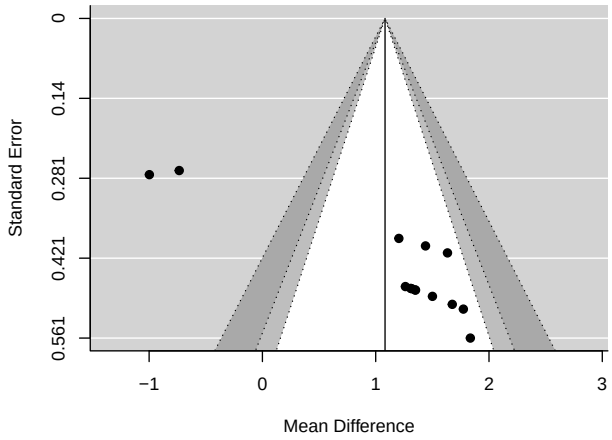
Standard Error
0
0.14
0.281
0.421
0.561
−1
0
1
2
3
Mean Difference

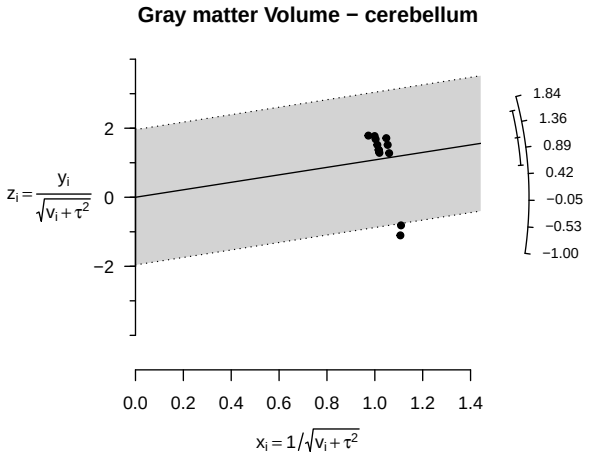
Gray matter Volume − cerebellum
$z_i = \frac{y_i}{\sqrt{v_i + \tau^2}}$
2
0
−2
0.0
0.2
0.4
0.6
0.8
1.0
1.2
1.4
$x_i = 1/\sqrt{v_i + \tau^2}$
1.84
1.36
0.89
0.42
−0.05
−0.53
−1.00

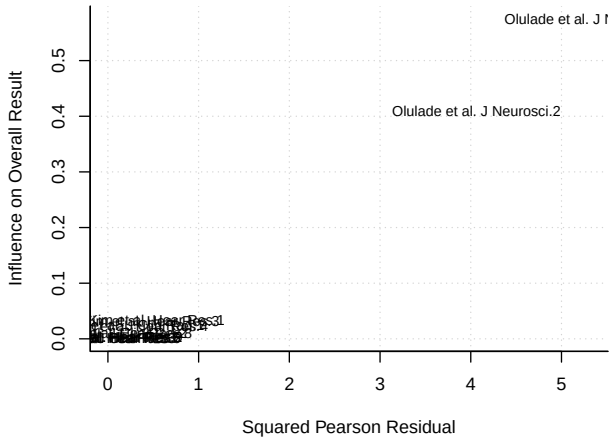
Influence on Overall Result
Olulade et al. J N
Olulade et al. J Neurosci.2
0.0
0.1
0.2
0.3
0.4
0.5
0
1
2
3
4
5
Squared Pearson Residual

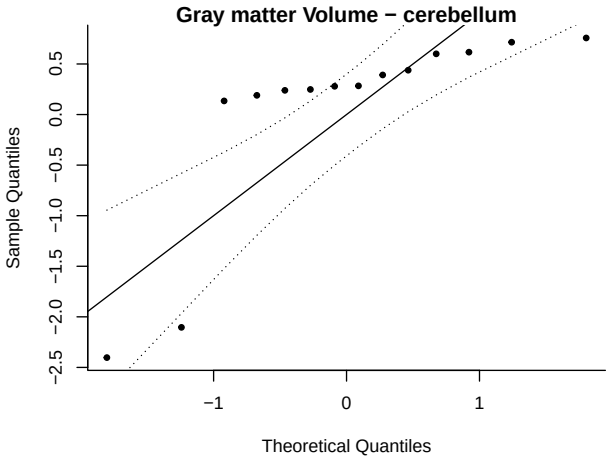
Gray matter Volume − cerebellum
Sample Quantiles
0.5
0.0
−0.5
−1.0
−1.5
−2.0
−2.5
−1
0
1
Theoretical Quantiles

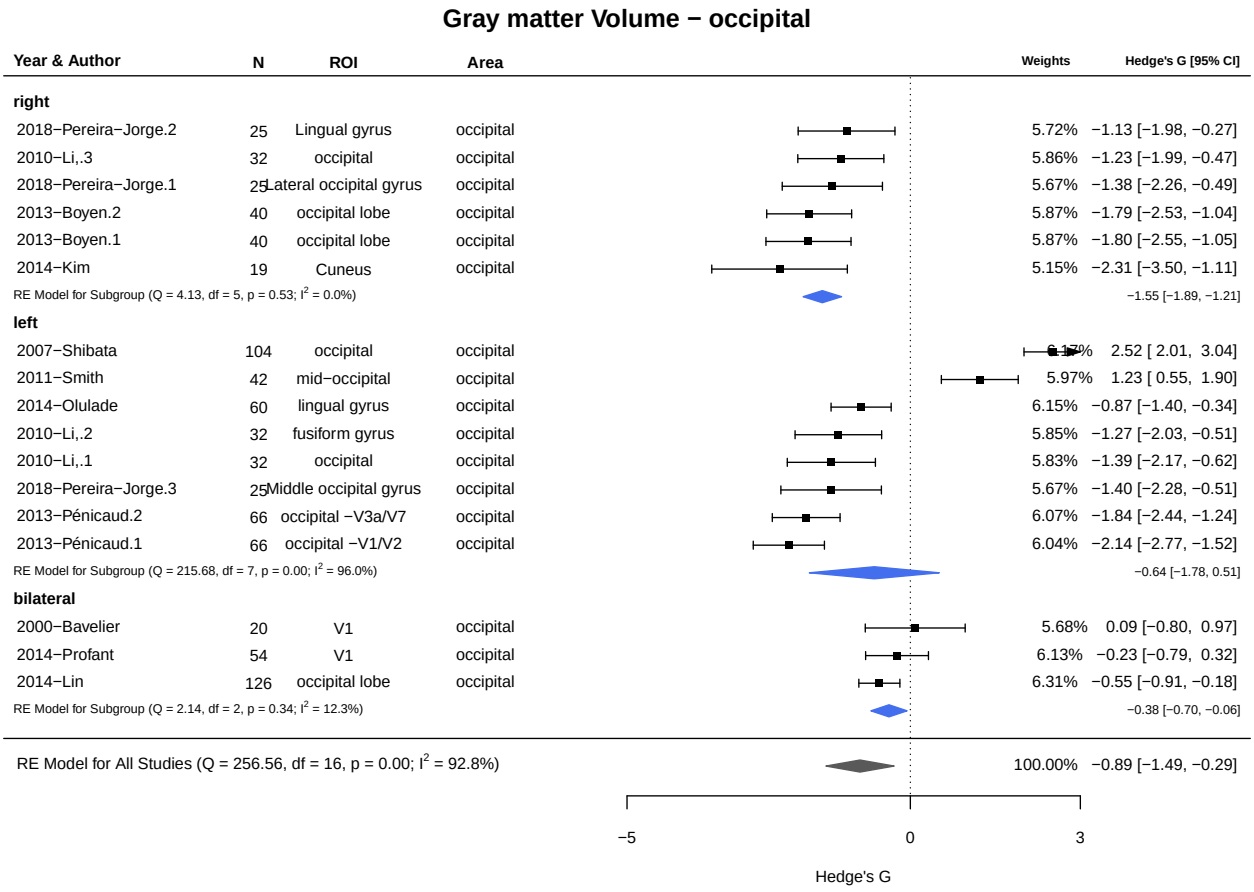
Gray matter Volume − occipital
Year & Author
N
ROI
Area
Weights
Hedge's G [95% CI]
right
2018−Pereira−Jorge.2 25 Lingual gyrus occipital 5.72% −1.13 [−1.98, −0.27]
2010−Li,.3 32 occipital occipital 5.86% −1.23 [−1.99, −0.47]
2018−Pereira−Jorge.1 25 Lateral occipital gyrus occipital 5.67% −1.38 [−2.26, −0.49]
2013−Boyen.2 40 occipital lobe occipital 5.87% −1.79 [−2.53, −1.04]
2013−Boyen.1 40 occipital lobe occipital 5.87% −1.80 [−2.55, −1.05]
2014−Kim 19 Cuneus occipital 5.15% −2.31 [−3.50, −1.11]
RE Model for Subgroup (Q = 4.13, df = 5, p = 0.53; I² = 0.0%) −1.55 [−1.89, −1.21]
left
2007−Shibata 104 occipital occipital 6.17% 2.52 [2.01, 3.04]
2011−Smith 42 mid−occipital occipital 5.97% 1.23 [0.55, 1.90]
2014−Olulade 60 lingual gyrus occipital 6.15% −0.87 [−1.40, −0.34]
2010−Li,.2 32 fusiform gyrus occipital 5.85% −1.27 [−2.03, −0.51]
2010−Li,.1 32 occipital occipital 5.83% −1.39 [−2.17, −0.62]
2018−Pereira−Jorge.3 25 Middle occipital gyrus occipital 5.67% −1.40 [−2.28, −0.51]
2013−Pénicaud.2 66 occipital −V3a/V7 occipital 6.07% −1.84 [−2.44, −1.24]
2013−Pénicaud.1 66 occipital −V1/V2 occipital 6.04% −2.14 [−2.77, −1.52]
RE Model for Subgroup (Q = 215.68, df = 7, p = 0.00; I² = 96.0%) −0.64 [−1.78, 0.51]
bilateral
2000−Bavelier 20 V1 occipital 5.68% 0.09 [−0.80, 0.97]
2014−Profant 54 V1 occipital 6.13% −0.23 [−0.79, 0.32]
2014−Lin 126 occipital lobe occipital 6.31% −0.55 [−0.91, −0.18]
RE Model for Subgroup (Q = 2.14, df = 2, p = 0.34; I² = 12.3%) −0.38 [−0.70, −0.06]
RE Model for All Studies (Q = 256.56, df = 16, p = 0.00; I² = 92.8%) 100.00% −0.89 [−1.49, −0.29]
−5
0
3
Hedge's G

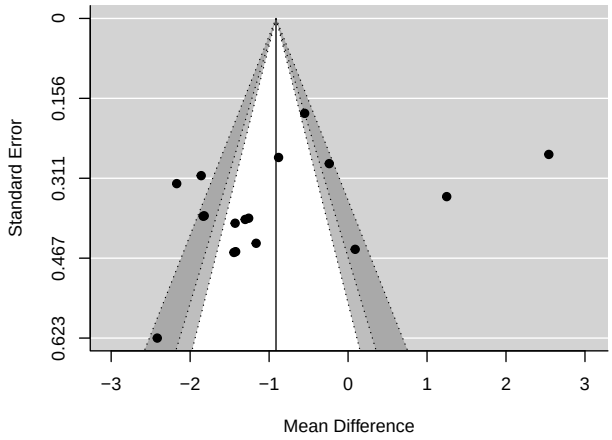
Standard Error
0
0.156
0.311
0.467
0.623
−3
−2
−1
0
1
2
3
Mean Difference

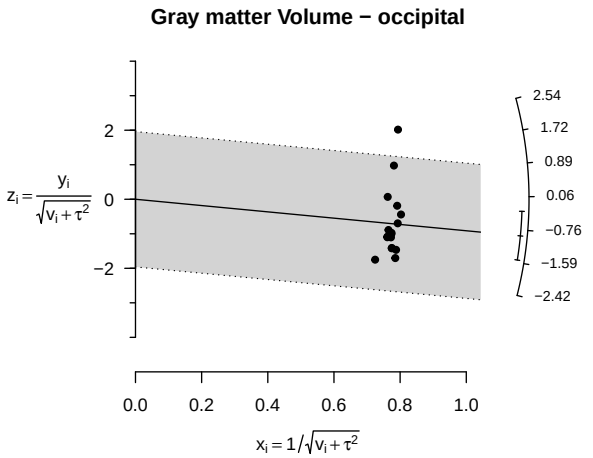
Gray matter Volume − occipital
$z_i = \frac{y_i}{\sqrt{v_i + \tau^2}}$
2
0
−2
2.54
1.72
0.89
0.06
−0.76
−1.59
−2.42
0.0
0.2
0.4
0.6
0.8
1.0
$x_i = 1/\sqrt{v_i + \tau^2}$

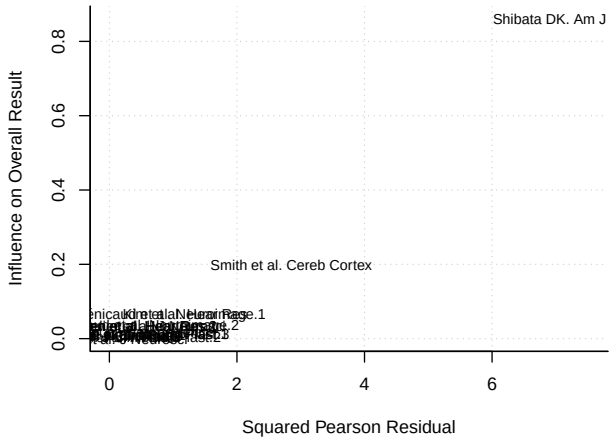
Influence on Overall Result
0.0
0.2
0.4
0.6
0.8
Shibata DK. Am J
Smith et al. Cereb Cortex
0
2
4
6
Squared Pearson Residual

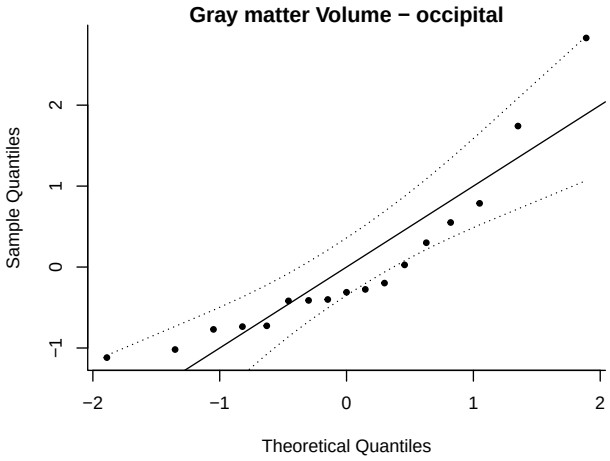
Gray matter Volume − occipital
Sample Quantiles
−1
0
1
2
−2
−1
0
1
2
Theoretical Quantiles

Gray matter Volume − insular cortex

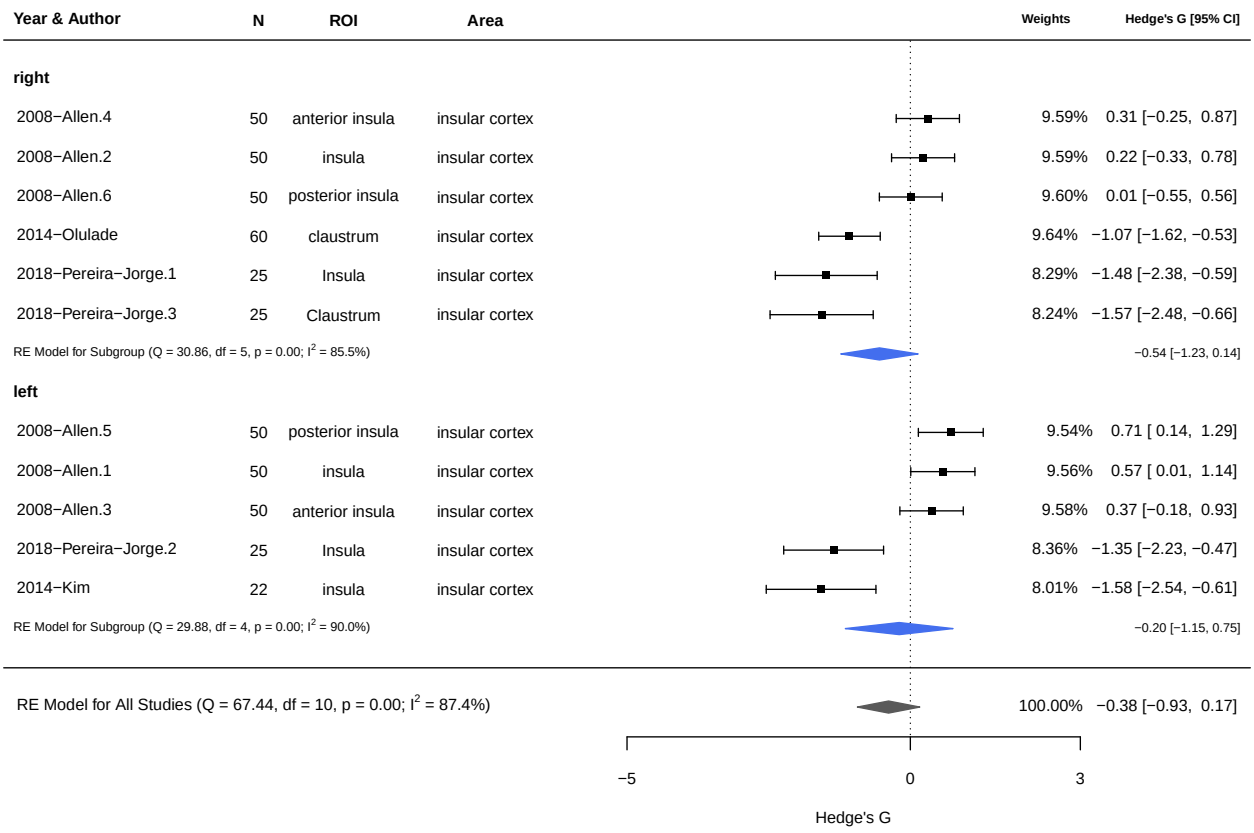

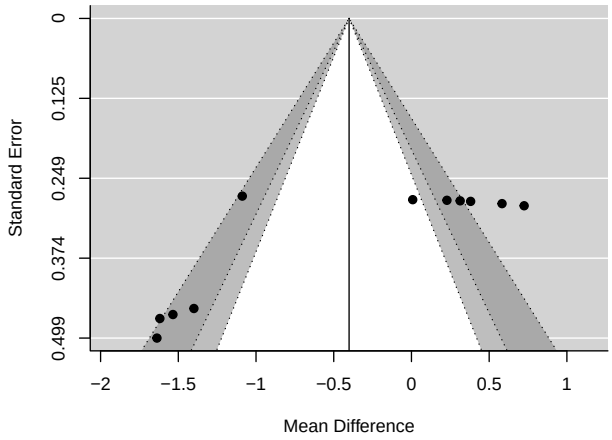
Standard Error
0
0.125
0.249
0.374
0.499
−2
−1.5
−1
−0.5
0
0.5
1
Mean Difference

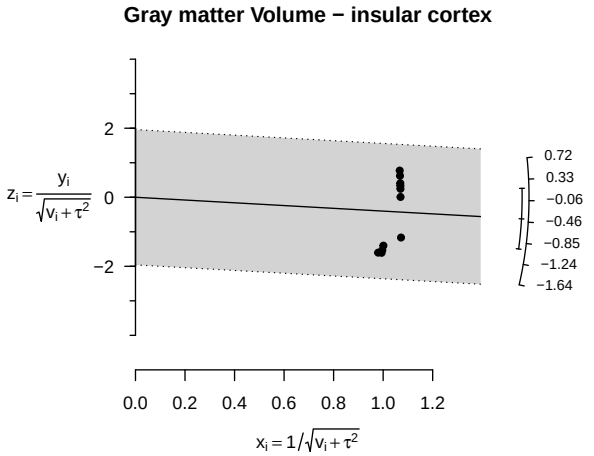
Gray matter Volume − insular cortex
$z_i = \frac{y_i}{\sqrt{v_i + \tau^2}}$
2
0
−2
0.72
0.33
−0.06
−0.46
−0.85
−1.24
−1.64
0.0
0.2
0.4
0.6
0.8
1.0
1.2
$x_i = 1/\sqrt{v_i + \tau^2}$

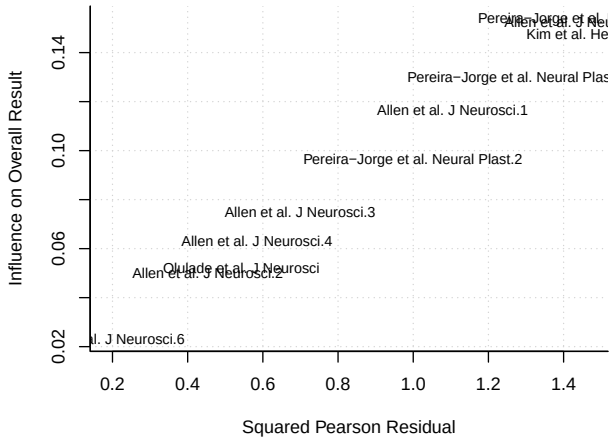
Influence on Overall Result
0.02
0.06
0.10
0.14
Pereira−Jorge et al.
Kim et al. He
Pereira−Jorge et al. Neural Plas
Allen et al. J Neurosci.1
Pereira−Jorge et al. Neural Plast.2
Allen et al. J Neurosci.3
Allen et al. J Neurosci.4
Oludade et al. J Neurosci
Allen et al. J Neurosci.2
l. J Neurosci.6
0.2
0.4
0.6
0.8
1.0
1.2
1.4
Squared Pearson Residual

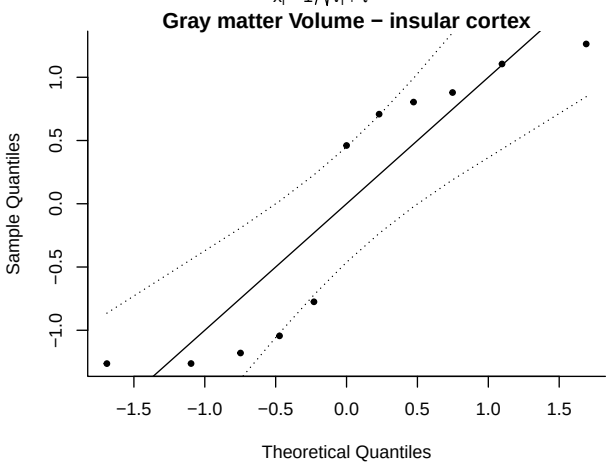
Gray matter Volume − insular cortex
Sample Quantiles
−1.0
−0.5
0.0
0.5
1.0
−1.5
−1.0
−0.5
0.0
0.5
1.0
1.5
Theoretical Quantiles

Meta-regressions of White Matter FA & Brain Areas: Random effects model no intercept covariated by Side

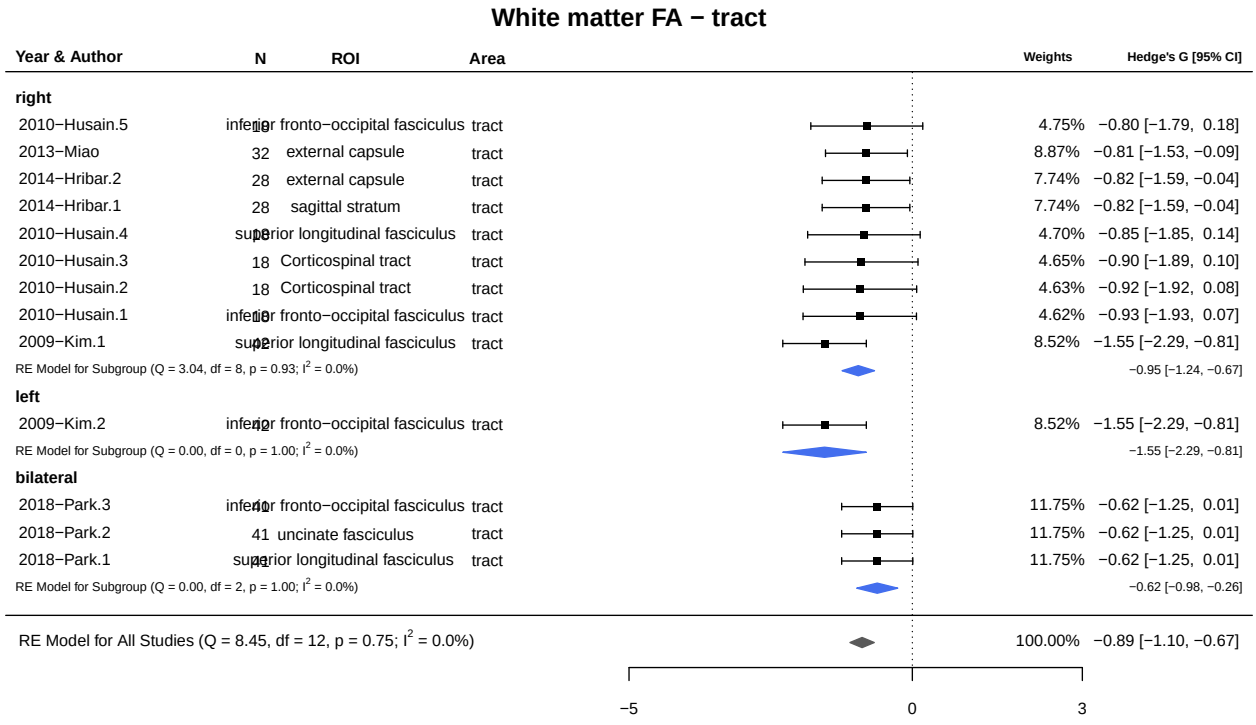

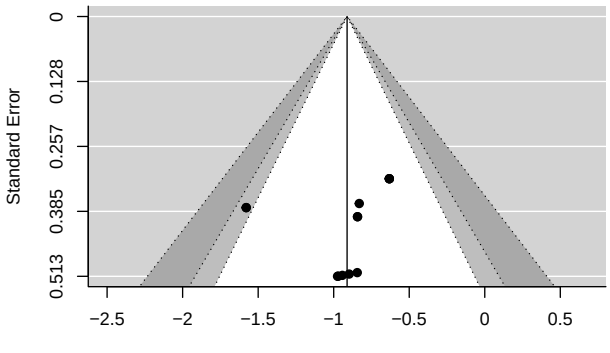

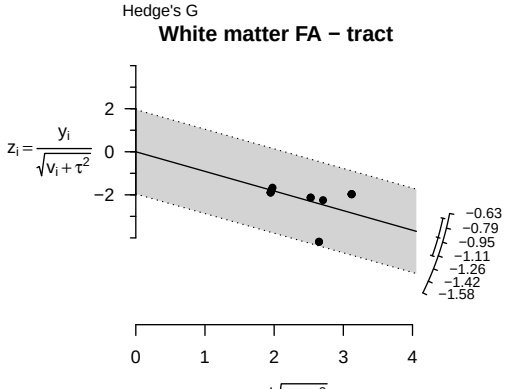

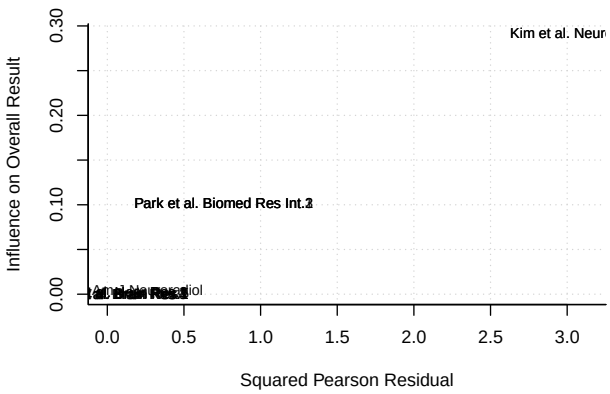

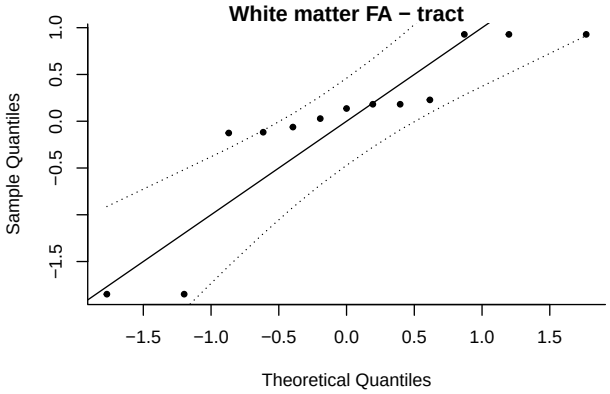

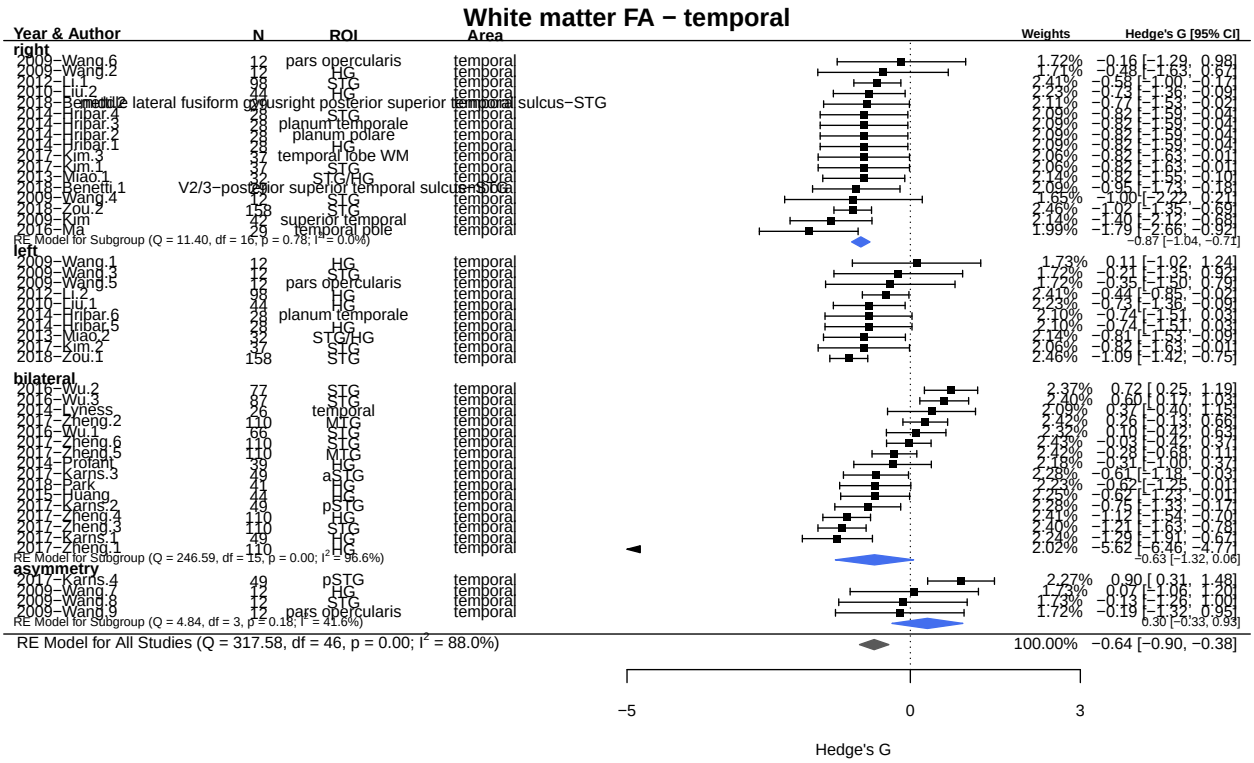

Error in rma(yi = hedgesG, vi = varG, data = meta.mod, measure = "MD", : Fisher scoring algorithm did

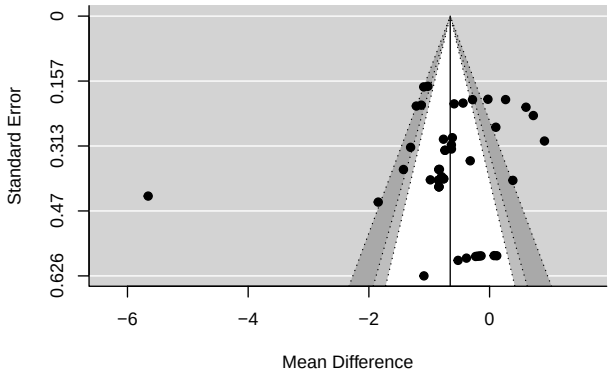

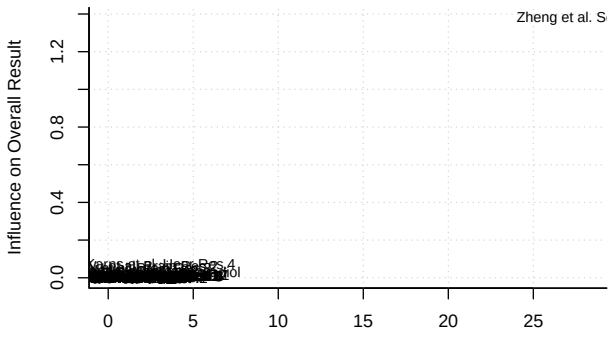

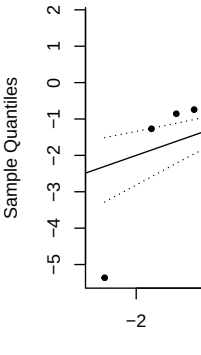

not converge. See 'help(rma)' for possible remedies.

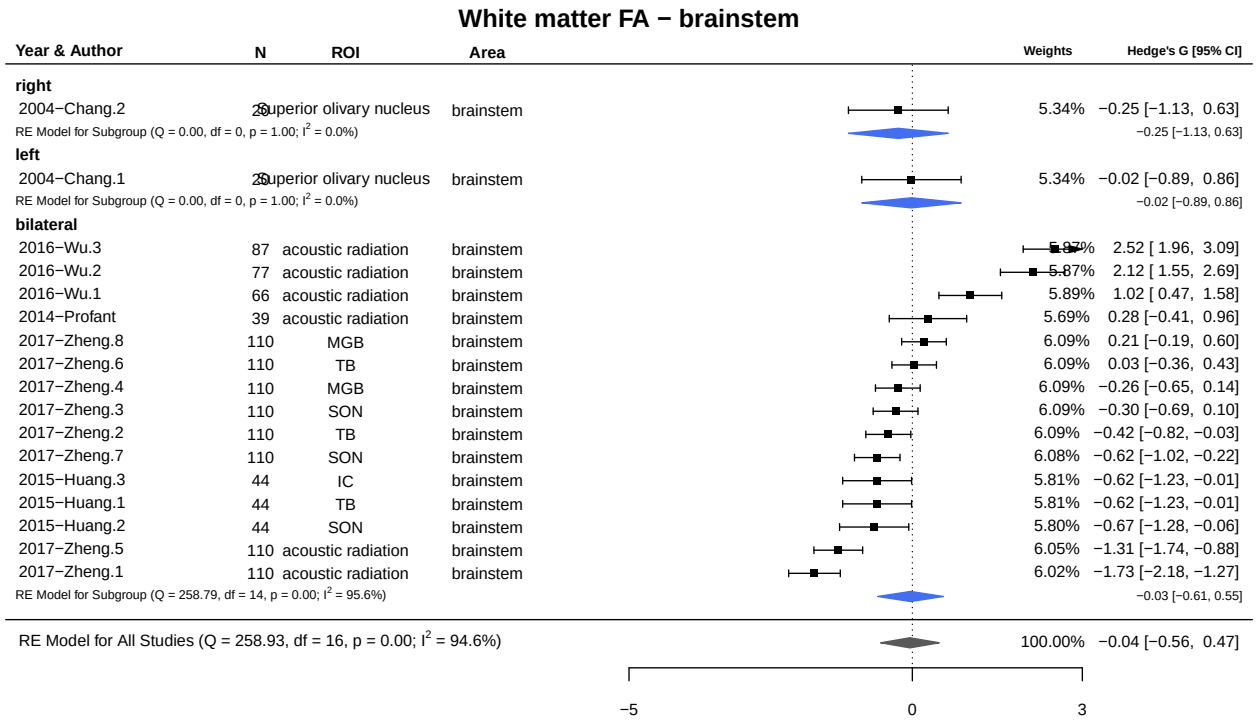
White matter FA − brainstem
Year & Author
N
ROI
Area
Weights
Hedge's G [95% CI]
right
2004−Chang.2 20 superior olivary nucleus brainstem 5.34% −0.25 [−1.13, 0.63]
RE Model for Subgroup (Q = 0.00, df = 0, p = 1.00; I² = 0.0%) −0.25 [−1.13, 0.63]
left
2004−Chang.1 20 superior olivary nucleus brainstem 5.34% −0.02 [−0.89, 0.86]
RE Model for Subgroup (Q = 0.00, df = 0, p = 1.00; I² = 0.0%) −0.02 [−0.89, 0.86]
bilateral
2016−Wu.3 87 acoustic radiation brainstem 5.87% 2.52 [1.96, 3.09]
2016−Wu.2 77 acoustic radiation brainstem 5.87% 2.12 [1.55, 2.69]
2016−Wu.1 66 acoustic radiation brainstem 5.89% 1.02 [0.47, 1.58]
2014−Profant 39 acoustic radiation brainstem 5.69% 0.28 [−0.41, 0.96]
2017−Zheng.8 110 MGB brainstem 6.09% 0.21 [−0.19, 0.60]
2017−Zheng.6 110 TB brainstem 6.09% 0.03 [−0.36, 0.43]
2017−Zheng.4 110 MGB brainstem 6.09% −0.26 [−0.65, 0.14]
2017−Zheng.3 110 SON brainstem 6.09% −0.30 [−0.69, 0.10]
2017−Zheng.2 110 TB brainstem 6.09% −0.42 [−0.82, −0.03]
2017−Zheng.7 110 SON brainstem 6.08% −0.62 [−1.02, −0.22]
2015−Huang.3 44 IC brainstem 5.81% −0.62 [−1.23, −0.01]
2015−Huang.1 44 TB brainstem 5.81% −0.62 [−1.23, −0.01]
2015−Huang.2 44 SON brainstem 5.80% −0.67 [−1.28, −0.06]
2017−Zheng.5 110 acoustic radiation brainstem 6.05% −1.31 [−1.74, −0.88]
2017−Zheng.1 110 acoustic radiation brainstem 6.02% −1.73 [−2.18, −1.27]
RE Model for Subgroup (Q = 258.79, df = 14, p = 0.00; I² = 95.6%) −0.03 [−0.61, 0.55]
RE Model for All Studies (Q = 258.93, df = 16, p = 0.00; I² = 94.6%) 100.00% −0.04 [−0.56, 0.47]
−5
0
3
Hedge's G

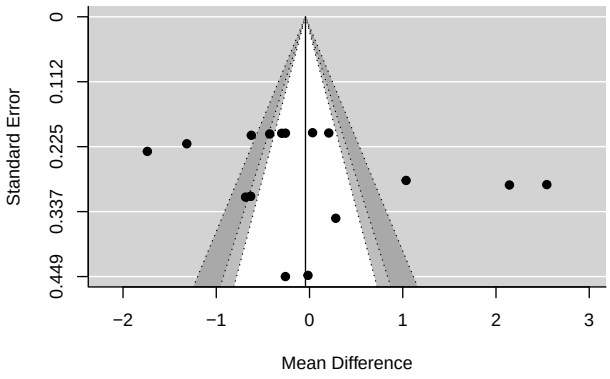
Standard Error
0
0.112
0.225
0.337
0.449
−2
−1
0
1
2
3
Mean Difference

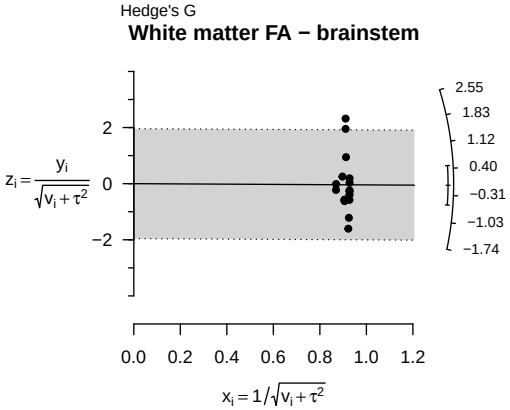
White matter FA − brainstem
$z_i = \frac{y_i}{\sqrt{v_i + \tau^2}}$
2
0
−2
2.55
1.83
1.12
0.40
−0.31
−1.03
−1.74
0.0
0.2
0.4
0.6
0.8
1.0
1.2
$x_i = 1/\sqrt{v_i + \tau^2}$

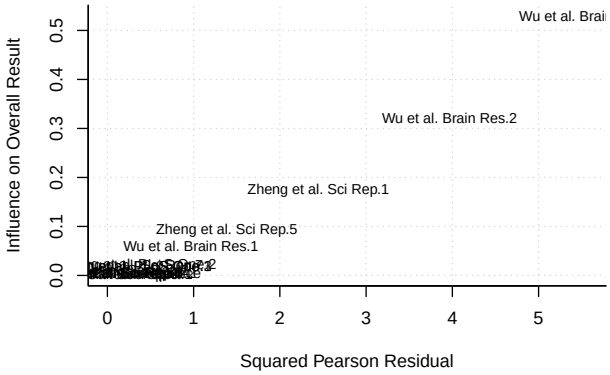
Influence on Overall Result
0.0
0.1
0.2
0.3
0.4
0.5
Wu et al. Brai
Wu et al. Brain Res.2
Zheng et al. Sci Rep.1
Zheng et al. Sci Rep.5
Wu et al. Brain Res.1
0
1
2
3
4
5
Squared Pearson Residual

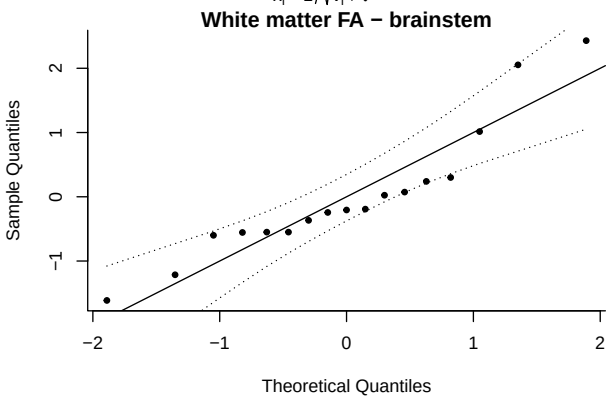
White matter FA − brainstem
Sample Quantiles
−1
0
1
2
−2
−1
0
1
2
Theoretical Quantiles

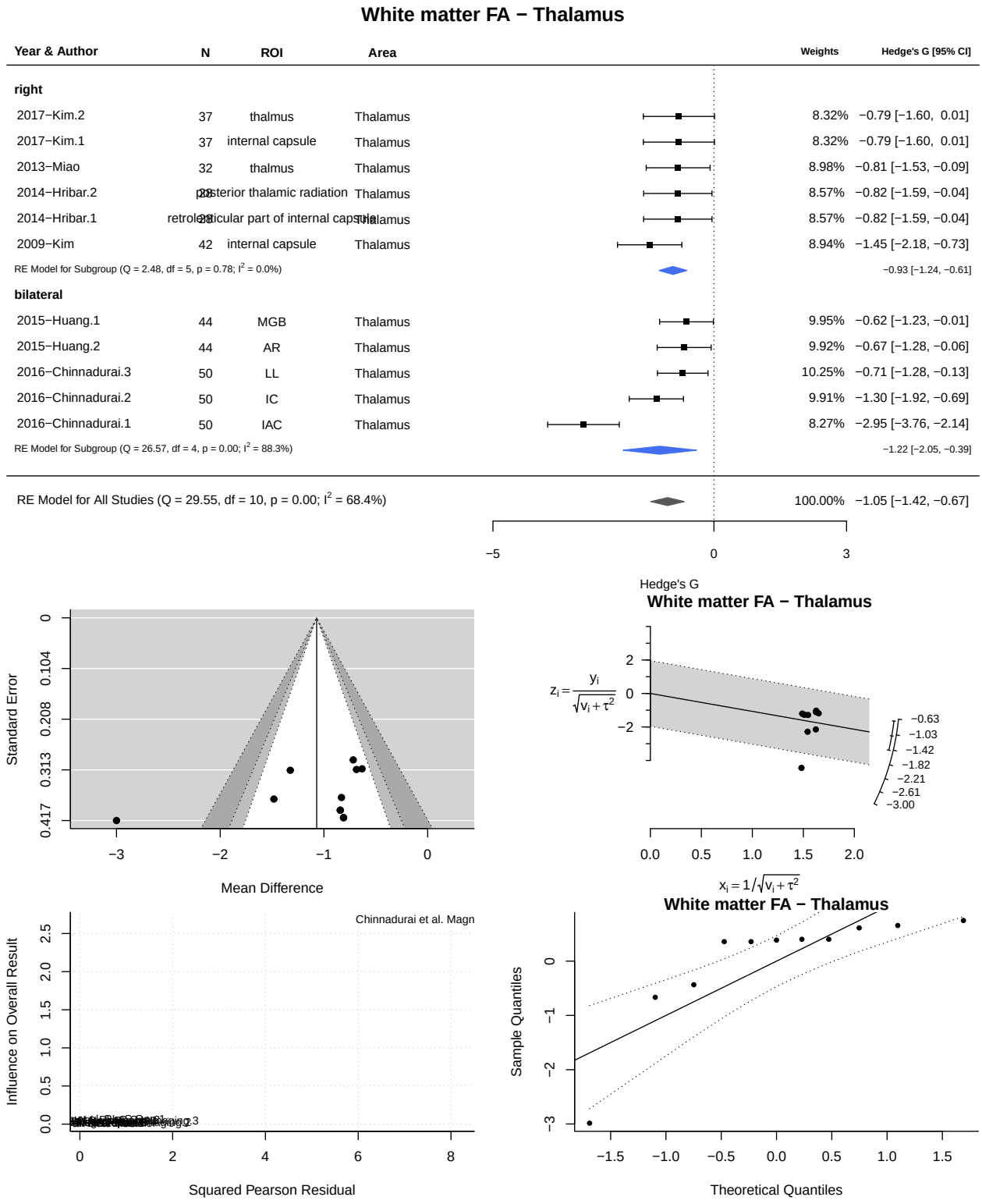
White matter FA − Thalamus
Year & Author
N
ROI
Area
Weights
Hedge's G [95% CI]
right
2017−Kim.2 37 thalmus Thalamus 8.32% −0.79 [−1.60, 0.01]
2017−Kim.1 37 internal capsule Thalamus 8.32% −0.79 [−1.60, 0.01]
2013−Miao 32 thalmus Thalamus 8.98% −0.81 [−1.53, −0.09]
2014−Hribar.2 28 posterior thalamic radiation Thalamus 8.57% −0.82 [−1.59, −0.04]
2014−Hribar.1 28 retrolenticular part of internal capsule Thalamus 8.57% −0.82 [−1.59, −0.04]
2009−Kim 42 internal capsule Thalamus 8.94% −1.45 [−2.18, −0.73]
RE Model for Subgroup (Q = 2.48, df = 5, p = 0.78; I² = 0.0%) −0.93 [−1.24, −0.61]
bilateral
2015−Huang.1 44 MGB Thalamus 9.95% −0.62 [−1.23, −0.01]
2015−Huang.2 44 AR Thalamus 9.92% −0.67 [−1.28, −0.06]
2016−Chinnadurai.3 50 LL Thalamus 10.25% −0.71 [−1.28, −0.13]
2016−Chinnadurai.2 50 IC Thalamus 9.91% −1.30 [−1.92, −0.69]
2016−Chinnadurai.1 50 IAC Thalamus 8.27% −2.95 [−3.76, −2.14]
RE Model for Subgroup (Q = 26.57, df = 4, p = 0.00; I² = 88.3%) −1.22 [−2.05, −0.39]
RE Model for All Studies (Q = 29.55, df = 10, p = 0.00; I² = 68.4%) 100.00% −1.05 [−1.42, −0.67]
−5
0
3
Hedge's G
Standard Error
0
0.104
0.208
0.313
0.417
−3
−2
−1
0
Mean Difference
White matter FA − Thalamus
$z_i = \frac{y_i}{\sqrt{v_i + \tau^2}}$
2
0
−2
−0.63
−1.03
−1.42
−1.82
−2.21
−2.61
−3.00
0.0
0.5
1.0
1.5
2.0
$x_i = 1/\sqrt{v_i + \tau^2}$
Influence on Overall Result
Chinnadurai et al. Magn
0.0
0.5
1.0
1.5
2.0
2.5
0
2
4
6
8
Squared Pearson Residual
White matter FA − Thalamus
Sample Quantiles
0
−1
−2
−3
−1.5
−1.0
−0.5
0.0
0.5
1.0
1.5
Theoretical Quantiles

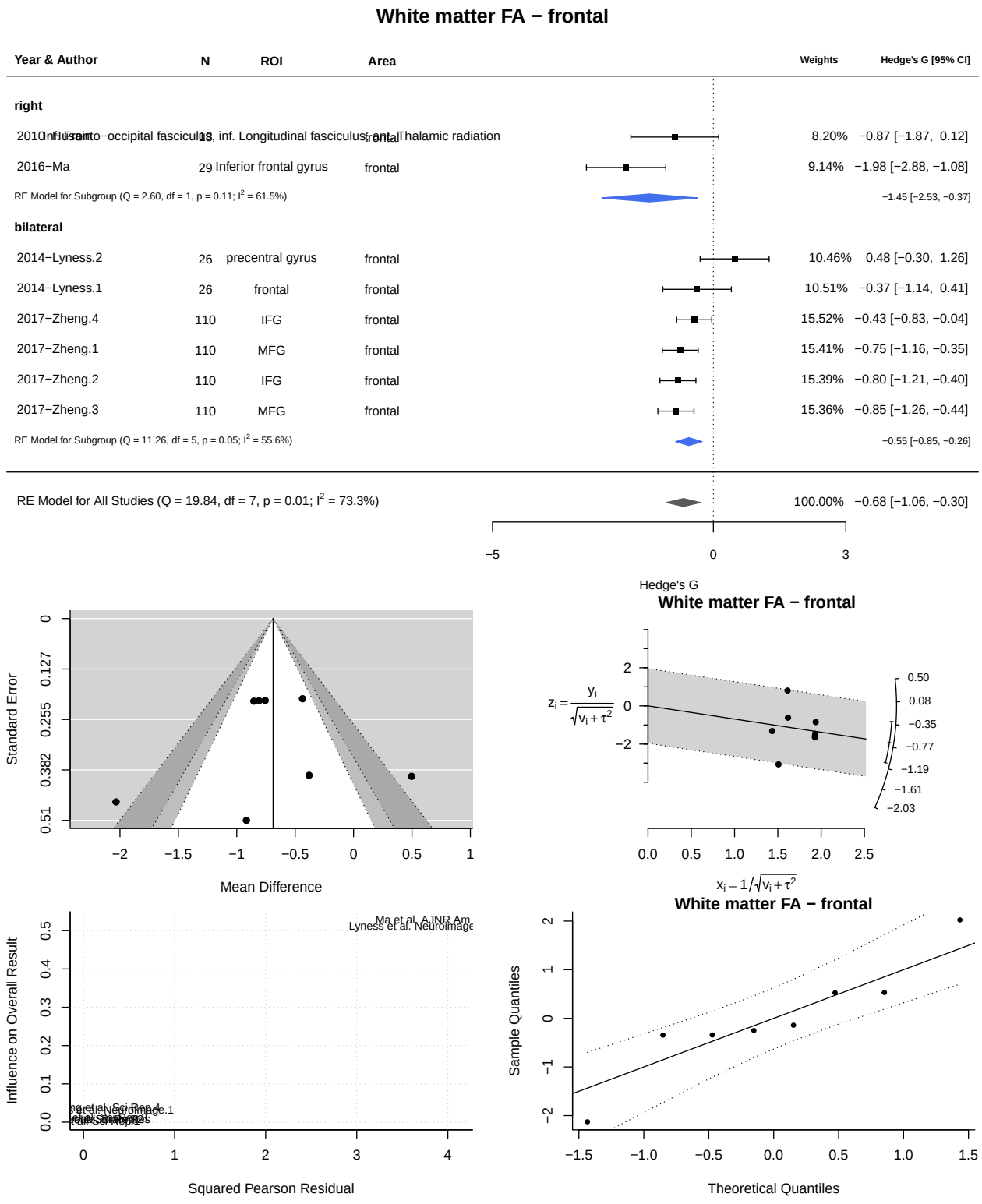
White matter FA − frontal
Year & Author
N
ROI
Area
Weights
Hedge's G [95% CI]
right
2010−Hua
18
Inf. Fronto−occipital fasciculus, inf. Longitudinal fasciculus, ant. Thalamic radiation
frontal
8.20% −0.87 [−1.87, 0.12]
2016−Ma
29
Inferior frontal gyrus
frontal
9.14% −1.98 [−2.88, −1.08]
RE Model for Subgroup (Q = 2.60, df = 1, p = 0.11; I² = 61.5%)
−1.45 [−2.53, −0.37]
bilateral
2014−Lyness.2
26
precentral gyrus
frontal
10.46% 0.48 [−0.30, 1.26]
2014−Lyness.1
26
frontal
frontal
10.51% −0.37 [−1.14, 0.41]
2017−Zheng.4
110
IFG
frontal
15.52% −0.43 [−0.83, −0.04]
2017−Zheng.1
110
MFG
frontal
15.41% −0.75 [−1.16, −0.35]
2017−Zheng.2
110
IFG
frontal
15.39% −0.80 [−1.21, −0.40]
2017−Zheng.3
110
MFG
frontal
15.36% −0.85 [−1.26, −0.44]
RE Model for Subgroup (Q = 11.26, df = 5, p = 0.05; I² = 55.6%)
−0.55 [−0.85, −0.26]
RE Model for All Studies (Q = 19.84, df = 7, p = 0.01; I² = 73.3%)
100.00% −0.68 [−1.06, −0.30]
−5
0
3
Hedge's G
Standard Error
0
0.127
0.255
0.382
0.51
−2
−1.5
−1
−0.5
0
0.5
1
Mean Difference
White matter FA − frontal
$z_i = \frac{y_i}{\sqrt{v_i + \tau^2}}$
2
0
−2
0.50
0.08
−0.35
−0.77
−1.19
−1.61
−2.03
0.0
0.5
1.0
1.5
2.0
2.5
$x_i = 1/\sqrt{v_i + \tau^2}$
Influence on Overall Result
Ma et al. AJNR Am
Lyness et al. NeuroImage
0.0
0.1
0.2
0.3
0.4
0.5
0
1
2
3
4
Squared Pearson Residual
White matter FA − frontal
Sample Quantiles
2
1
0
−1
−2
−1.5
−1.0
−0.5
0.0
0.5
1.0
1.5
Theoretical Quantiles

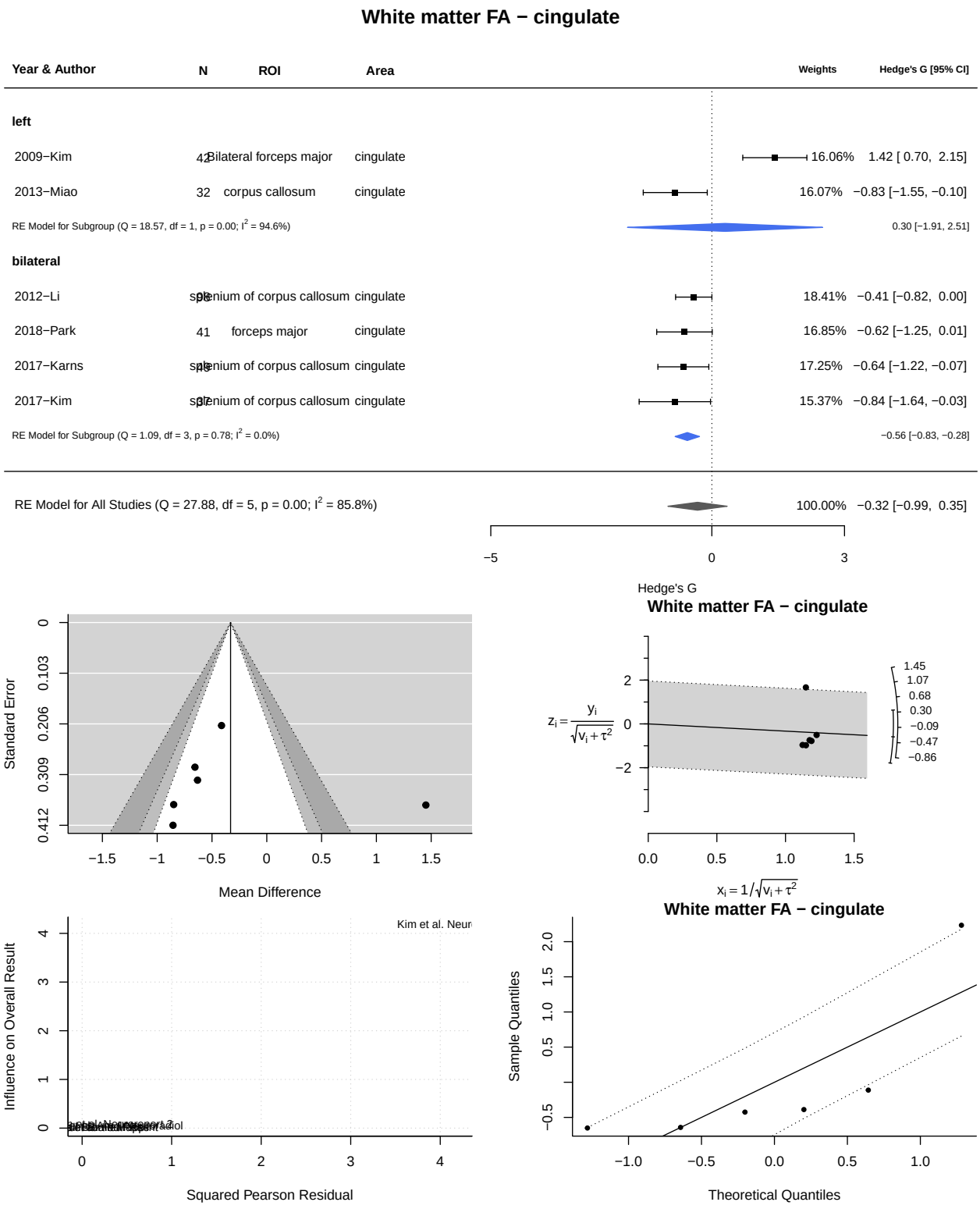
White matter FA − cingulate
Year & Author
N
ROI
Area
Weights
Hedge's G [95% CI]
left
2009−Kim 42 Bilateral forceps major cingulate 16.06% 1.42 [0.70, 2.15]
2013−Miao 32 corpus callosum cingulate 16.07% −0.83 [−1.55, −0.10]
RE Model for Subgroup (Q = 18.57, df = 1, p = 0.00; I² = 94.6%) 0.30 [−1.91, 2.51]
bilateral
2012−Li 98 splenium of corpus callosum cingulate 18.41% −0.41 [−0.82, 0.00]
2018−Park 41 forceps major cingulate 16.85% −0.62 [−1.25, 0.01]
2017−Karns 48 splenium of corpus callosum cingulate 17.25% −0.64 [−1.22, −0.07]
2017−Kim 97 splenium of corpus callosum cingulate 15.37% −0.84 [−1.64, −0.03]
RE Model for Subgroup (Q = 1.09, df = 3, p = 0.78; I² = 0.0%) −0.56 [−0.83, −0.28]
RE Model for All Studies (Q = 27.88, df = 5, p = 0.00; I² = 85.8%) 100.00% −0.32 [−0.99, 0.35]
−5
0
3
Hedge's G
Standard Error
0
0.103
0.206
0.309
0.412
−1.5
−1
−0.5
0
0.5
1
1.5
Mean Difference
White matter FA − cingulate
$z_i = \frac{y_i}{\sqrt{v_i + \tau^2}}$
2
0
−2
1.45
1.07
0.68
0.30
−0.09
−0.47
−0.86
0.0
0.5
1.0
1.5
$x_i = 1/\sqrt{v_i + \tau^2}$
Influence on Overall Result
Kim et al. Neur
0
1
2
3
4
Squared Pearson Residual
White matter FA − cingulate
Sample Quantiles
−0.5
0.5
1.0
1.5
2.0
−1.0
−0.5
0.0
0.5
1.0
Theoretical Quantiles

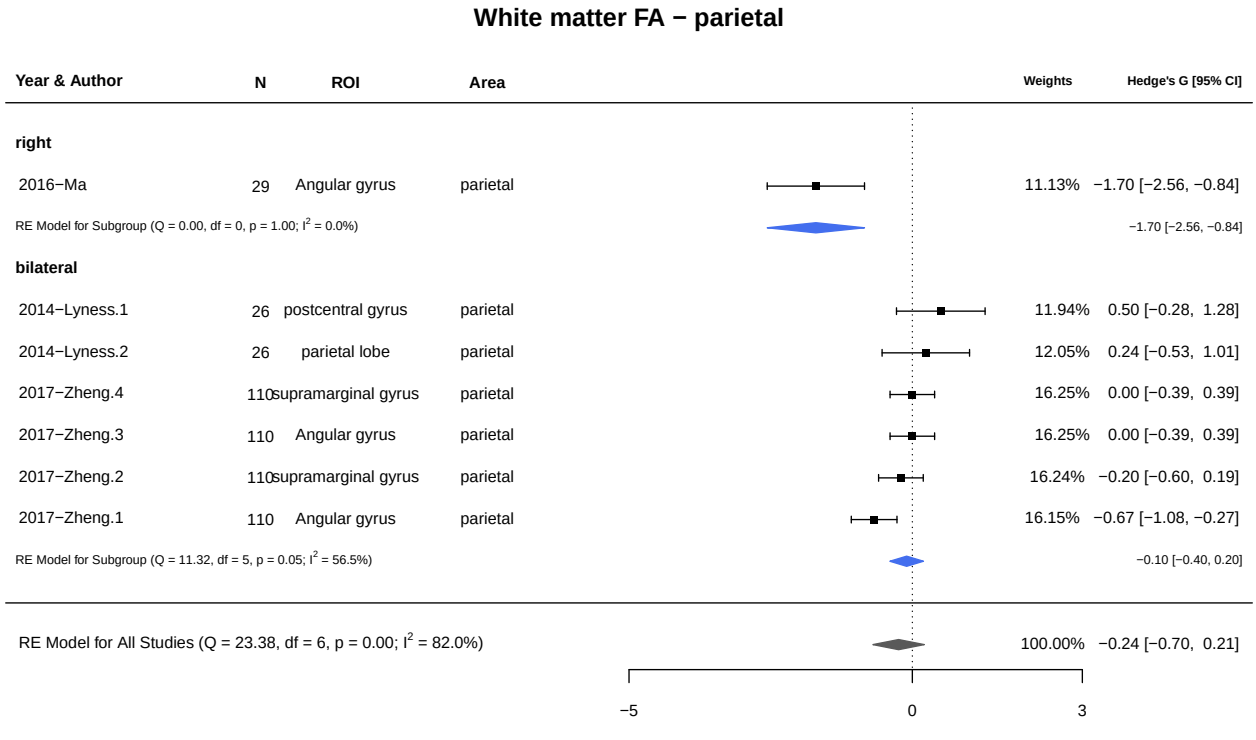
White matter FA − parietal
Year & Author
N
ROI
Area
Weights
Hedge's G [95% CI]
right
2016−Ma 29 Angular gyrus parietal 11.13% −1.70 [−2.56, −0.84]
RE Model for Subgroup (Q = 0.00, df = 0, p = 1.00; I² = 0.0%) −1.70 [−2.56, −0.84]
bilateral
2014−Lyness.1 26 postcentral gyrus parietal 11.94% 0.50 [−0.28, 1.28]
2014−Lyness.2 26 parietal lobe parietal 12.05% 0.24 [−0.53, 1.01]
2017−Zheng.4 110 supramarginal gyrus parietal 16.25% 0.00 [−0.39, 0.39]
2017−Zheng.3 110 Angular gyrus parietal 16.25% 0.00 [−0.39, 0.39]
2017−Zheng.2 110 supramarginal gyrus parietal 16.24% −0.20 [−0.60, 0.19]
2017−Zheng.1 110 Angular gyrus parietal 16.15% −0.67 [−1.08, −0.27]
RE Model for Subgroup (Q = 11.32, df = 5, p = 0.05; I² = 56.5%) −0.10 [−0.40, 0.20]
RE Model for All Studies (Q = 23.38, df = 6, p = 0.00; I² = 82.0%) 100.00% −0.24 [−0.70, 0.21]
−5
0
3
Hedge's G

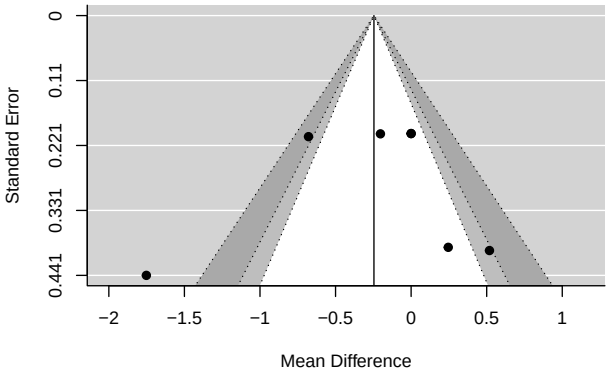
Standard Error
0
0.11
0.221
0.331
0.441
−2
−1.5
−1
−0.5
0
0.5
1
Mean Difference

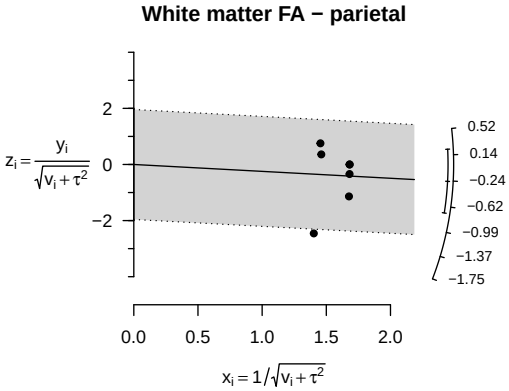
White matter FA − parietal
$z_i = \frac{y_i}{\sqrt{v_i + \tau^2}}$
2
0
−2
0.52
0.14
−0.24
−0.62
−0.99
−1.37
−1.75
0.0
0.5
1.0
1.5
2.0
$x_i = 1/\sqrt{v_i + \tau^2}$

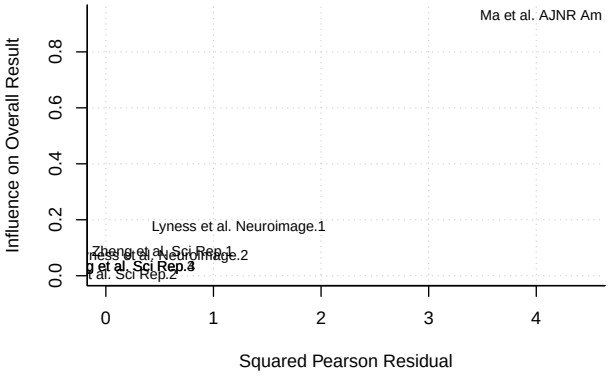
Influence on Overall Result
0.0
0.2
0.4
0.6
0.8
Ma et al. AJNR Am
Lyness et al. Neuroimage.1
Zheng et al. Sci Rep.1
ness et al. Neuroimage.2
g et al. Sci Rep.3
l et al. Sci Rep.2
0
1
2
3
4
Squared Pearson Residual

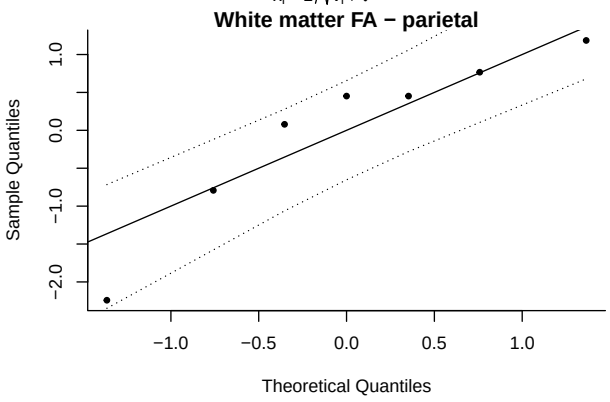
White matter FA − parietal
Sample Quantiles
1.0
0.0
−1.0
−2.0
−1.0
−0.5
0.0
0.5
1.0
Theoretical Quantiles

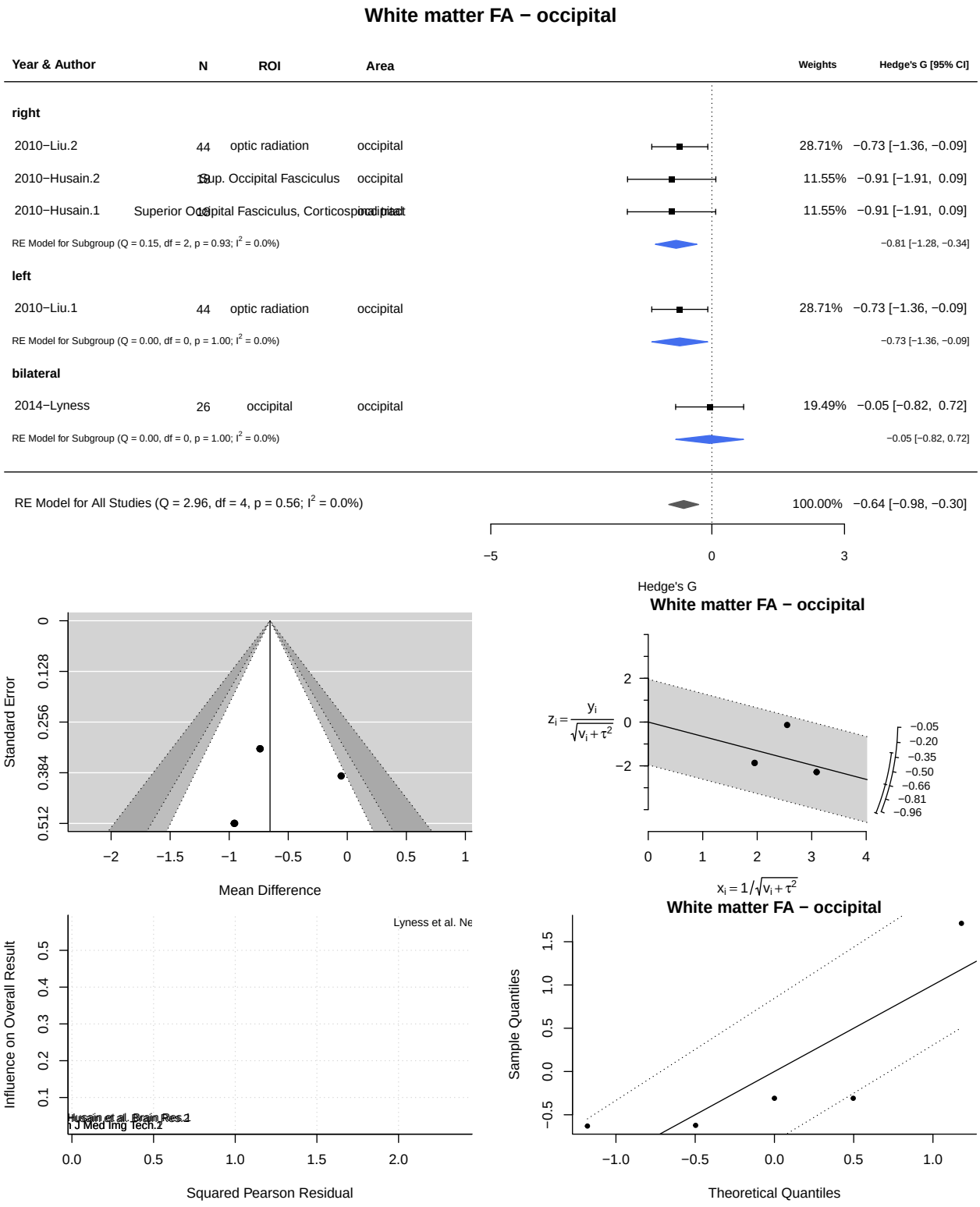
White matter FA − occipital
Year & Author
N
ROI
Area
Weights
Hedge's G [95% CI]
right
2010−Liu.2 44 optic radiation occipital 28.71% −0.73 [−1.36, −0.09]
2010−Husain.2 18 Sup. Occipital Fasciculus occipital 11.55% −0.91 [−1.91, 0.09]
2010−Husain.1 18 Superior Occipital Fasciculus, Corticospinal tract occipital 11.55% −0.91 [−1.91, 0.09]
RE Model for Subgroup (Q = 0.15, df = 2, p = 0.93; I² = 0.0%) −0.81 [−1.28, −0.34]
left
2010−Liu.1 44 optic radiation occipital 28.71% −0.73 [−1.36, −0.09]
RE Model for Subgroup (Q = 0.00, df = 0, p = 1.00; I² = 0.0%) −0.73 [−1.36, −0.09]
bilateral
2014−Lyness 26 occipital occipital 19.49% −0.05 [−0.82, 0.72]
RE Model for Subgroup (Q = 0.00, df = 0, p = 1.00; I² = 0.0%) −0.05 [−0.82, 0.72]
RE Model for All Studies (Q = 2.96, df = 4, p = 0.56; I² = 0.0%) 100.00% −0.64 [−0.98, −0.30]
−5
0
3
Hedge's G
Standard Error
0
0.128
0.256
0.384
0.512
−2
−1.5
−1
−0.5
0
0.5
1
Mean Difference
White matter FA − occipital
$z_i = \frac{y_i}{\sqrt{v_i + \tau^2}}$
2
0
−2
−0.05
−0.20
−0.35
−0.50
−0.66
−0.81
−0.96
0
1
2
3
4
$x_i = 1/\sqrt{v_i + \tau^2}$
Influence on Overall Result
0.1
0.2
0.3
0.4
0.5
Lyness et al. Ne
Husain et al. Brain Res 1
i J Med Img Tech 2
0.0
0.5
1.0
1.5
2.0
Squared Pearson Residual
White matter FA − occipital
Sample Quantiles
−0.5
0.0
0.5
1.0
1.5
−1.0
−0.5
0.0
0.5
1.0
Theoretical Quantiles

Meta-regressions of White Matter Volume & Brain Areas: Random effects model no intercept covariated by Side

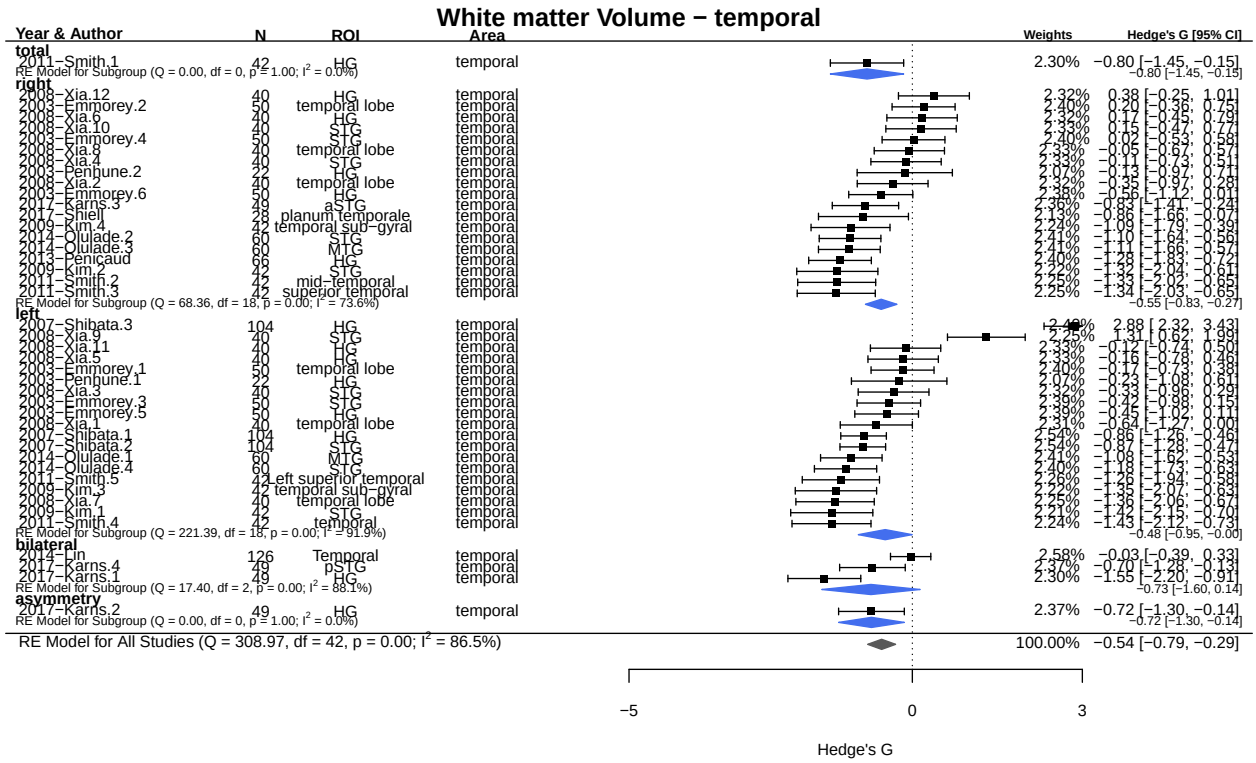

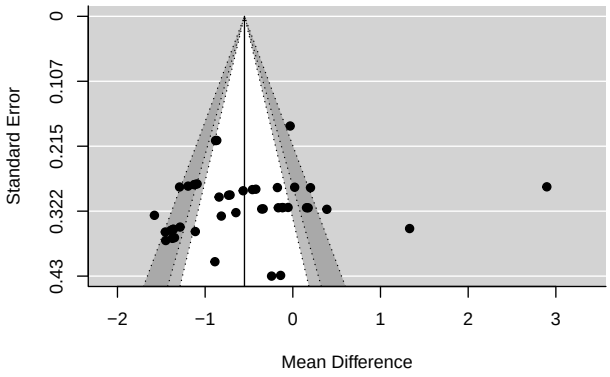

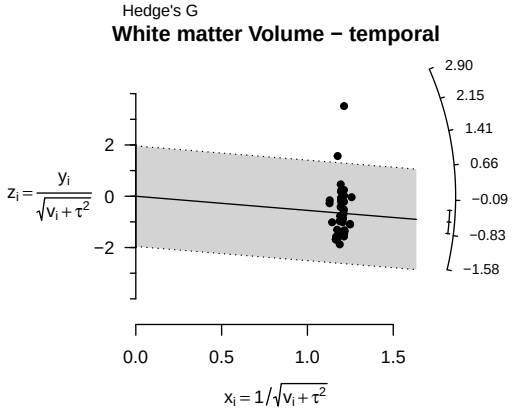

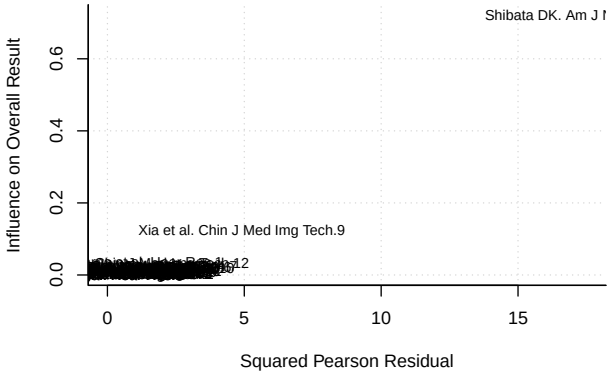

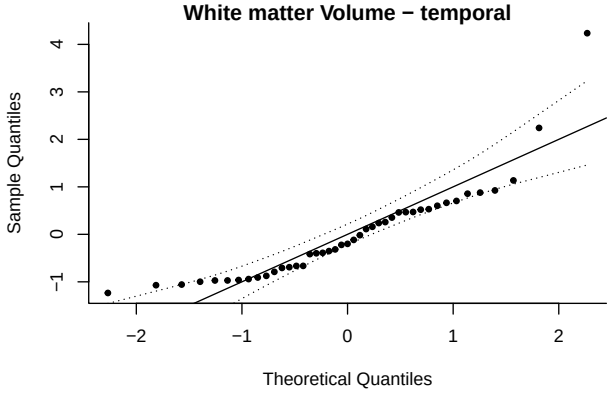

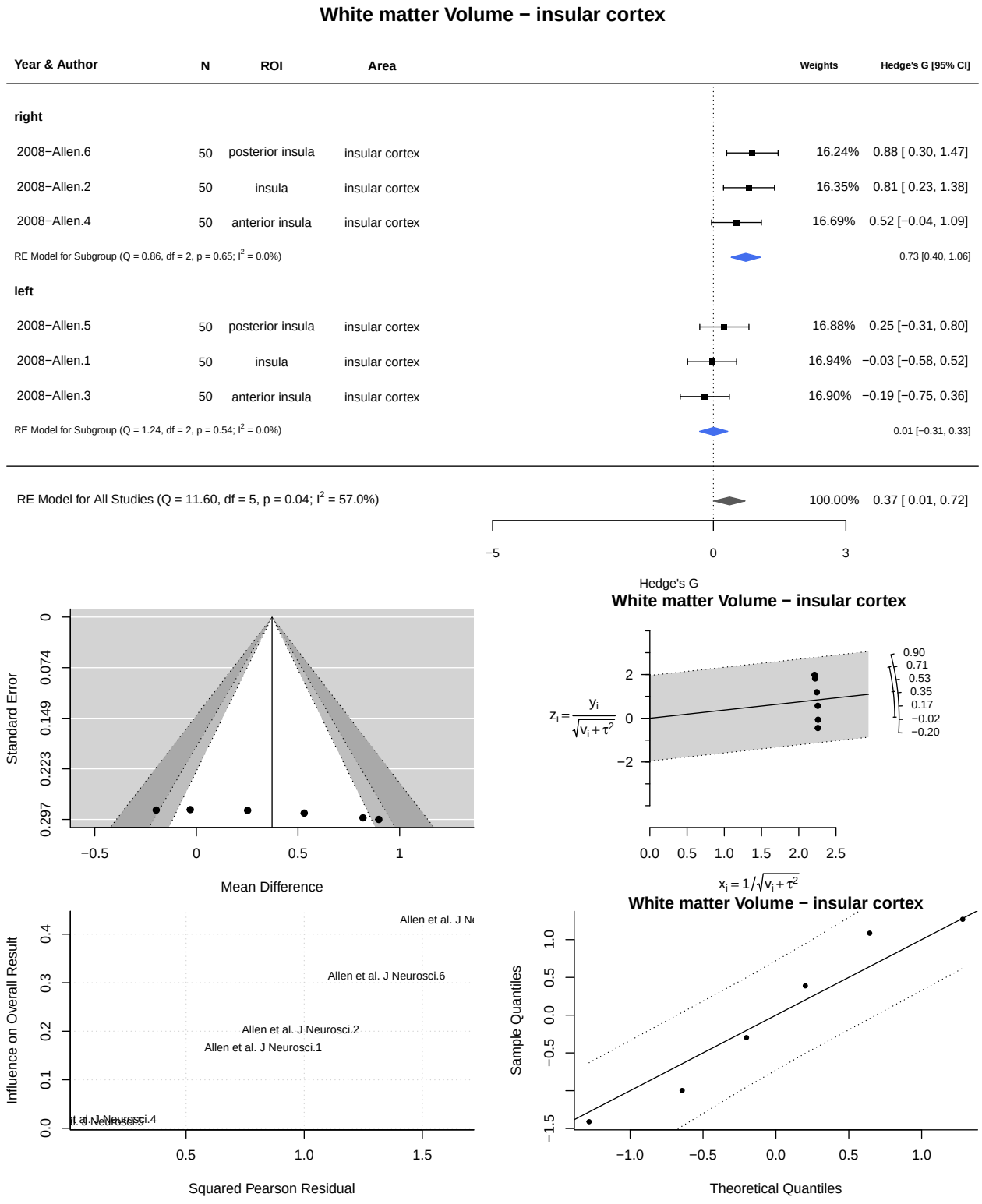
White matter Volume − insular cortex
Year & Author
N
ROI
Area
Weights
Hedge's G [95% CI]
right
2008−Allen.6 50 posterior insula insular cortex 16.24% 0.88 [0.30, 1.47]
2008−Allen.2 50 insula insular cortex 16.35% 0.81 [0.23, 1.38]
2008−Allen.4 50 anterior insula insular cortex 16.69% 0.52 [−0.04, 1.09]
RE Model for Subgroup (Q = 0.86, df = 2, p = 0.65; I² = 0.0%) 0.73 [0.40, 1.06]
left
2008−Allen.5 50 posterior insula insular cortex 16.88% 0.25 [−0.31, 0.80]
2008−Allen.1 50 insula insular cortex 16.94% −0.03 [−0.58, 0.52]
2008−Allen.3 50 anterior insula insular cortex 16.90% −0.19 [−0.75, 0.36]
RE Model for Subgroup (Q = 1.24, df = 2, p = 0.54; I² = 0.0%) 0.01 [−0.31, 0.33]
RE Model for All Studies (Q = 11.60, df = 5, p = 0.04; I² = 57.0%) 100.00% 0.37 [0.01, 0.72]
−5
0
3
Hedge's G
Standard Error
0
0.074
0.149
0.223
0.297
−0.5
0
0.5
1
Mean Difference
White matter Volume − insular cortex
$z_i = \frac{y_i}{\sqrt{v_i + \tau^2}}$
2
0
−2
0.90
0.71
0.53
0.35
0.17
−0.02
−0.20
0.0
0.5
1.0
1.5
2.0
2.5
$x_i = 1/\sqrt{v_i + \tau^2}$
Influence on Overall Result
0.0
0.1
0.2
0.3
0.4
Allen et al. J Neurosci.6
Allen et al. J Neurosci.2
Allen et al. J Neurosci.1
0.5
1.0
1.5
Squared Pearson Residual
White matter Volume − insular cortex
Sample Quantiles
−1.5
−0.5
0.0
0.5
1.0
−1.0
−0.5
0.0
0.5
1.0
Theoretical Quantiles

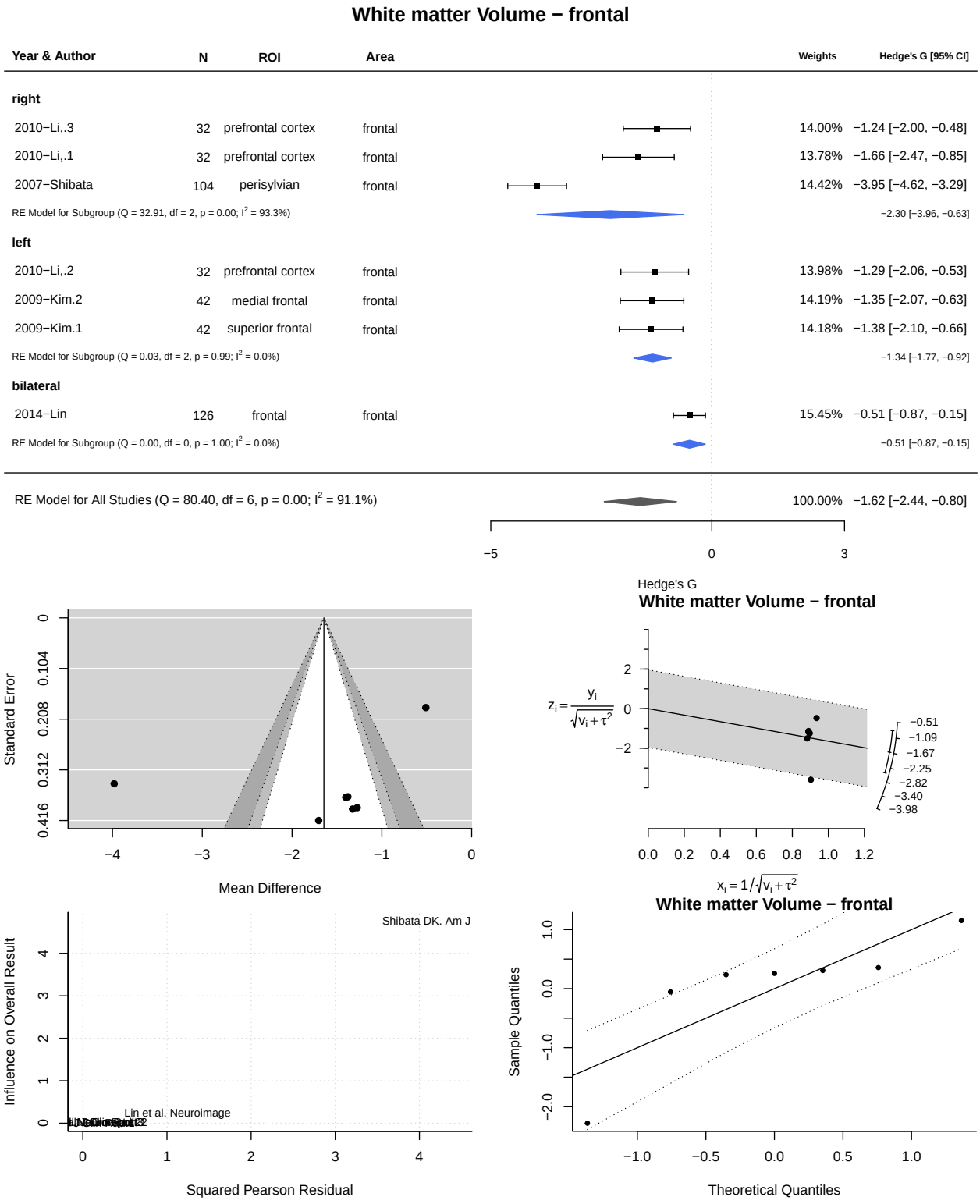
White matter Volume − frontal
Year & Author
N
ROI
Area
Weights
Hedge's G [95% CI]
right
2010−Li,.3 32 prefrontal cortex frontal 14.00% −1.24 [−2.00, −0.48]
2010−Li,.1 32 prefrontal cortex frontal 13.78% −1.66 [−2.47, −0.85]
2007−Shibata 104 perisylvian frontal 14.42% −3.95 [−4.62, −3.29]
RE Model for Subgroup (Q = 32.91, df = 2, p = 0.00; I² = 93.3%) −2.30 [−3.96, −0.63]
left
2010−Li,.2 32 prefrontal cortex frontal 13.98% −1.29 [−2.06, −0.53]
2009−Kim.2 42 medial frontal frontal 14.19% −1.35 [−2.07, −0.63]
2009−Kim.1 42 superior frontal frontal 14.18% −1.38 [−2.10, −0.66]
RE Model for Subgroup (Q = 0.03, df = 2, p = 0.99; I² = 0.0%) −1.34 [−1.77, −0.92]
bilateral
2014−Lin 126 frontal frontal 15.45% −0.51 [−0.87, −0.15]
RE Model for Subgroup (Q = 0.00, df = 0, p = 1.00; I² = 0.0%) −0.51 [−0.87, −0.15]
RE Model for All Studies (Q = 80.40, df = 6, p = 0.00; I² = 91.1%) 100.00% −1.62 [−2.44, −0.80]
−5
0
3
Hedge's G
Standard Error
0
0.104
0.208
0.312
0.416
−4
−3
−2
−1
0
Mean Difference
White matter Volume − frontal
$z_i = \frac{y_i}{\sqrt{v_i + \tau^2}}$
2
0
−2
−0.51
−1.09
−1.67
−2.25
−2.82
−3.40
−3.98
0.0
0.2
0.4
0.6
0.8
1.0
1.2
$x_i = 1/\sqrt{v_i + \tau^2}$
Shibata DK. Am J
Lin et al. Neuroimage
Influence on Overall Result
0
1
2
3
4
Squared Pearson Residual
White matter Volume − frontal
Sample Quantiles
1.0
0.0
−1.0
−2.0
−1.0
−0.5
0.0
0.5
1.0
Theoretical Quantiles

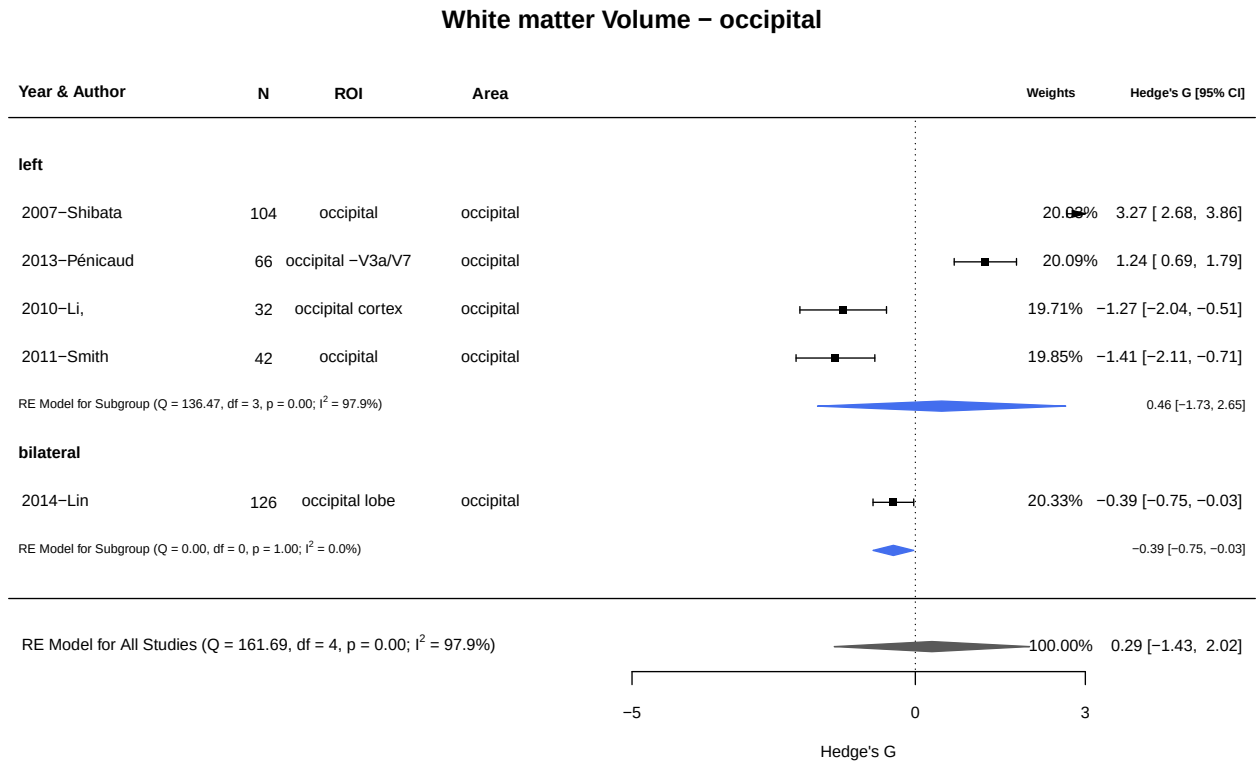
White matter Volume − occipital
Year & Author
N
ROI
Area
Weights
Hedge's G [95% CI]
left
2007−Shibata 104 occipital occipital 20.08% 3.27 [2.68, 3.86]
2013−Pénicaud 66 occipital −V3a/V7 occipital 20.09% 1.24 [0.69, 1.79]
2010−Li, 32 occipital cortex occipital 19.71% −1.27 [−2.04, −0.51]
2011−Smith 42 occipital occipital 19.85% −1.41 [−2.11, −0.71]
RE Model for Subgroup (Q = 136.47, df = 3, p = 0.00; I² = 97.9%) 0.46 [−1.73, 2.65]
bilateral
2014−Lin 126 occipital lobe occipital 20.33% −0.39 [−0.75, −0.03]
RE Model for Subgroup (Q = 0.00, df = 0, p = 1.00; I² = 0.0%) −0.39 [−0.75, −0.03]
RE Model for All Studies (Q = 161.69, df = 4, p = 0.00; I² = 97.9%) 100.00% 0.29 [−1.43, 2.02]
−5
0
3
Hedge's G

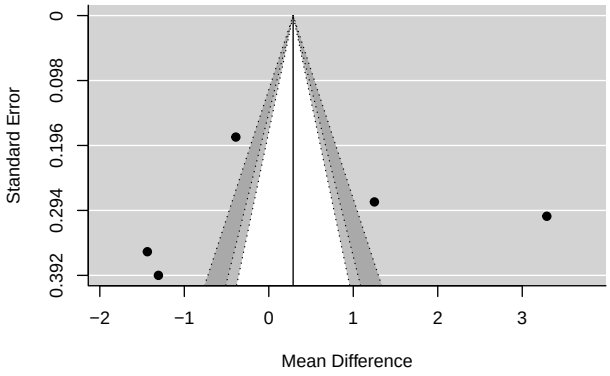
Standard Error
0
0.098
0.196
0.294
0.392
−2
−1
0
1
2
3
Mean Difference

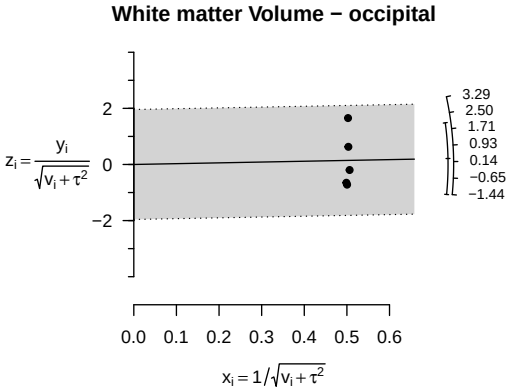
White matter Volume − occipital
$z_i = \frac{y_i}{\sqrt{v_i + \tau^2}}$
2
0
−2
3.29
2.50
1.71
0.93
0.14
−0.65
−1.44
0.0 0.1 0.2 0.3 0.4 0.5 0.6
$x_i = 1/\sqrt{v_i + \tau^2}$

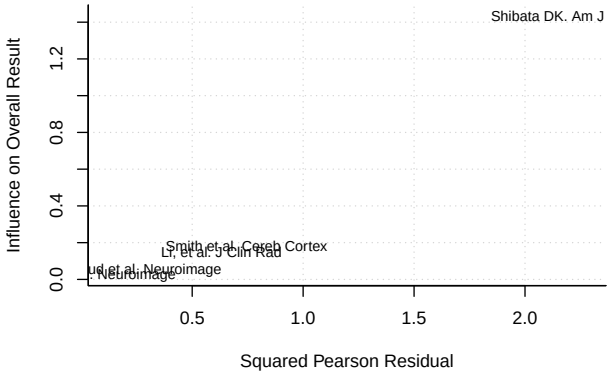
Influence on Overall Result
0.0
0.4
0.8
1.2
Shibata DK. Am J
Smith et al. Cereb Cortex
Li, et al. J Clin Rad
ud et al. Neuroimage
Neuroimage
0.5
1.0
1.5
2.0
Squared Pearson Residual

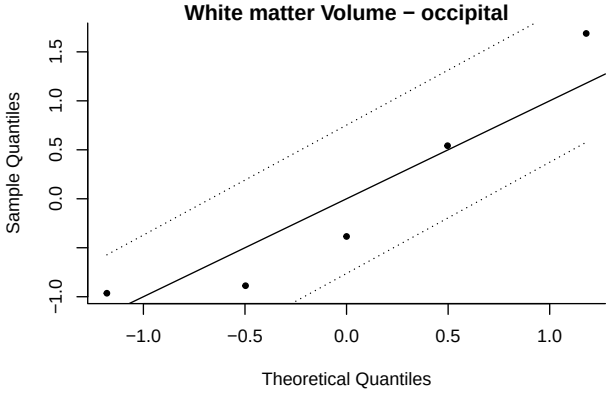
White matter Volume − occipital
Sample Quantiles
−1.0
0.0
0.5
1.0
1.5
−1.0
−0.5
0.0
0.5
1.0
Theoretical Quantiles

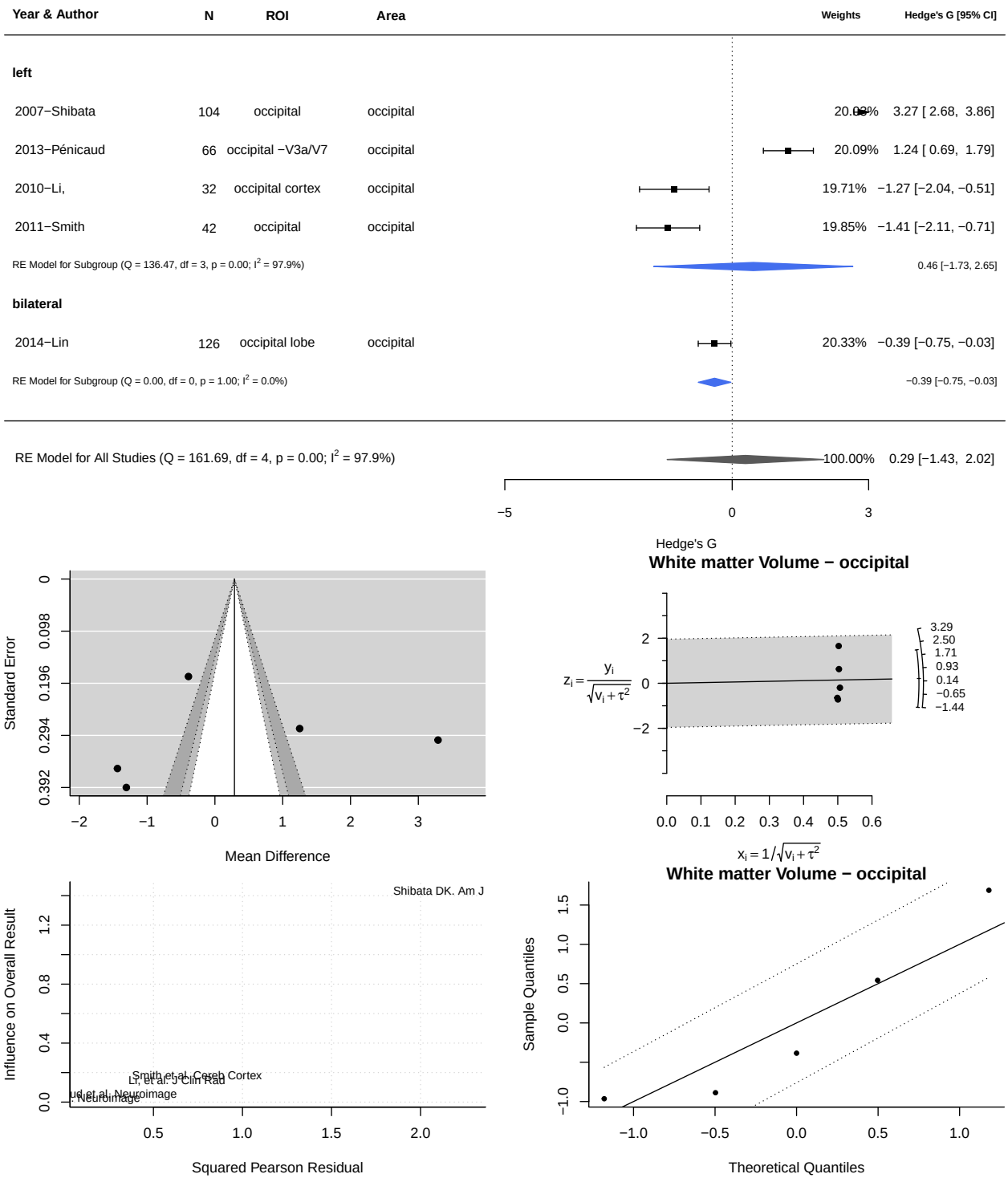
White matter Volume − occipital
Year & Author
N
ROI
Area
Weights
Hedge's G [95% CI]
left
2007−Shibata 104 occipital occipital 20.00% 3.27 [2.68, 3.86]
2013−Pénicaud 66 occipital −V3a/V7 occipital 20.09% 1.24 [0.69, 1.79]
2010−Li, 32 occipital cortex occipital 19.71% −1.27 [−2.04, −0.51]
2011−Smith 42 occipital occipital 19.85% −1.41 [−2.11, −0.71]
RE Model for Subgroup (Q = 136.47, df = 3, p = 0.00; I² = 97.9%) 0.46 [−1.73, 2.65]
bilateral
2014−Lin 126 occipital lobe occipital 20.33% −0.39 [−0.75, −0.03]
RE Model for Subgroup (Q = 0.00, df = 0, p = 1.00; I² = 0.0%) −0.39 [−0.75, −0.03]
RE Model for All Studies (Q = 161.69, df = 4, p = 0.00; I² = 97.9%) 100.00% 0.29 [−1.43, 2.02]
−5
0
3
Hedge's G

Standard Error
0
0.098
0.196
0.294
0.392
−2
−1
0
1
2
3
Mean Difference

White matter Volume − occipital
$z_i = \frac{y_i}{\sqrt{v_i + \tau^2}}$
2
0
−2
3.29
2.50
1.71
0.93
0.14
−0.65
−1.44
0.0
0.1
0.2
0.3
0.4
0.5
0.6
$x_i = 1/\sqrt{v_i + \tau^2}$

Influence on Overall Result
0.0
0.4
0.8
1.2
Shibata DK. Am J
Smith et al. Cereb Cortex
Li, et al. J Clin Rad
Neuroimage
0.5
1.0
1.5
2.0
Squared Pearson Residual

White matter Volume − occipital
Sample Quantiles
−1.0
0.0
0.5
1.0
1.5
−1.0
−0.5
0.0
0.5
1.0
Theoretical Quantiles

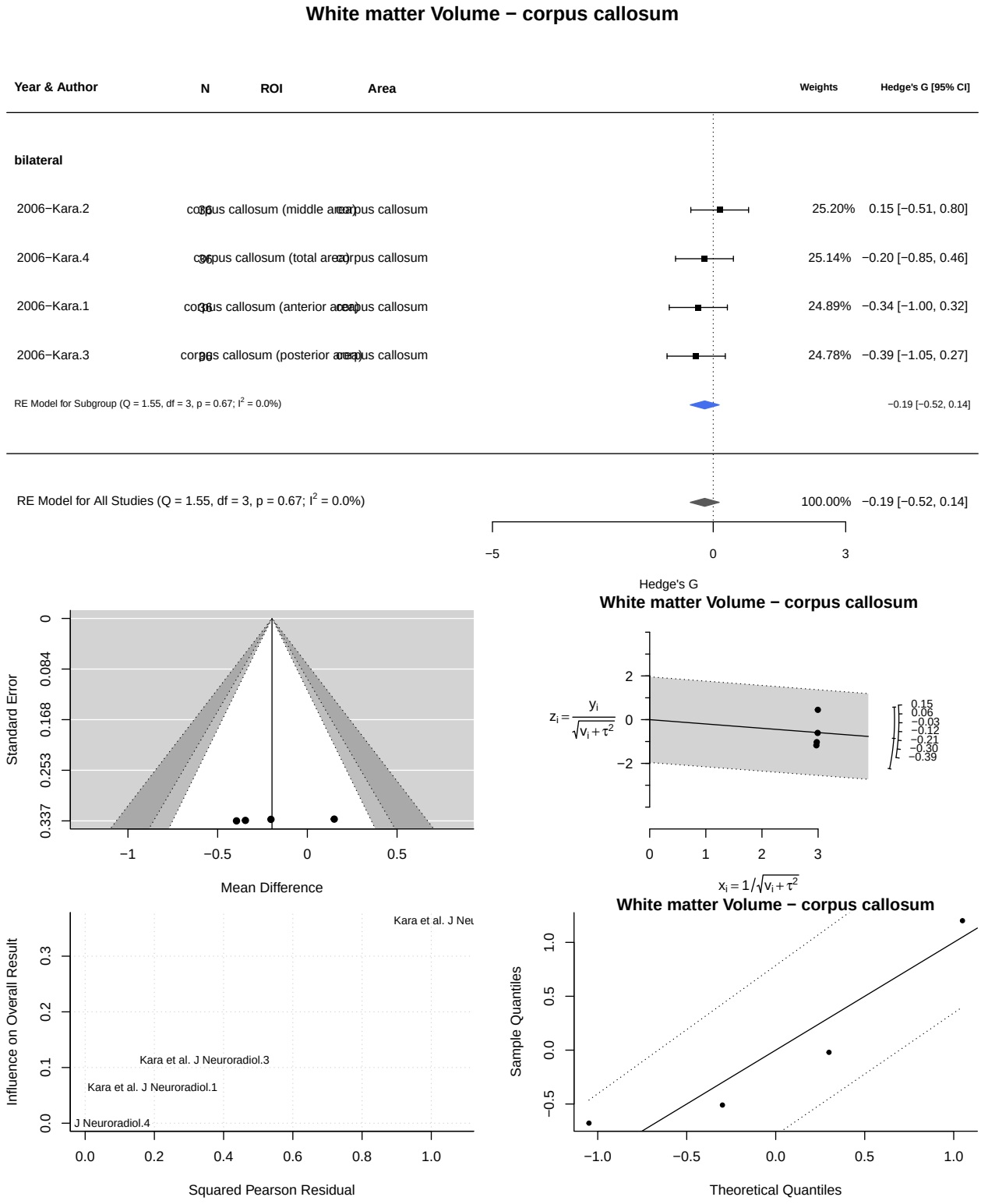
White matter Volume − corpus callosum
Year & Author
N
ROI
Area
Weights
Hedge's G [95% CI]
bilateral
2006−Kara.2
corpus callosum (middle area)
corpus callosum
25.20%
0.15 [−0.51, 0.80]
2006−Kara.4
corpus callosum (total area)
corpus callosum
25.14%
−0.20 [−0.85, 0.46]
2006−Kara.1
corpus callosum (anterior area)
corpus callosum
24.89%
−0.34 [−1.00, 0.32]
2006−Kara.3
corpus callosum (posterior area)
corpus callosum
24.78%
−0.39 [−1.05, 0.27]
RE Model for Subgroup (Q = 1.55, df = 3, p = 0.67; I² = 0.0%)
−0.19 [−0.52, 0.14]
RE Model for All Studies (Q = 1.55, df = 3, p = 0.67; I² = 0.0%)
100.00%
−0.19 [−0.52, 0.14]
−5
0
3
Hedge's G
Standard Error
0
0.084
0.168
0.253
0.337
−1
−0.5
0
0.5
Mean Difference
White matter Volume − corpus callosum
2
0
−2
0
1
2
3
0.15
0.06
−0.03
−0.12
−0.21
−0.30
−0.39
Influence on Overall Result
0.0
0.1
0.2
0.3
Kara et al. J Neuroradiol.3
Kara et al. J Neuroradiol.1
J Neuroradiol.4
0.0
0.2
0.4
0.6
0.8
1.0
Squared Pearson Residual
White matter Volume − corpus callosum
Sample Quantiles
−0.5
0.0
0.5
1.0
−1.0
−0.5
0.0
0.5
1.0
Theoretical Quantiles

Supplementary material: Forest-plots of other Measures

Hesch gyrus FA white matter

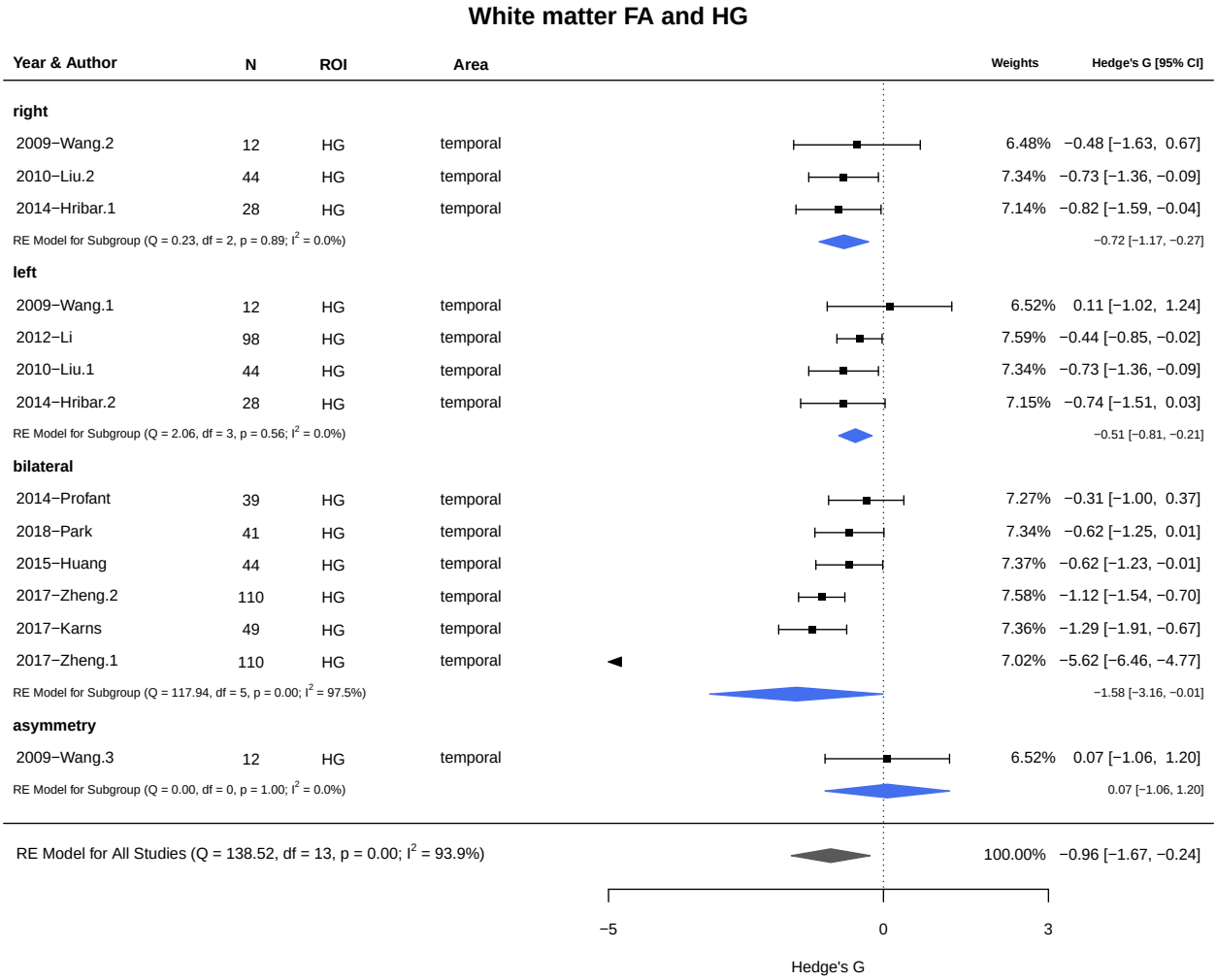

STG Volume White matter

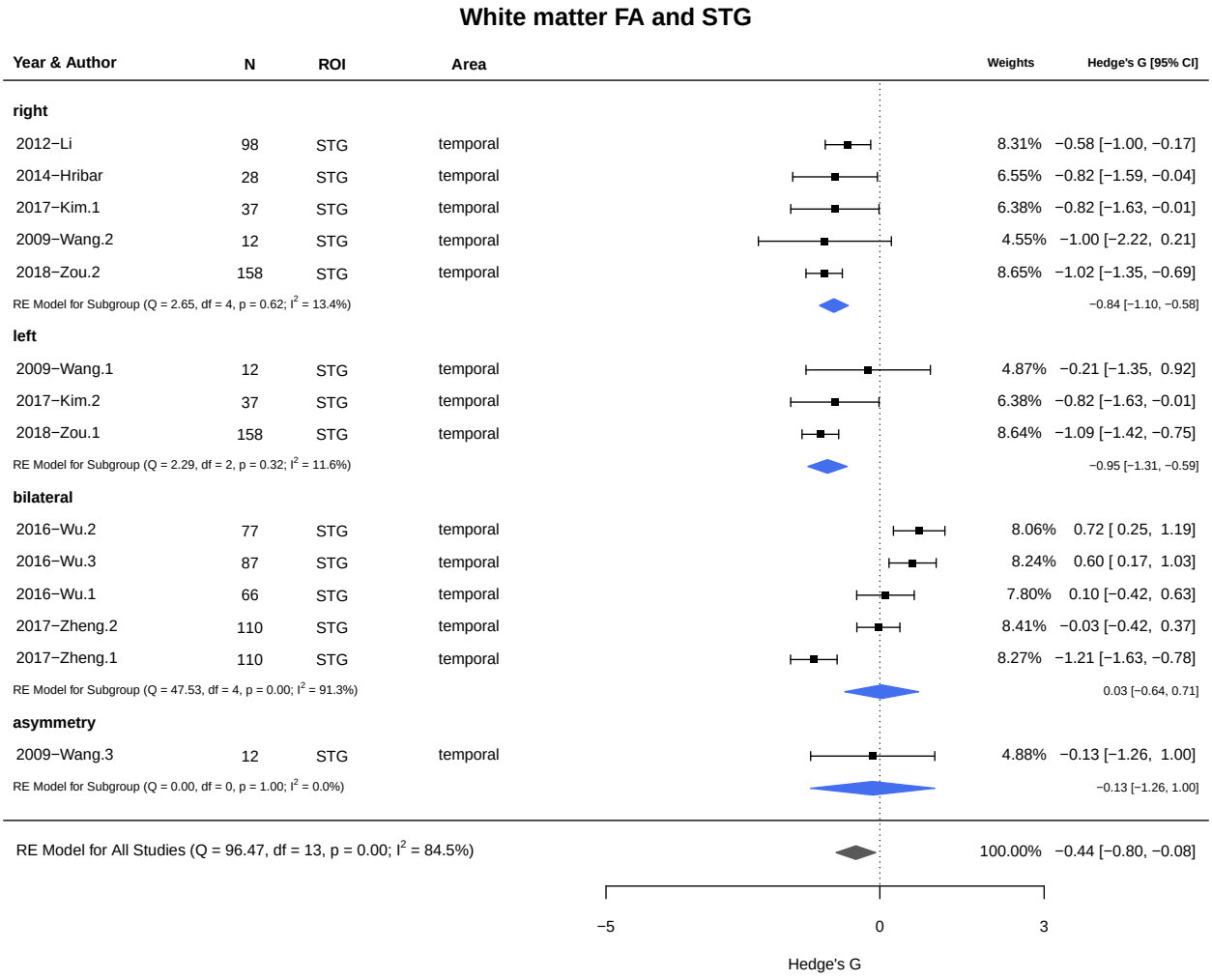

Measures of White matter Integrity

White matter: RD

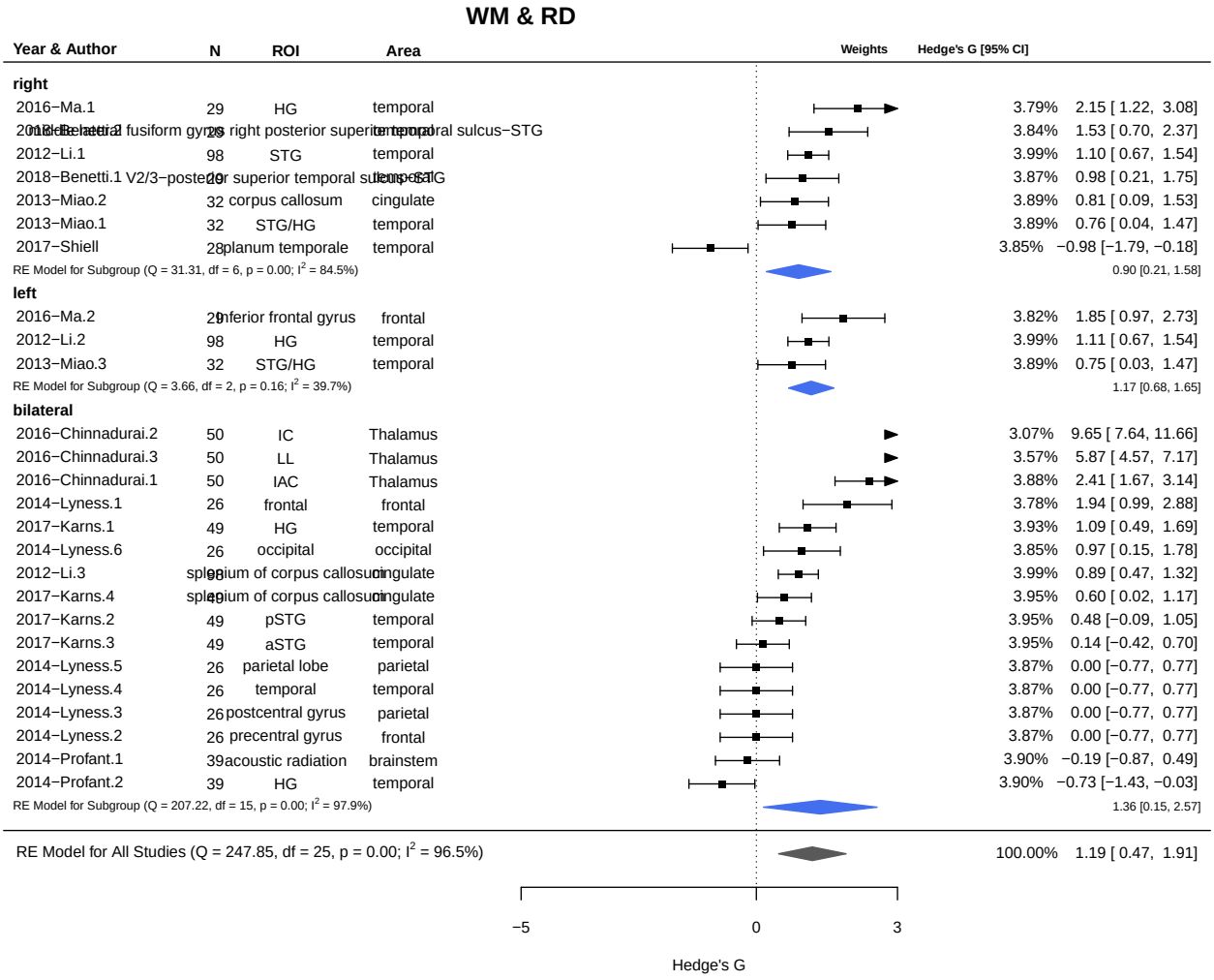

White matter: MD

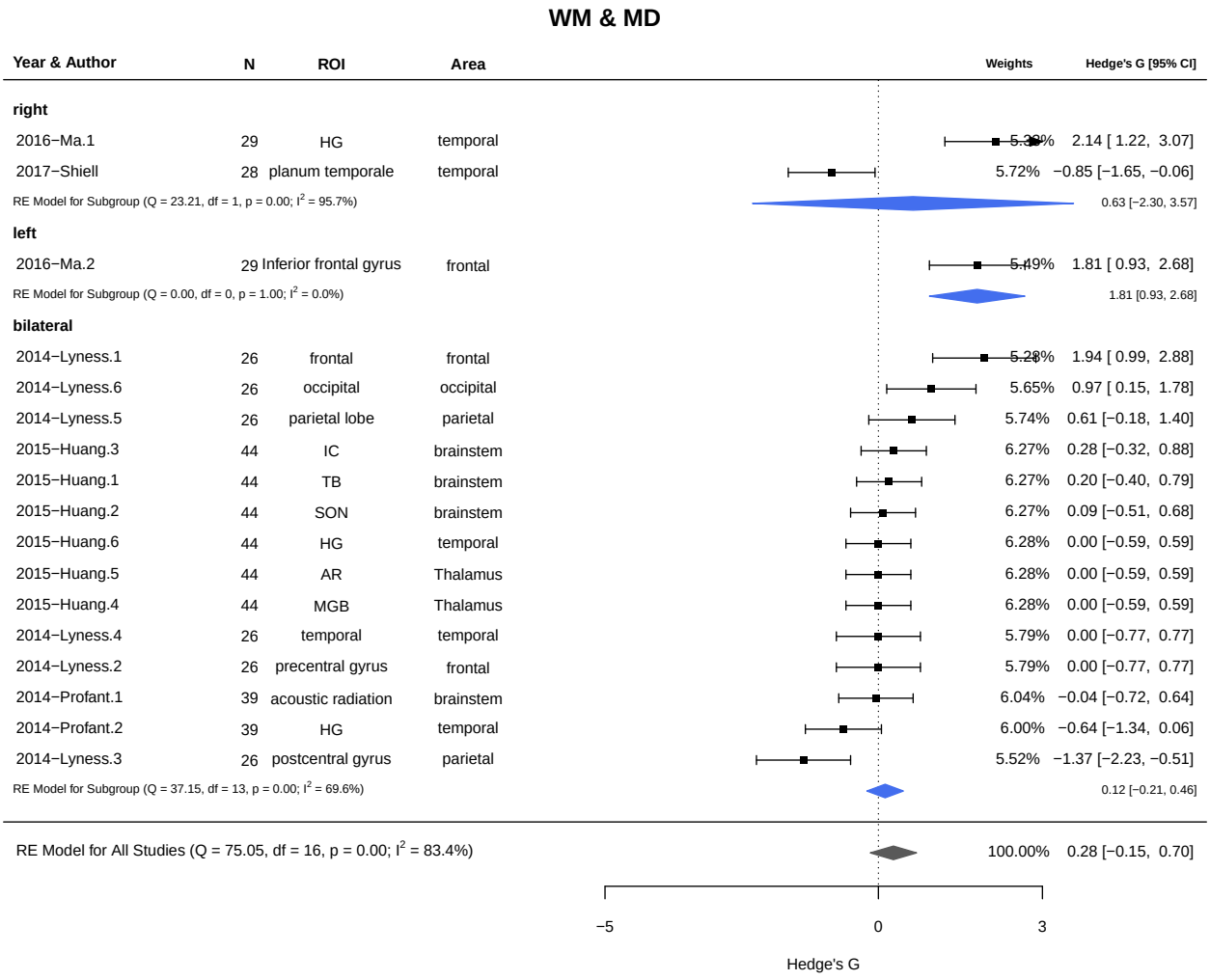

White matter: Mean Kurtosis

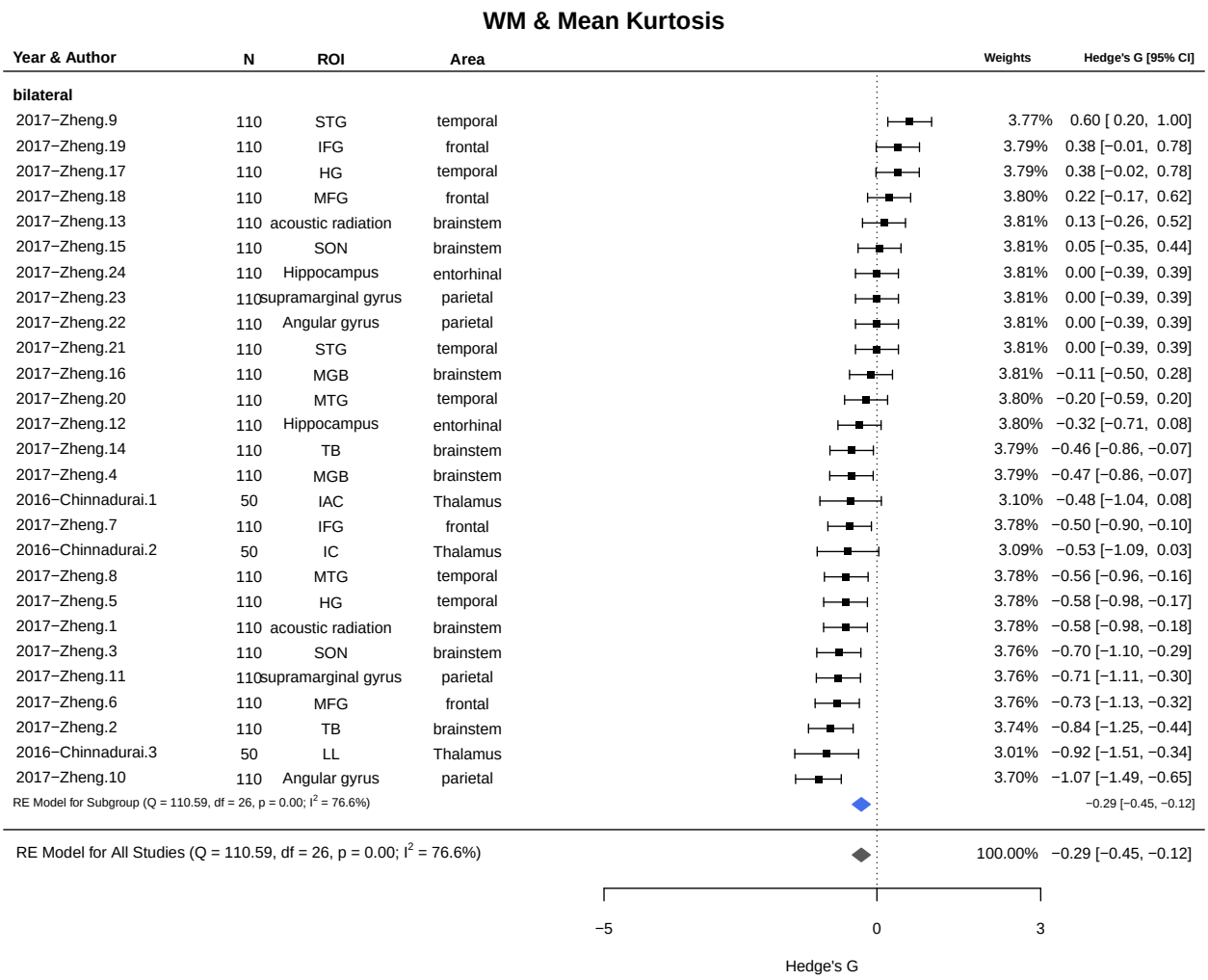

White matter: AD

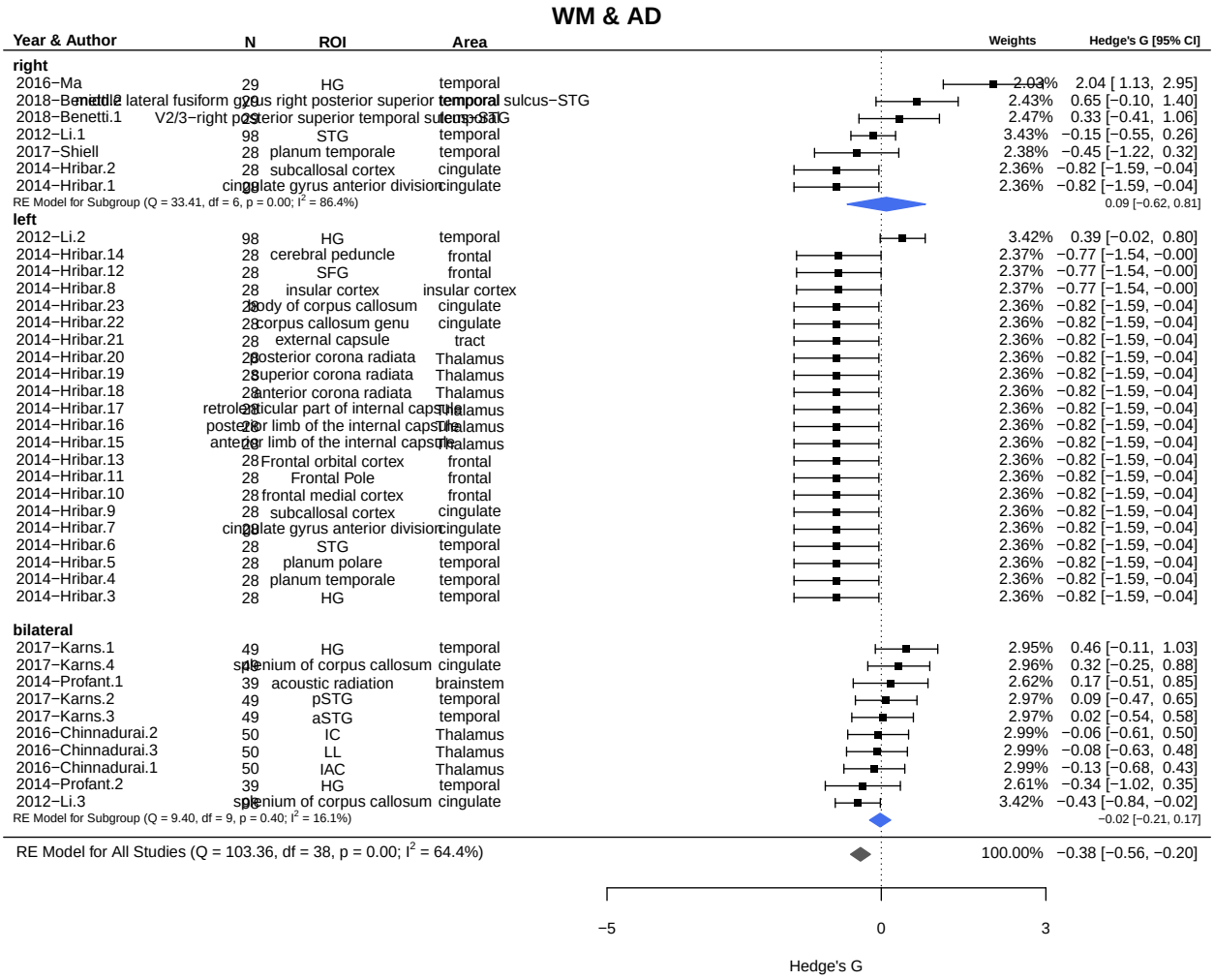

Error in rma(yi = hedgesG, vi = varG, data = meta.mod, measure = "MD", : Fisher scoring algorithm did not converge. See 'help(rma)' for possible remedies.

Other Measures of White Matter

White matter: Thickness

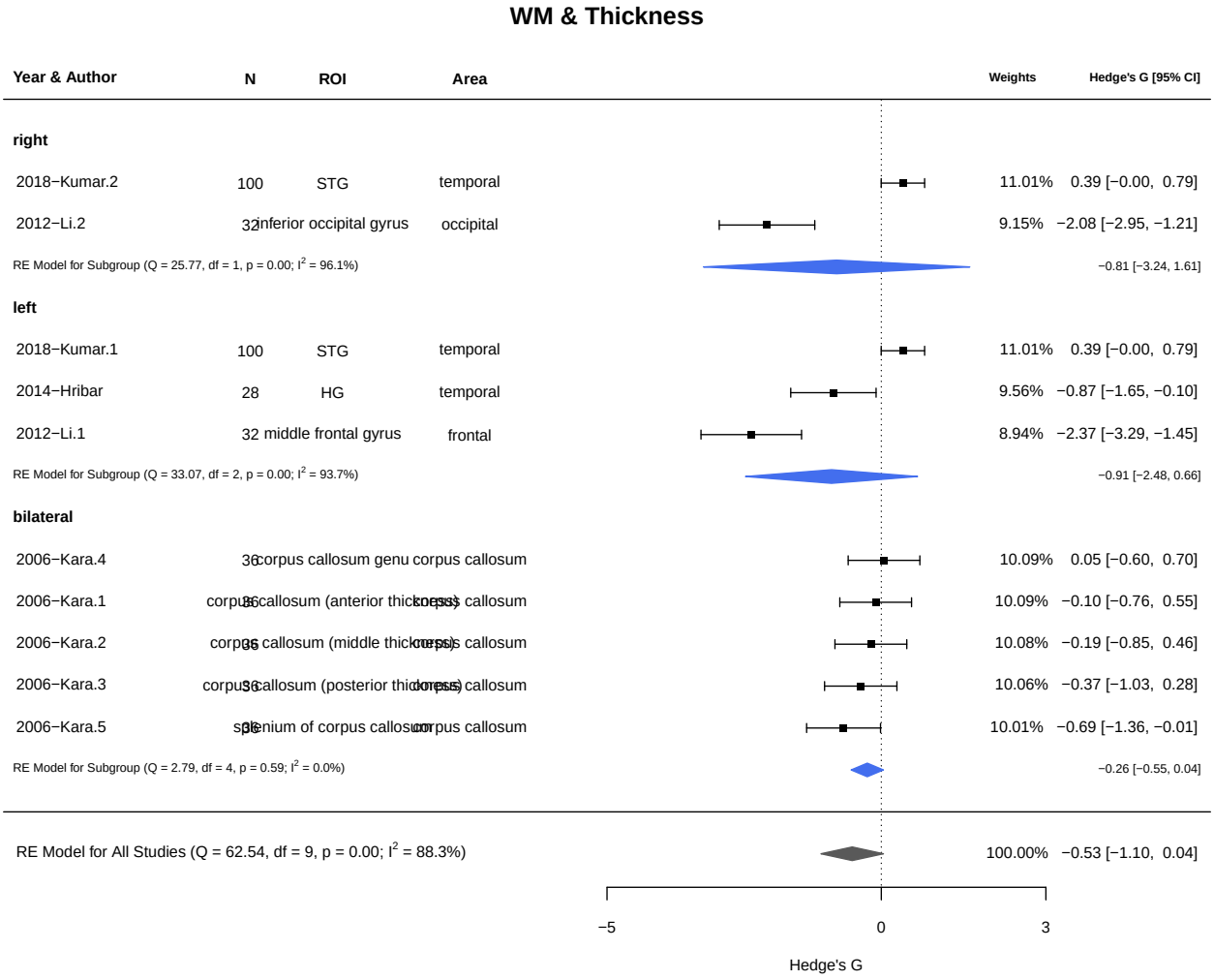

White matter: VBM

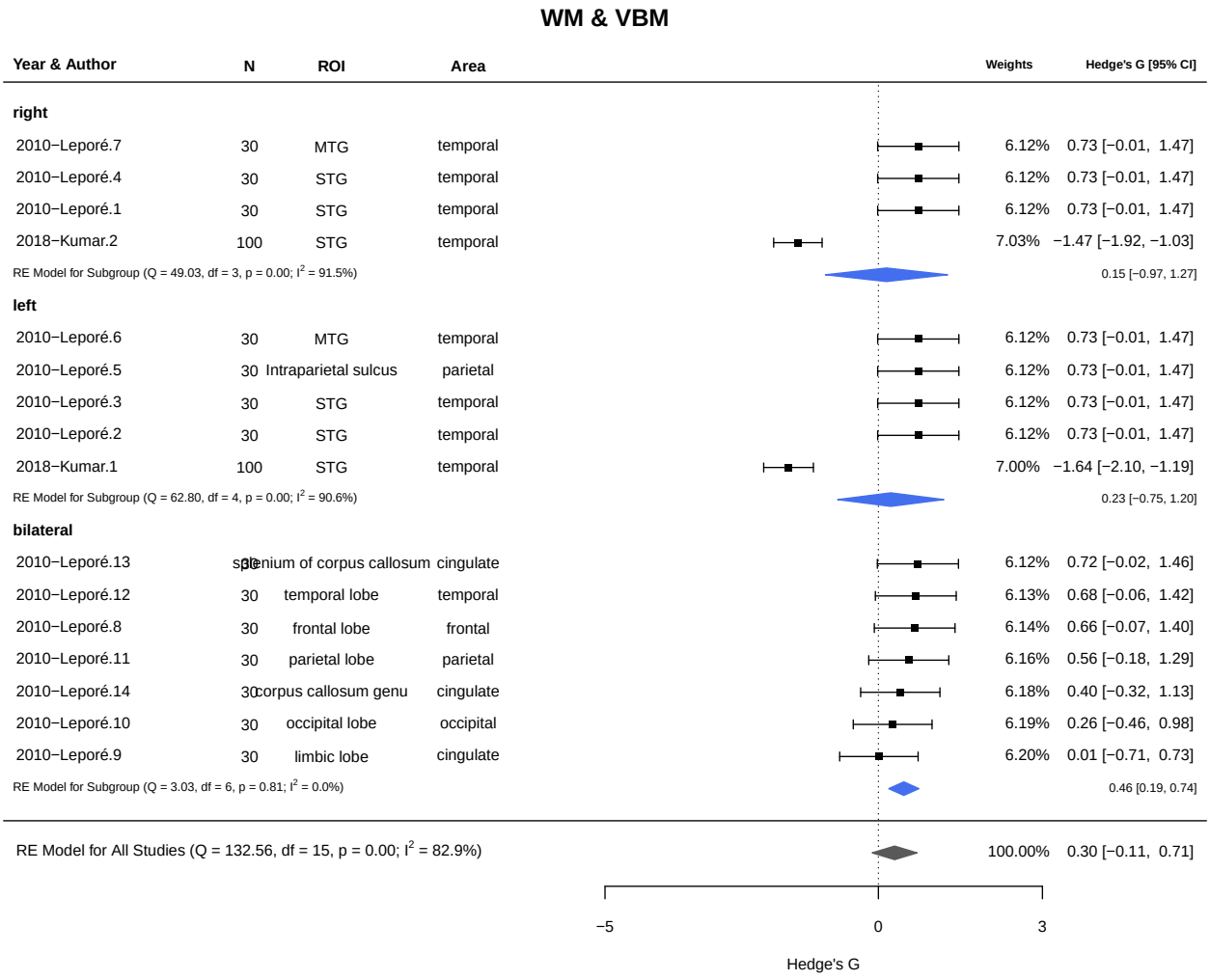

Meta Plots

The L'Abbé plot

In a L'Abbé plot (based on L'Abbé, Detsky, & O'Rourke, 1987), the arm-level outcomes for two experimental groups (e.g., treatment and control group) are plotted against each other. is treatment versus effect, since you have the cohen's d this should be relatively simple.
> WE DON'T HAVE TWO EXPERIMENTAL GROUPS

Baujat plot to identify studies contributing to heterogeneity

The plot shows the contribution of each study to the overall Q-test statistic for heterogeneity on the horizontal axis versus the influence of each study (defined as the standardized squared difference between the overall estimate based on a fixed-effects model with and without the ith study included in the model) on the vertical axis 2.17. Funnel plot to illustrate publication bias

Galbraith plot

Radial plot (radial) of variables and cohen's d - Galbraith, Rex (1988). "Graphical display of estimates having differing standard errors". Technometrics. Technometrics, Vol. 30, No. 3. 30 (3): 271–281.
2.18.2. We want to see this type of error plot over time for our patient cohorts by age. we want this for each measure WM and GM versus age on the x-axis so we can see GM and WM over time! Do a monte carlo simulation to connect different age population and create the error.
For a fixed-effects model, the plot shows the inverse of the standard errors on the horizontal axis against the individual observed effect sizes or outcomes standardized by their corresponding standard errors on the vertical axis. On the right hand side of the plot, an arc is drawn corresponding to the individual observed effect sizes or outcomes. A line projected from (0,0) through a particular point within the plot onto this arc indicates the value of the individual observed effect size or outcome for that point.

Resources

We are following Preferred Reporting Items for Systematic Reviews and Meta-Analyses guidelines: Moher, D., Liberati, A., Tetzlaff, J., Altman, D. G., and Prisma Group. (2009). Preferred reporting items for systematic reviews and meta-analyses: the PRISMA statement. PLoS Med. 6:e1000097. doi: 10.1371/journal.pmed.1000097 AND https://www.bmj.com/content/339/bmj.b2535

- https://stackoverflow.com/questions/14426637/how-to-do-bubble-plot
- https://www.researchgate.net/publication/296680807_Menstrual_hygiene_management_among_adolescent_girls_in_India_A_Systematic_review_and_meta-analysis/figures?lo=1

Good explanation of some of the plots:

- https://ora.ox.ac.uk/objects/uuid:ff78831d-6f82-4187-97cc-349058e9abde/download_file?file_format=pdf&safe_filename=Rahimi%2Bet%2Bal%252C%2BData%2Bvisualisation%2Bfor%2Bmeta-analysis.pdf&type_of_work=Journal+article